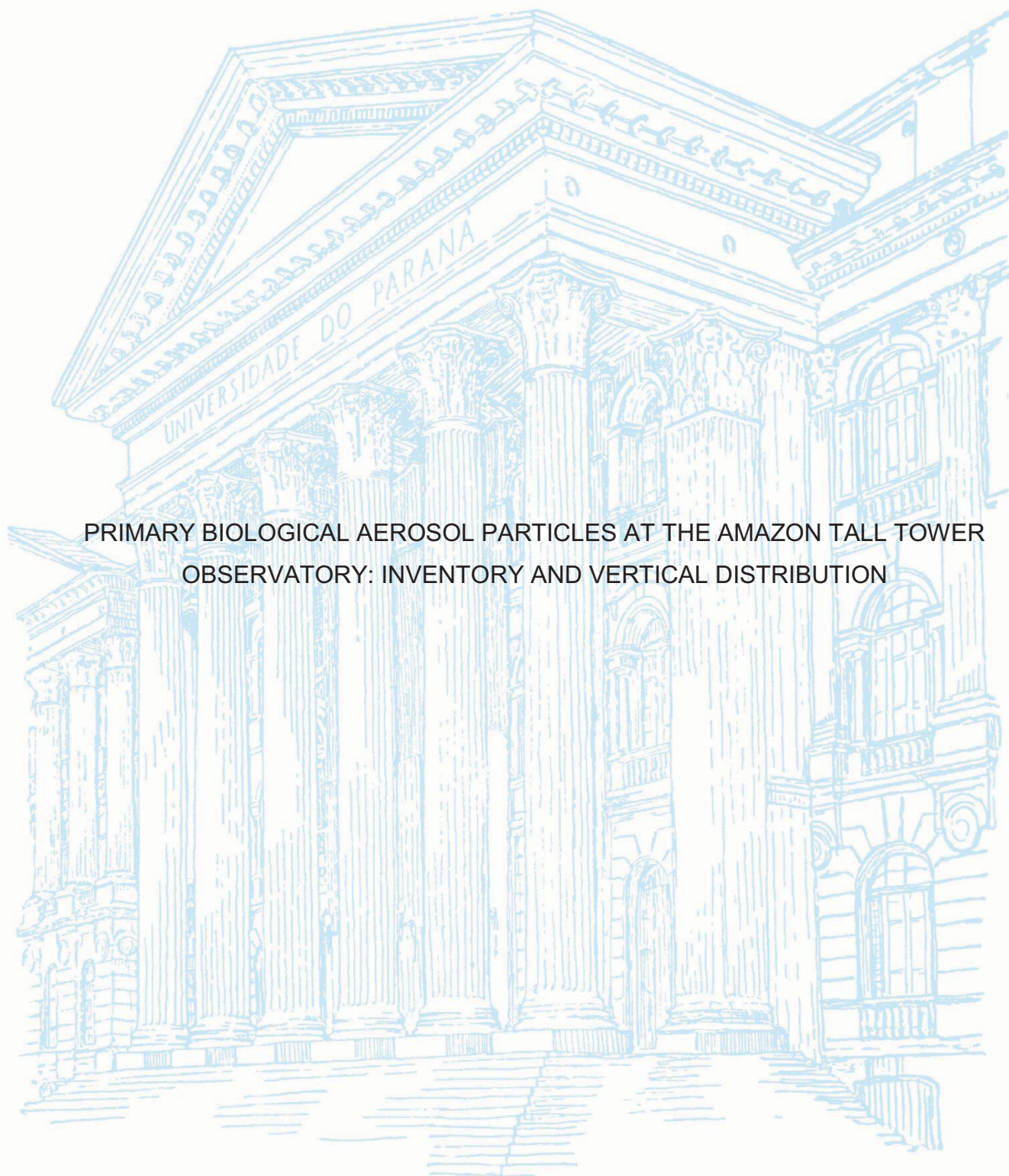


UNIVERSIDADE FEDERAL DO PARANÁ

CYBELLI GONÇALVES GREGÓRIO BARBOSA



PRIMARY BIOLOGICAL AEROSOL PARTICLES AT THE AMAZON TALL TOWER
OBSERVATORY: INVENTORY AND VERTICAL DISTRIBUTION

CURITIBA

2018

CYBELLI GONÇALVES GREGÓRIO BARBOSA

PRIMARY BIOLOGICAL AEROSOL PARTICLES AT THE AMAZON TALL TOWER
OBSERVATORY: INVENTORY AND VERTICAL DISTRIBUTION

Tese apresentada ao curso de Pós-Graduação
em Engenharia de Recursos Hídricos e
Ambiental, Setor de Tecnologia, Universidade
Federal do Paraná, como requisito parcial à
obtenção do título de Doutor.

Orientador: Prof. Dr. Ricardo H. M. Godoi

Coorientador: Dr. Philip E. Taylor

CURITIBA

2018

Catálogo na Fonte: Sistema de Bibliotecas, UFPR
Biblioteca de Ciência e Tecnologia

B238p

Barbosa, Cybelli Gonçalves Gregório

Primary biological aerosol particles at the Amazon tall tower observatory: inventory and vertical distribution / Cybelli Gonçalves Gregório Barbosa. – Curitiba, 2018.

Tese - Universidade Federal do Paraná, Setor de Tecnologia, Programa de Pós-Graduação em Engenharia de Recursos Hídricos e Ambiental, 2018.

Orientador: Ricardo Henrique Moreton Godoi – Coorientador: Philip Earl Taylor.

1. Aerossóis. 2. Pólen. 3. Distribuição vertical (Hidrobiologia). 4. Amazônia. I. Universidade Federal do Paraná. II. Godoi, Ricardo Henrique Moreton. III. Taylor, Philip Earl. IV. Título.

CDD: 551.527

Bibliotecário: Elias Barbosa da Silva CRB-9/1894



MINISTÉRIO DA EDUCAÇÃO
SETOR TECNOLOGIA
UNIVERSIDADE FEDERAL DO PARANÁ
PRÓ-REITORIA DE PESQUISA E PÓS-GRADUAÇÃO
PROGRAMA DE PÓS-GRADUAÇÃO ENGENHARIA DE
RECURSOS HÍDRICOS E AMBIENTAL

TERMO DE APROVAÇÃO

Os membros da Banca Examinadora designada pelo Colegiado do Programa de Pós-Graduação em ENGENHARIA DE RECURSOS HÍDRICOS E AMBIENTAL da Universidade Federal do Paraná foram convocados para realizar a arguição da Tese de Doutorado de **CYBELLI GONCALVES GREGORIO BARBOSA**, intitulada: **"PRIMARY BIOLOGICAL AEROSOL PARTICLES AT THE AMAZON TALL TOWER OBSERVATORY: INVENTORY AND VERTICAL DISTRIBUTION"**, após terem inquirido a aluna e realizado a avaliação do trabalho, são de parecer pela sua Aprovação no rito de defesa.


A outorga do título de Doutor está sujeita à homologação pelo colegiado, ao atendimento de todas as indicações e correções solicitadas pela banca e ao pleno atendimento das demandas regimentais do Programa de Pós-Graduação.

Curitiba, 23 de Maio de 2018.


RICARDO HENRIQUE MORETON GODOI(UFPR)
(Presidente da Banca Examinadora)


JOSÉ EDUARDO GONÇALVES(UFPR)


MICHAEL MANNICH(UFPR)


THEOTONIO MENDES PAULIQUEVIS
JUNIOR(UNIFESP)


PHILIP EARL TAYLOR(DEAKIN)


BETTINA WEBER(MPIC)

*Everything that can possibly go wrong,
will go wrong.*

Edward Murphy

RESUMO

Partículas de aerossol biológicas primárias (primary biological aerosol particles - PBAP) são essenciais como fonte de nutriente e na dispersão de material reprodutivo. Pólen e esporos de fungos são considerados potenciais núcleos gigantes de condensação de nuvens sobre florestas tropicais. Portanto, eles provavelmente influenciam nos processos de precipitação em escala local e regional. A distribuição vertical de partículas grossas sobre a floresta foi analisada utilizando medições na Torre Alta de Observação da Amazônia (Amazon Tall Tower Observatory - ATTO), no Brasil. Esta é a primeira caracterização de dispersão e transporte vertical de bioaerossóis atmosféricos até 300 m de altura para a Amazônia central. Campanhas de amostragem foram conduzidas durante ambas as estações, seca e chuvosa, de 2015 a 2017. Um amostrador volumétrico de esporos (tipo Hirst) foi utilizado para coletar partículas na torre a 25, 40, 60, 80 e 300 metros de altura acima do nível do solo. As amostras foram imageadas com microscopia ótica e a série temporal de abundância de bioaerossol foi obtida baseada na classificação, quantificação e identificação morfológica. Grãos de pólen, esporos de fungos e farnos, e resíduos da copa como fragmentos de folhas e insetos, ceras e glândulas de plantas, decresceram em abundância da copa (30 a 35 m) até 300 m de altura. Precipitação, umidade relativa e direção e velocidade do vento tiveram uma forte influência na distribuição vertical dessas PBAP. Partículas de pólen foram encontradas na faixa de tamanho de 10 a 95 μm , com maior frequência de 10 a 30 μm . Grandes grãos de pólen estavam ausentes bem acima da copa, exceto durante eventos de tempestade. Pólen acima da copa raramente apareceram rompidos. A baixa precipitação através da estação seca de 2015, registrada durante um evento de El Niño, foi correlacionado com um acréscimo no número de PBAP suspensos, devido ao aumento na emissão e/ou decréscimo na remoção proporcionada pela chuva. Para 60 e 80 m, houveram diferenças significativas ($p\text{-valor} < 0,01$) entre concentrações de pólen e fungos de dia e a noite. A composição relativa de PBAP é similar ao longo do ano, apesar das diferenças de altura e estação. Fora de eventos de tempestade, aerossóis primários grossos mensurados, especialmente pólen maiores que 10 μm de diâmetro, podem geralmente sofrer menos arrastamento atmosférico e ter menos influência nos processos atmosféricos.

Palavras-chave: Partículas de aerossol biológicas primárias, polén, distribuição vertical, Torre Alta de Observação da Amazônia, Amazônia.

ABSTRACT

Primary biological aerosol particles (PBAP) are essential as a nutrient source and for dispersal of reproductive material. Pollen and fungal spores are considered potential giant cloud condensation nuclei over tropical rainforests. Thus, they likely influence local and regional scale precipitation processes. The vertical distribution of coarse particles above the rainforest was analysed using tower-based measurements at the Amazon Tall Tower Observatory (ATTO) in Brazil. This is the first characterization of airborne bioaerosol emission and vertical transport up to 300 m height for the central Amazon. Sampling campaigns were conducted during both the wet and dry seasons from 2015 to 2017. A Recording Volumetric Spore Sampler (Hirst-type) was used to collect particles on the tower at heights of 25, 40, 60, 80 and 300 m above ground level. Samples were imaged with optical microscopy, and time series of bioaerosol abundance were obtained based on morphological classification, quantification and identification. Pollen grains, fungal spores, fern spores and canopy debris, such as leaf and insect fragments, as well as plant waxes and glands, decreased in abundance from the canopy (around 30~35 m) to 300 m height. Precipitation, relative humidity, and wind direction and speed had a strong influence on the vertical distribution of those PBAP. Pollen particles were found in the size range of 10 to 95 μm , with higher frequency from 10 to 30 μm . Large pollen grains were absent high above the canopy except during some thunderstorm events. Pollen above the canopy rarely appeared ruptured. The low rainfall across the 2015 dry season, recorded during an El Niño event, correlated with an increased number of suspended PBAP, due to an increased emission and/or decreased rain-related scavenging. For 60 and 80m, there were significant ($p\text{-value} < 0.01$) differences between day and night concentrations of pollen and fungi. The relative PBAP composition is similar throughout the year, despite season and height difference. Outside of storm events, measured coarse primary aerosols, especially pollen larger than 10 μm in diameter, might generally undergo less atmospheric entrainment and have less influence on atmospheric processes.

Key-words: primary biological aerosol particles (PBAP), pollen, vertical distribution, Amazon Tall Tower Observatory (ATTO), Amazon.

LIST OF FIGURES

FIGURE 1: Scheme of the Atmospheric Boundary Layer structure: Surface, Convective Mixed, Stable and Residual Layers up to the capping inversion.	19
FIGURE 2: Scheme of vertical motions in the boundary layer, air mass subsidence related to divergence in the surface, and air updraft related to convergence.	20
FIGURE 3: Scheme of cloud condensation nuclei (CCN) formation from bioaerosols emitted from the surface and consequent dry or wet deposition on the surface.	23
FIGURE 4: Optical view of pollen grains: Pinaceae, Sphagnaceae, Pteridaceae, Oculopollis, and 3D SEM view of Oculopollis (from left to right).	25
FIGURE 5: Scheme of pollen production for a flowering plant: simplified steps from the flower parts description until the pollen release from the anther. Out of scale.	25
FIGURE 6: Simplified scheme of an ascospore reproduction based on an ascus, up to the hyphae formation at the germination phase. Out of scale.	27
FIGURE 7: Simplified scheme of a basidiospore reproduction from the basidia cell until the spores dispersion. Out of scale.	27
FIGURE 8: Simplified scheme of a fern reproduction based on the sporulation where the several spores are released into the atmosphere. Out of scale.	28
FIGURE 9: Sampling site location: Amazon Tall Tower Observatory (ATTO) almost 200 km northeast of Manaus, the capital of Amazonas state in Brazil. ...	32
FIGURE 10: Image of the tall towers at the research site where the sampler(s) were installed: INSTANT tower: 80 m height (left) and ATTO tower: 320 m height (right).	32
FIGURE 11: The Sporewatch spore sampler: Scheme of the external view describing the parts attached to the main body, with the internal view in detail showing the rotating drum (left), and image of the sampler installed at the tower (right).	35
FIGURE 12: Scheme of the steps followed during sampling: (1) tape preparation with adhesive for sampling, (2) after sampling the tape was divided, (3) mounted onto glass slides (4) with a coverslip, (5) and then stored for longitudinal optical scanning.	36
FIGURE 13: Normal Q-Q plot for each category with the respective distribution in dots (vertical axis) and the Normal Quantiles line marked in red (horizontal axis).	42
FIGURE 14: Pictures of biological particles sampled showing the morphology of the selected categories: (A) Pollen grains, (B) Fungal spores, (C) Fern	

spores, (D) Unknown particles, (E) Soot particles and (F) Canopy debris. Scale: 50 μm	43
FIGURE 15: Density distribution (black line) and accumulated distribution (dotted blue line) for each category with all sampled heights integrated. All the horizontal axis are in concentration unit (particles m^{-3}): Pollen (top left), Fungal spores (top right), Fern spores (center left), Soot (center right), Unknown particles (bottom left) and Debris canopy (bottom right).....	45
FIGURE 16: Relative histogram (black lines) and log-normal distribution (red line) for the size (from 3 to 100 μm) of all particles sampled, integrating all the categories and seasons at each sampled height: 40 m (top left), 60 m (top right), 80 m (bottom left) and 300 m (bottom right).	46
FIGURE 17: Examples of the size difference for pollen grains collected across all heights. The scale bar is marked.	47
FIGURE 18: Histogram of absolute frequency for size distribution of pollen grains at each sampled height, with both seasons integrated for 40 and 80 m: 40 m (top left), 60 m (top right), 80 m (bottom left) and 300 m (bottom right). The total number of pollen sampled is detailed in blue and the percentage up to 20 μm is marked in red.....	47
FIGURE 19: Fungal spores major division at each height, with integrated seasons: 40 m (top left), 60 m (top right), 80 m (bottom left) and 300 m (bottom right).....	48
FIGURE 20: Accumulated monthly Precipitation (top) for the site and monthly Relative humidity range (bottom): minimum and maximum values measured at 80 m height, from 2015 to 2017. All the sampling periods with valid results are highlighted in red with the considered season specified.....	50
FIGURE 21: Mean and maximum monthly Wind Speed values (top) and monthly Temperature range with minimum and maximum values (bottom), from 2015 to 2017. Sampling periods with valid results highlighted in red. All the values correspond to the height of 80 m.	51
FIGURE 22: Bar plot of particles concentration by category: pollen, fungal spores, fern spores, unknown particles, soot and canopy debris, sampled during dry season periods from 2015 to 2017 at 40, 60 and 80 m (vertical axis out of scale).	53
FIGURE 23: Bar plot of particles concentration by category: pollen, fungal spores, fern spores, unknown particles, soot and canopy debris, sampled during wet season periods at 40, 80 and 300 m, from 2015 to 2017 (vertical axis out of scale).	53
FIGURE 24: Seasonal median concentration of fern, fungal spores, pollen, soot and unknown particles for 40 m height. Interquartile ranges are represented on the top of each columns.	54

FIGURE 25: Seasonal median concentration of fern, fungal spores, pollen, soot and unknown particles for 80 m height. Interquartile ranges are represented on the top of each columns.....	54
FIGURE 26: Boxplot of pollen concentrations (particle m^{-3}) for each hour interval (in local time): dry season at 40 m (top left), wet season at 40 m (top right), dry season at 80 m (center left), wet season at 80 m (center right), 60 m (bottom left), and 300 m (bottom right). Number of events recorded during each hour interval is in gray above each boxplot.	56
FIGURE 27: Each pollen occurrence (with size diameter marked in blue dots) and maximum wind speed (black dotted line), in hourly resolution during thunderstorms in January 2015, for 80 m height.....	59
FIGURE 28: Samples from 80 m height, 10 th January 2015: only a few particles observed for long hours (top left), a large variety of particles sampled during thunderstorm event around 6 am (top right and bottom right/left), and larger size of pollen particle sampled at 80 m height (bottom right) also during a thunderstorm, probably from <i>Podocarpaceae</i> family (giant hyaline particle on the left).	60
FIGURE 29: High density of particles sampled during a wind gust event at 80 m, on 3 rd April at 1pm during the 2015 wet season. Larger concentration of canopy debris and fungal spores.	61
FIGURE 30: Wind rose chart for the wet season sampling period at 80 m height from 9 th to 24 th January 2015.	62
FIGURE 31: High variety of particles sampled at 60 m, on 19 th September 2015 at 6 am, local time. All the categories are evenly represented during the sampling period.....	63
FIGURE 32: Wind rose chart for the dry season period sampled at 60 m height, from 16 th September to 20 th November 2015.....	64
FIGURE 33: Unique larger pollen grain collected at 60 m during 2015 dry season, on 14 th October 2015 at 8 pm.	65
FIGURE 34: Wind rose for 40 m height during dry season (left), for 15 th September to 7 th October 2016 and wet season (right), from 29 th November to 16 th December 2016.	66
FIGURE 35: Wind rose chart for the dry season period sampled at 80 m height, from 15 th September to 7 th October 2016.....	67
FIGURE 36: Backward trajectories reaching the site by the end of the sampling period on December 2016 (left) and April 2017 (right) at 300 m, showing the dominance of northeasterly air masses for the period.	67
FIGURE 37: Example of a typical sample from 300 m during the wet season with a clear background and few collected particles, including biological ones, on 30 th March 2017 at 11am.	68

FIGURE 38: Example of an atypical observation during the mid wet season at 300 m, showing high density of small particles, up to 15 μm , on 3 rd April 2015 at 6 pm.....	69
FIGURE 39: Air mass backtrajectories 3 days prior to the sampling with lightning occurrence highlighted in a map (top) and an electric field profile with number of strikes (bottom). Dark blue dots are the highest frequency of strikes reaching the air mass.	71
FIGURE 40: Image of a pollen rupture experiment. The particle on the left is still intact and the one on the right released the contents into the microdroplet of liquid that condensed around each pollen grain. Experiments performed in a controlled environment with up to 94 % relative humidity.	72
FIGURE 41: Pictures of damaged pollen grains sampled from 2015 to 2017, occurred at all sampled heights. Different types and sizes of particles can be observed. All the images are in the same scale: 25 μm	73
FIGURE 42: Example of a sample from 80 m height with the Pollen trap on the 26 th of September 2016, 8h (local time).	92
FIGURE 43: Wind rose from September 17 th to October 7 th 2016, at 80 m height. .	92
FIGURE 44: Images with 1000x magnification of particles from 8 to 16 μm sampled with fiberfilm filter, scale bar: 10 μm . Example of Iron-containing particles with minor oxygen compounds (left) and Si-, O-containing particle (right).	94
FIGURE 45: Images with 1000x magnification of particles from 4 to 8 μm sampled with fiberfilm filter, scale bar: 10 μm . Example of biological particles (top left), Si-, O-, N-containing particles (top right), salt and mineral particles (bottom left and right).	95
FIGURE 46: Elemental composition spectrum (left) from the central particle (left) and colour image highlighting K-(orange), Na-(yellow), Mg-(purple) containing particle (right).	95
FIGURE 47: Images with 1000x magnification of particles from 2 to 4 μm sampled with fiberfilm filter, scale bar: 10 μm . Example of C-, O-containing amorphous particles (left), and Si-, O-, Na- and Mg-containing particles (right).	96

LIST OF CHARTS AND TABLES

CHART 1: Monthly distribution of the sampling periods by height, regardless the year of the sampling. Months with sampling for each height are marked in green.	37
CHART 2: Examples of bioaerosols categorized for this project: pollen, fungal, fern, moss, soot and debris. The particles were redimensioned and the scale for each category is shown.	39
CHART 3: Monthly sampling calendar with the periods marked in green: valid samples and results, or red: invalid samples, results not used.	41
TABLE 1: Description of sampling periods with pollen trap, according to the height, with total sampled hours. Periods of simultaneous sampling at different heights are specified.	36
TABLE 2: Total and valid sampled hours according to the height.	40
TABLE 3: Summary of pollen, fungi and fern results with median and maximum values for each height at each sampled season. All values are in one-hour time resolution.	58
TABLE 4: Particle concentration sampled with Pollen trap during the dry season of 2016. Median results in number of particle per cubic meter of air, averaged over 24 h.	91
TABLE 5: Total particle concentration for fractionated particle sampling using the PIXE cascade impactor during the dry season of 2016.	93
TABLE 6: Relative cluster classification of single particles in the range of 2 to 16 μm sampled at 80 m height during 2016 dry season. Results in percentage (%).	96

LIST OF ABBREVIATIONS AND SYMBOLS

ABL	Atmospheric Boundary Layer
ATTO	Amazon Tall Tower Observatory
CO _{2e}	carbon dioxide equivalent
CCN	Cloud condensation nuclei
EPA	Environmental Protection Agency (EUA)
INPA	National Institute of Amazonian Research - Instituto de Pesquisas da Amazônia
IPCC	Intergovernmental Panel on Climate Change
ITCZ	Intertropical Convergence Zone
PBA	Primary Biological Aerosol
PBAP	Primary Biological Aerosol Particles
PM	Particulate Matter
PM ₁	Particulate Matter with aerodynamic diameter up to 1 µm
PM _{2.5}	Particulate Matter with aerodynamic diameter up to 2.5 µm
PM ₁₀	Particulate Matter with aerodynamic diameter up to 10 µm
SOA	Secondary Organic Aerosol

SUMMARY

1	INTRODUCTION	15
1.1	HYPOTHESIS.....	17
1.2	AIMS	17
2	LITERATURE REVIEW	18
2.1	GLOBAL ATMOSPHERIC CIRCULATION	18
2.1.1	Atmospheric Boundary Layer.....	18
2.1.2	Physical transport mechanisms	19
2.2	ATMOSPHERIC PARTICLES.....	21
2.2.1	General classification of atmospheric particles	21
2.2.2	Particle formation and emission to the atmosphere	22
2.2.3	Biological particles in the atmosphere.....	24
2.3	ATMOSPHERIC PARTICLES OVER THE AMAZON RAINFOREST	28
3	METHODS	32
3.1	SAMPLING SITE	32
3.2	SAMPLING EQUIPMENT	34
3.3	SAMPLING PERIODS	36
3.4	MICROSCOPY ANALYSIS	38
3.5	SAMPLE VALIDATION AND DATA TREATMENT	40
4	RESULTS AND DISCUSSION	43
4.1	MORPHOLOGY AND VERTICAL DISTRIBUTION OF BIOLOGICAL PARTICLES.....	43
4.2	METEOROLOGICAL PATTERN AND SEASONAL DISTRIBUTION.....	49
4.3	BIOGENIC PARTICLE VERTICAL DISTRIBUTION	59
4.4	INCIDENCE OF POLLEN RUPTURE AT THE AMAZON REGION.....	70
5	CONCLUSION	75
	REFERENCES.....	78
	APPENDIX A: ADHESIVE RECIPE AND PREPARATION	88
	APPENDIX B: TOTAL PARTICULATE MATTER AND BIOGENIC FRACTION	90
	APPENDIX C: BIOAEROSOL ATLAS	98

1 INTRODUCTION

Biological particles are abundant in the atmosphere and follow an essential path in the dissemination of biological organisms and reproductive material. Also, they are important components for air chemistry and physics. These suspended particles can influence the surface's energy by scattering and absorbing radiation and can initiate the formation of clouds and precipitation as cloud condensation and ice nuclei (ANDREAE; CRUTZEN, 1997; PÖSCHL, 2005, 2010). Primary biological aerosol particles (PBAP), such as pollen, bacteria, fungal and fern spores, viruses, and fragments of animals and plants, are directly emitted from the biosphere remaining in suspension according to its size and density (ELBERT et al., 2007; DESPRES et al., 2012).

Primary biological particles typically belong to the coarse fraction of atmospheric particulate matter, with aerodynamic diameter from 10 to 100 micrometers. Those particles and components are also found in intermediate and fine fractions, like most fungal spores, small fragments, and excretions of plants and animals, bacteria, viruses, carbohydrates, proteins, waxes, ions, (TAYLOR et al., 2004; PÖSCHL, 2005). The possible driven mechanisms (like turbulence and long-range transport) and effects (as nucleation or health effects) of those particles in the atmosphere are frequently discussed (TAYLOR; JONSSON, 2004; SUN; ARIYA, 2006; ELBERT et al., 2007; STEINER et al., 2015).

Although different types of investigations, including airborne and tower-based measurements, have been performed to understand the dispersion and physical behaviour of long-distance and short-range transport of pollen grains (RAYNOR et al., 1973; MANDRIOLI et al., 1984; SOFIEV et al., 2006), the data obtained from these studies are restricted in their representativeness because of the limited number of observed pollen events, the lack of continuous airborne measurements, and the limited height coverage of tower-based measurements. Therefore, observations of the vertical distribution and abundance of pollen are a need to more accurately determine pollen dispersion and transport.

Raynor et al. (1973) and Hart et al. (1994) reported that the vertical distribution of pollen is highly correlated with meteorological conditions, and their findings are based on vertically resolved measurements using towers. Since the maximum height of their sampling was limited to 108 m, these tower-based studies did not take account

of the distribution of pollen up to the top of the planetary boundary layer, and into the free troposphere. The presence of pollen in samples collected by aircraft suggested that a substantial abundance of pollen was prolonged at heights over 1 km. These results corroborated the hypothesis that recurring meteorological conditions favour vertical exchange and long-range transport of pollen (MANDRIOLI et al., 1984).

In order to understand and predict temporal and spatial characteristics of pollen, pollen-forecasting models have been developed (VAZQUEZ et al., 2003). The models utilize pollen concentration data observed by *in situ* aerobiological monitors near the surface (PORSBJERG et al., 2003). However, there is convincing evidence that long-range transported pollen can significantly enhance pollen concentrations at both the surface and at elevated altitudes above the receptor sites. Especially in these cases, temporally and vertically resolved data of pollen concentration are expected to improve the forecasting capability of these models.

Meteorological events combined with an analysis of pollen morphology, suggest that rupture of airborne pollen can occur. These micron-sized particles might influence cloud formation (STEINER et al., 2015). Strong downdrafts and dry, cold outflows distinguish thunderstorm rain from frontal rain (STULL, 2011). The weather system of a mature thunderstorm likely entrains pollen grains into the cloud base, where pollen rupture would be enhanced, then transports the nano and micro-sized fragments of pollen debris to ground level where outflows distribute them ahead of the rain. Examining the morphology of pollen during thunderstorms could assist in understanding these events. Therefore, to understand and predict pollen release, dispersal, and transport, it is necessary to simultaneously measure the vertical distribution of pollen associated with meteorological parameters.

1.1 HYPOTHESIS

Studies performed at high altitude suggest that primary biological aerosol particles, such as pollen grains, are evenly distributed across the atmospheric boundary layer. These concepts, first developed in the 1970's, based on North American and European measurements, proposed a relatively linear vertical pattern of biogenic particles dispersal throughout the atmospheric boundary layer.

Considering that the tropical rainforest is a large source of PBAP, it is opportune to examine the entrainment of bioaerosols using tower-based measurements. Regarding the transport mechanism of particles and the development of the atmospheric boundary layer structure, vertical pollen abundance should follow a pattern of exponential decrease.

1.2 AIMS

The present study proposes to seasonally and vertically evaluate the Primary Biological Aerosol Particles suspended in a pristine atmosphere of the Amazon rainforest.

In order to achieve the main goal, these specific aims were targeted:

- Quantify the seasonal distribution of PBAP, during dry and wet periods;
- Measure the vertical distribution of biogenic particles at different tower-based heights;
- Catalogue the types of biological aerosol particles;
- Record the incidences of pollen rupture related to meteorological conditions.

2 LITERATURE REVIEW

2.1 GLOBAL ATMOSPHERIC CIRCULATION

2.1.1 Atmospheric Boundary Layer

Horizontally, the global circulation around the planet surface can be visualized in three major cells. In the Northern Hemisphere, the major winds at the Equator's region are directed from West, and in the Southern Hemisphere, from the East. Around the zero latitude, the trade winds are from Northeast and Southeast, respectively, driving the major winds and jets easterly in low-pressure zones. At this region, between the Hadley cells, the variation is known as Intertropical Convergence Zone (ITCZ), and its seasonal oscillation along with other meteorological conditions, are responsible for weather changes in the region (STULL, 2011).

The South American climate system presents some features like the ITCZ, maintained by the transient moisture flux from the Amazon (MARENGO, 2012). The specific local topography, heating and moisture conditions over the Amazon Basin at the Equator's line are responsible for the climate intra-seasonal pattern on the region.

The seasonality over South America is strongly related to the annual cycle of the Convergence Zone and the surface temperature gradients (GRIMM, 2010). The rainfall over South America is also influenced by the El Niño Southern Oscillation, an upper-low level circulation anomaly that perturbs the global circulation (GRIMM and TEDESCHI, 2009; TEDESCHI, CAVALCANTI and GRIMM, 2012).

Vertically, the atmosphere around the Earth's planet is structured in layers according to the pressure and density profile. The troposphere, the first layer above the ground's surface, below around 10 km, is characterized by an exponential drop of density and air pressure with altitude increase. Within the troposphere, the layer directly above, and influenced by the surface, is known as the atmospheric boundary layer (ABL), and extends up to 3 km, as shown in FIGURE 1. The layer above is known as the free troposphere (GRIMM, 2010).

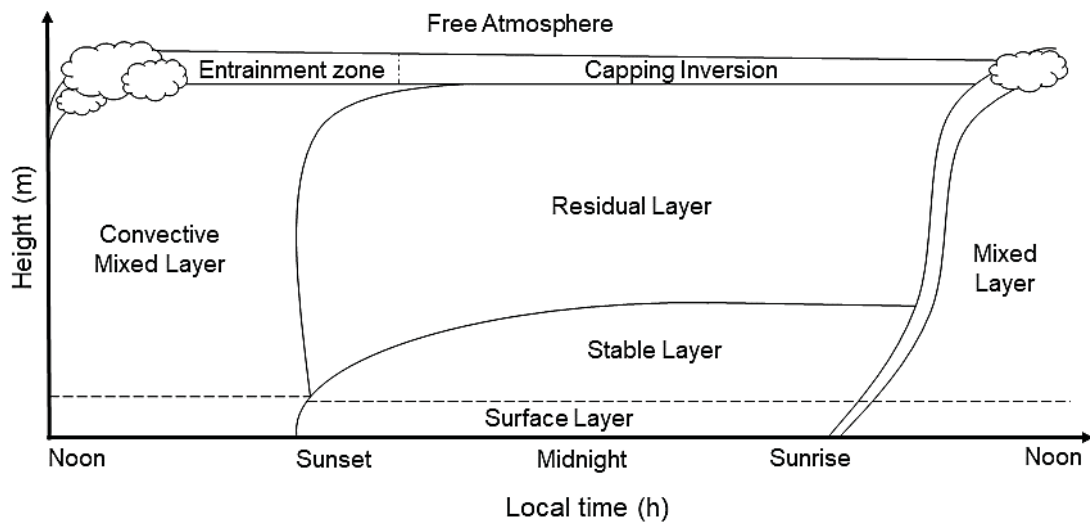


FIGURE 1: Scheme of the Atmospheric Boundary Layer structure: Surface, Convective Mixed, Stable and Residual Layers up to the capping inversion.

SOURCE: adapted from STULL (2003).

The ABL is characterized by a diurnal cycle, based on the temperature surface variation that, once transported to the air, can drive turbulence processes. All the subsequent processes are mainly concentrated to the ABL extension, with the free troposphere being barely perturbed by the changes on the ground. Heat and moisture can increase the turbulence and the development of the different structures inside the ABL: mixed or convective layer (very turbulent) during sunlight hours, residual layer (less turbulent) and stable boundary layer during nocturnal periods. Depending on the vertical temperature profile, particles or substances emitted from the surface can be dispersed or trapped according to the ABL development structure (STULL, 2003; 2011).

2.1.2 Physical transport mechanisms

Long-range transport in the atmosphere generally occurs in the free troposphere. To achieve long-range transport, the substance must reach the edge or beyond the ABL.

Vertical motions are related to atmosphere stability, which is related to the moisture content and temperature profile above ground level. The lapse rate of an air mass and the conditions around defines the convergence and divergence motions horizontally, which leads to updrafts or downdrafts vertically, FIGURE 2.

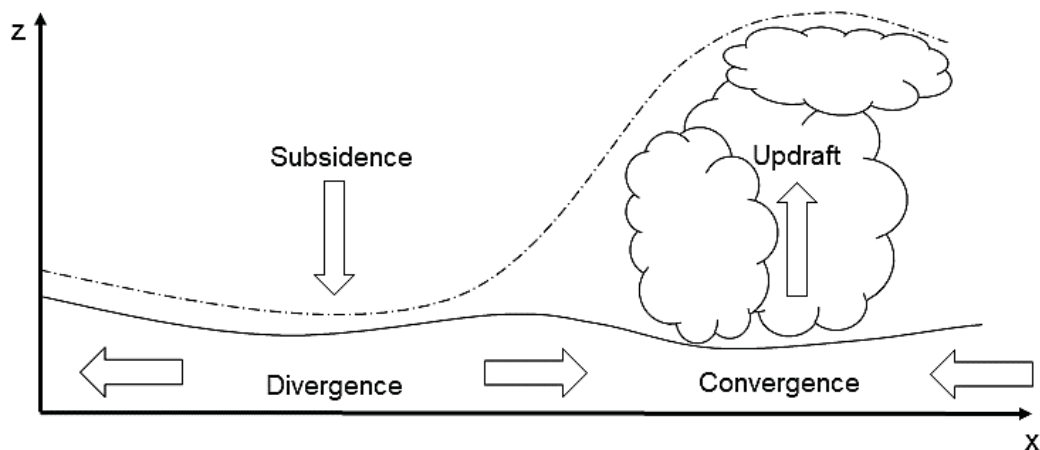


FIGURE 2: Scheme of vertical motions in the boundary layer, air mass subsidence related to divergence in the surface, and air updraft related to convergence.

SOURCE: adapted from STULL (2003).

Over high-pressure surface, the divergence motion is feed by air mass subsidence just above, illustrated in FIGURE 2. The opposite occurs over low-pressure surface when the convergence leads to a rising up mass and can also cause updrafts.

The instability can lead to air gusts and convection with the lifting and mixture of the air mass. One weather event related to atmospheric instability is a thunderstorm, when high moisture and unstable air gets lifted and forms fronts. The rapid updrafts and downdrafts promote a disturbance in the air, and lightning (an electric current charge between the clouds and the ground's surface) that can also perturb and damage suspended particles. Over arid or semi-arid regions, winds gust from a dry cold front lead to a dust storm (a storm with no rain) whereby sand/dust is suspended and resuspended from the ground. (STULL, 2003).

The Sahara is the largest source of desert dust to the atmosphere (GINOUX et al., 2012). Studies have revealed the extent of the influence of Saharan dust on nutrient dynamics and biogeochemical cycling in both oceanic and terrestrial ecosystems in North Africa and far beyond, due to frequent long-range transport across the Atlantic Ocean, the Mediterranean Sea, and the Red Sea, and on to the Americas, Europe, and the Middle East (GOUDIE; MIDDLETON, 2001; HOORNAERT et al., 2003; YU et al., 2015; LONGO et al., 2016; RAVELO-PEREZ et al., 2016; SALVADOR et al., 2016).

2.2 ATMOSPHERIC PARTICLES

2.2.1 General classification of atmospheric particles

Substances present in the air may be formed and emitted from natural or anthropogenic sources and among the pollutants stands the particulate matter (PM). This one plays an important role in the atmosphere, influencing and being influenced by the climate system.

Atmospheric particles or PM can be described as a complex mixture of solid particles and liquid droplets in sufficient size and density to remain in suspension in the atmosphere (EPA, 2013). Particles are mainly classified according to their size. The aerodynamic diameter of 2.5 μm separates two main aerosol categories: coarse mode, and fine mode that can present chemical compounds and/or metals adsorbed on the surface (EPA 2011, 2013).

The mobility and residence time in the atmosphere is defined by the particle size and density. This might be small enough to allow the transport to regions far from the source and, according to the prevailing meteorological conditions, influence distant regions and countries, even transporting pollution overseas and across continents. In general, the larger the diameter of the particles, the lower the residence time in suspension. Very fine particles remain suspended for considerable periods and can be transported to remote and uninhabited regions such as deserts and the poles. The composition of the suspended particle determines their potential influence on the environment (MARTIN et al., 2010).

In general, the smaller the fragment in suspension, the greater the possibility of agglomeration, coagulation and condensation of gases onto the surface, or even the formation of new particles (BUSECK; ADACHI, 2008). The shape and content of each particle can be defined by the formation process. In this case, it is possible to differentiate between particles formed naturally from particles that have resulted from human activities (ZHAO et al., 2013). In both cases, emission rates are highly variable and the impact cannot be fully understood or measured.

In addition to the PM physical characteristics (size) and chemical (elemental) composition, the climate and weather variables are extremely important in the transport of these particles to local, regional (EPA, 2011), and even intercontinental range

(ANDREAE et al., 2015). Particles physical characterization and chemical composition are determined by location and atmospheric conditions of the source region.

2.2.2 Particle formation and emission to the atmosphere

The composition of each particle varies according to location, weather conditions and source. Primary particles are directly emitted from the source, whereas secondary particles are formed in the atmosphere from gases and/or smaller particles. In a forest region, favorable conditions lead to the formation or growth of a new particle by nucleation or condensation, defined as a secondary organic aerosol – SOA, from a light volatile organic compound exposed to solar radiation and air humidity (PERRAUT et al., 2012; FUENTES et al., 2016).

Pollen grains, fern spores, large fungal spores, and other large primary biological aerosol particles, are directly emitted from the biosphere to the atmosphere, and typically belong to the coarse fraction of air particulate matter, with aerodynamic diameters up to 100 μm . PBA and components are also found in intermediate and fine fractions of air particulate matter, with aerodynamic diameters less than 10 μm (PM₁₀), 2.5 μm (PM_{2.5}), and 1 μm (PM₁), respectively: most fungal spores, small fragments and excretions of plants and animals, bacteria, viruses (TAYLOR et al., 2004), carbohydrates, proteins, waxes, ions, are in this size range (PÖSCHL, 2005).

Primary bioaerosols are generally considered efficient cloud condensation nucleus (CCN) due to their wettability and size (ANDREAE; ROSENFELD, 2008; ARIYA et al., 2009). Large bioaerosols, such as pollen grains, can act as giant CCNs (FIGURE 3). This means that they can develop cloud drops under lower supersaturation conditions than other types of aerosol. They can also rapidly grow, facilitating the formation of rain due to their ability to absorb large amounts of water. Thus, there is a geometric increase of grain size with increase in relative humidity (DINGLE, 1966; MOHLER et al., 2007; POPE, 2010; STEINER et al., 2015). This mechanism seems to dominate the formation of secondary organic particulate particles in the Amazon forest (PÖHLKER et al., 2013). The link between biogenic particle emissions and cloud properties in the rainforest ecosystem seems even stronger and more direct than previously thought.

Another particle formation process may initiate from nanoparticles, which create larger particles by agglutination or condensation of gases and other materials

on the surface. Salts are also cores for particle growth, mainly by hygroscopicity (high moisture absorption). Hydrophobic, hydrophilic or hygroscopic characteristics are crucial for the growth of particles and enable the formation of cloud condensation nuclei (BUSECK; ADACHI, 2008; KOEHLER et al., 2009; DESPRES et al., 2012). Hydrophilic substances strongly facilitate droplet nucleation (PETTERS; KREIDENWEIS, 2007; ANDREAE; ROSENFELD, 2008).

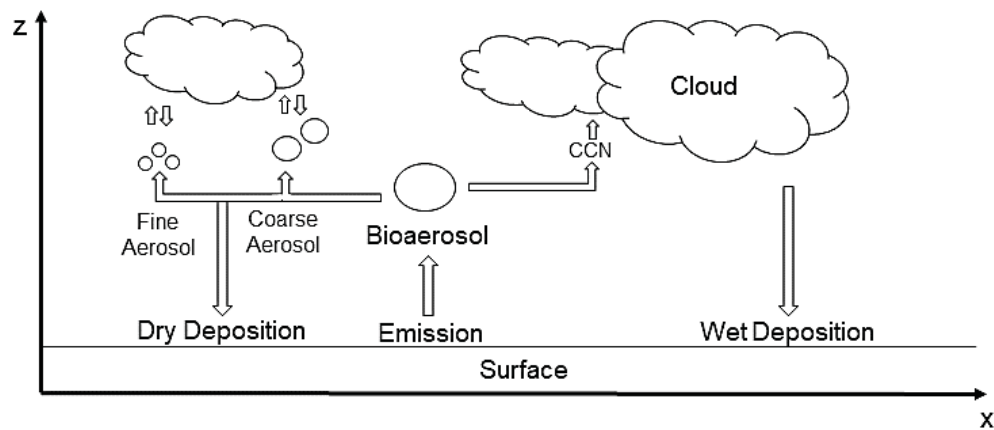


FIGURE 3: Scheme of cloud condensation nuclei (CCN) formation from bioaerosols emitted from the surface and consequent dry or wet deposition on the surface.

SOURCE: adapted from ARIYA et al. (2009).

In general, smaller particles have greater relative surface area, increasing the number of physical and chemical reactions and the formation of other particles. The composition is determined by the availability of substances derived from primary sources. This process helps in tracking the particle, relating the characteristic composition to possible generating sources (LOWRY et al., 2012).

Fine particles can be emitted into the atmosphere by several sources: industrial activities, fuel burning in automotive vehicles (especially Diesel engine) and biomass burning (ANDRADE et al., 2012). The source determines the composition of the particle and this may be organic compounds, acids, or heavy metals, for example. Generally, the incomplete burning of fossil fuels and organic material generates large amounts of carbonaceous particulates, therefore, elemental carbon is an abundant constituent of PM in urban areas (EPA, 2011; ZHAO et al., 2013).

Regarding the elemental composition of the particles, the presence of Aluminium, Silicon, Iron, Calcium, or Titanium, for example, can categorize the source as terrigenous, abundant in soil composition (MAENHAUT et al., 1989). Sodium and

Chlorine, are directly related to the marine source (WOROBIEC et al., 2007). Industrial activities and fossil fuel burning are usually related to elements such as Chromium, Manganese, Nickel, and Lead (TRAPP; MILLERO; PROSPERO, 2010; ARTAXO et al., 2013). Potassium, Phosphorus, and Zinc are considered biological tracers, while Sulphur, Potassium and Chlorine may also be associated with biomass burning (YAMASOE et al., 2000), just to mention a few examples.

To quantify the anthropogenic carbonaceous fraction present in PM over natural sources is a challenge pursued worldwide (ANDREAE; GELENCSEI, 2006; BOND, 2013). Soot particles have high porosity and ability to adsorb other substances in the vapour phase, especially organic compounds (SANDRADEWI et al., 2008), and also present high rates of absorption and refraction of electromagnetic radiation, as defined by Buseck et al. (2012). In the present work, the term soot is used to describe a set of amorphous black particles consisting primarily of carbonaceous matter.

2.2.3 Biological particles in the atmosphere

Biological particles are emitted directly to the atmosphere from biological organisms, such as microorganisms, plants, and animals, and this includes fragments from tissues and cells. Pollen is commonly the largest, in size, of those particles observed in the atmosphere. Pollen grains are reproductive plant cells with a hard wall that protects the sperm cells, nuclei and other cytoplasmic content (DEPRES et al., 2012).

The exine, external layer of the grain, is a waxy or resinous wall, chemically and mechanically resistant, developed to facilitate the dispersion, by wind or animal agent, through its sculptural features (KAPP, 1975). The rupture of the pollen exine naturally occurs during germination, and empty shells, derived from pollen grain rupture with consequent content release, are also included in atmospheric pollen counts (GROTE et al., 2000; TAYLOR et al., 2002, 2004; MIGUEL et al., 2006; ZHOU, 2014; STEINER et al., 2015).

The pollen grain has a shape factor related to the feature of the exine particle. The size, shape, sculptural structure, and polarity (the number, spatial orientation, and arrangement of the microspores and apertures, e.g. germination regions, are the guides (keys) for pollen identification (KAPP, 1975). These morphological characteristics are genetically determined and used to microscopically identify the

species. The FIGURE 4 shows some examples of pollen grains. Sizes and shapes are variable, from circular, elliptical, long, triangular and semicircular to boat-shaped (AGASHE; CAULTON, 2009; HESSE et al., 2009).

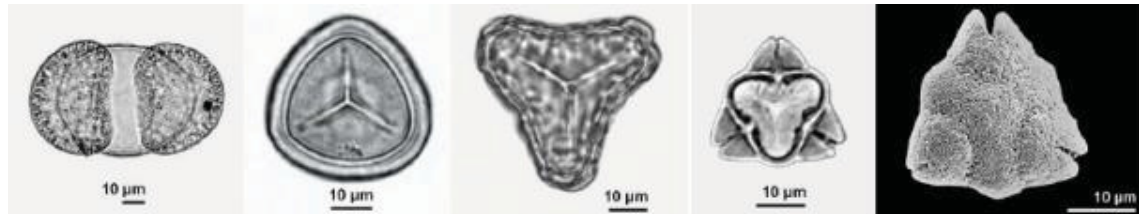


FIGURE 4: Optical view of pollen grains: Pinaceae, Sphagnaceae, Pteridaceae, Oculopollis, and 3D SEM view of Oculopollis (from left to right).

SOURCE: HESSE et al. (2009).

Pollen production occurs in the anthers for flowering and seed plants, as shown in FIGURE 5. Each anther of a flower produces up to several thousands of pollen grains, and anthers exert and dehisce according to changes in the temperature and relative humidity, respectively, releasing the pollen grains at the atmosphere. The emission of pollen from the open anther mainly relies on wind or animal disturbance (COLINVAUX; OLIVEIRA; PATINO, 2005; HESSE et al., 2009). Once in the air, the dispersal depends on meteorological conditions, being positively correlated with temperature, relative humidity, and wind speed and negatively correlated with precipitation (DEPRES et al., 2012).

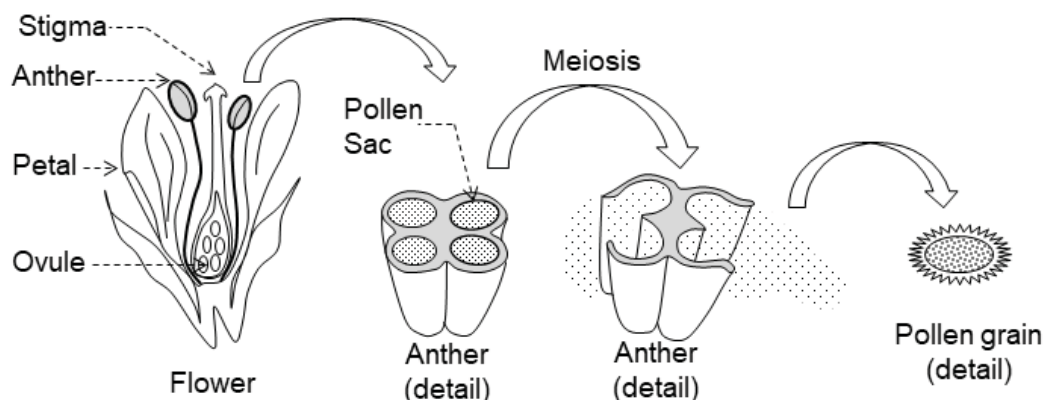


FIGURE 5: Scheme of pollen production for a flowering plant: simplified steps from the flower parts description until the pollen release from the anther. Out of scale.

SOURCE: adapted from KAPP (1975).

Vertical entrainment plays an important part in long-range dispersion and is related to, and controlled by, convection and inversion layers. This issue is not well covered in the published literature since there is a paucity of measurements at fixed heights well above ground level. During aircraft measurements, high concentrations of aerosol particles were found being transported from the free troposphere into the boundary layer by strong convective downdrafts during precipitation events. This rapid vertical motion may influence cloud properties and climate (WANG et al., 2016).

For vertical pollen measurements, earliest methods used adhesive-coated slides in hot air balloons, and by the mid 20th-century samplings were also performed with aircrafts. In 1937, Rempe stated that 40% of the ground concentration of pollen could be found at 2000 m height. In 1984, Mandrioli et al., concluded that pollen grains were evenly distributed over the first 1 km. However, in 2003, Graham et al., recorded high variations in pollen abundance within the first 50 meters above ground.

There have been major limitations with appropriate equipment for quantitative assessment. But, with those first results, the concept that pollen and other giant particles are readily dispersed across the atmospheric boundary layer up to 2000 m above ground level was disseminated (RAYNOR et al., 1973; MANDRIOLI et al., 1984; HART et al., 1994).

Although pollen grains, and large fungal spores, have a sedimentation velocity of approximately 2.5 cm s^{-1} in quiescent air, recent attempts at modelling ground-based concentrations of pollen have relied on the assumption of an even distribution across the lower atmosphere. Further to this, it is believed that pollen grains are regularly transported over long distances. For example, grass pollen detected in Melbourne, Australia, was believed to be mainly sourced from extensive pastures that ring the city and are located 30 km from the sampler site (DE MORTON et al., 2011). Recent advances in ground-based LIDAR technology reinforce this assumption of high vertical displacement (NOH et al., 2013; SICARD et al., 2016; RAO et al., 2017), although direct observations remain lacking.

Another group of highly diverse bioaerosols that is common on the Earth's surface is fungal spores. Spores are as small as a few micrometers in size, usually spherical, spheroidal or elongated in shape (GABEY et al., 2010; HUSSEIN et al., 2013). Spores are often actively released by osmotic pressure or surface tension during the sexual and/or asexual stage of the organism. The release mechanisms are different in the major groups of fungi, as Ascomycota release ascospores (FIGURE 6)

in a wet state, whereas Basidiomycota release basidiospores (FIGURE 7) in a dry state. Conidiospores are asexual spores produced from hyphae by both groups of fungi. Ascospore and basidiospore are airborne dominant (ELBERT et al., 2007; FRÖHLICH-NOWOISKY et al., 2009; DEPRES et al., 2012).

Fern and mosses spores, released by cryptogamic plants, can also be found suspended in the atmosphere. Near the source, they can be the dominant groups (GRAHAM et al., 2003). Fern spores (FIGURE 8) are usually produced by meiosis where the sporulation generate a single type of spore or two distinct spores (male and female). Many fern spores present a 'kidney' shape (KAPP, 1975).

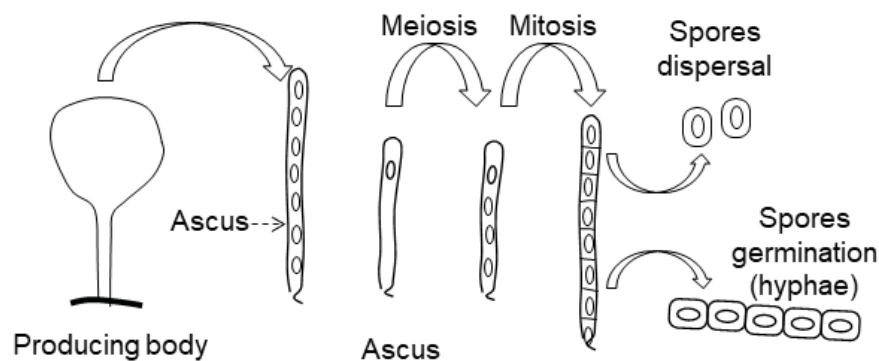


FIGURE 6: Simplified scheme of an ascospore reproduction based on an ascus, up to the hyphae formation at the germination phase. Out of scale.

SOURCE: adapted from PIEPENBRING (2015).

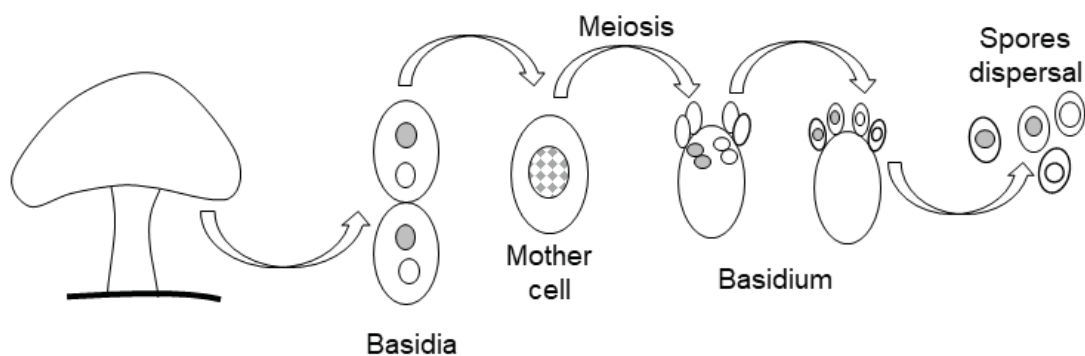


FIGURE 7: Simplified scheme of a basidiospore reproduction from the basidia cell until the spores dispersion. Out of scale.

SOURCE: adapted from HØILAND (2007).

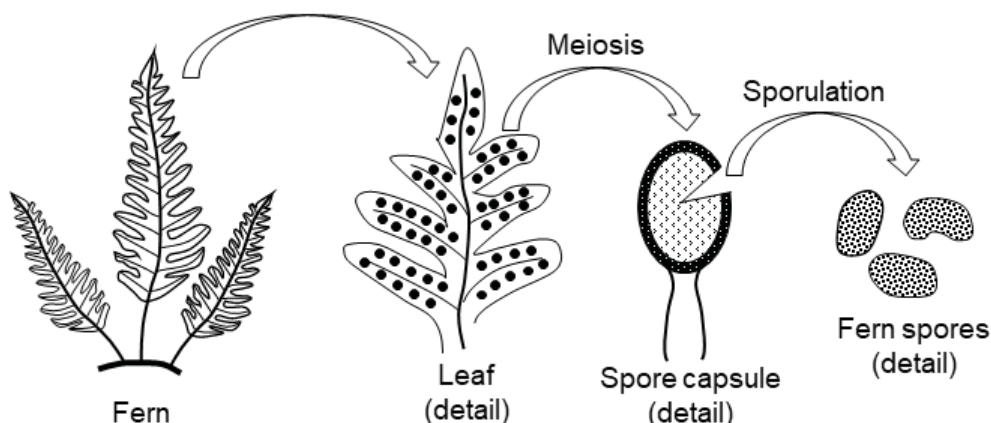


FIGURE 8: Simplified scheme of a fern reproduction based on the sporulation where the several spores are released into the atmosphere. Out of scale.
SOURCE: adapted from KRUPP (2011).

The quantity of PBA globally emitted into the atmosphere has been estimated at less than 10 to as much as 1000 Tg per year (PENNER, 1995; JAENICKE, 2005; WINIWARTER et al., 2009; HOOSE et al., 2010; WOMACK et al., 2015). The wide range is due to the measuring limitations and diverse methods applied. The IPCC estimates approximately 80 Tg only for pollen emission into the atmosphere each year across the globe (IPCC, 2013).

2.3 ATMOSPHERIC PARTICLES OVER THE AMAZON RAINFOREST

The large extent of the rainforest at the Amazon Basin, the largest tropical forest (GARSTANG et al., 1988; ARAGÃO, 2012; DOUGHTY et al., 2015) releases natural biogenic aerosols such as microorganisms, pollen, and spores, as well as secondary particles formed by volatile organic compounds emitted by the forest throughout the year. So, the Amazon Basin is an important region for the atmospheric particles study (ANDREAE et al., 1990, 2015).

In order to evaluate the influence of the forest on the climate, it is important to understand the natural sources of atmospheric aerosols. In this context, the Amazon Basin is considered one of the few continental regions where such particles can be studied under almost natural conditions (pristine during the wet season), emitting a high aerosol load, driven mainly by an intense interaction between the biosphere and the atmosphere (PAULIQUEVIS et al., 2012; HUFFMAN et al., 2013).

The variability in the PM composition and concentration in the region is influenced by aspects such as: transport of dust and soot from the African continent to the northeast coast of South America reaching the Amazon; vertical transport which enables the particles redistribution; fires occurrence which increases PM emissions; boundary layer mixing gradient that affects day and night particle distribution; and the high variability of primary particles (MARTIN et al., 2010).

Brazil's northern region is characterized by a rainy equatorial climate with spatial and seasonal temperature homogeneity, a result of the incident solar radiation that separates the two predominant seasons: rainy and dry (FISH; MARENGO; NOBRE, 1996). The rain distribution along the months of the year can change between October and May. In years with El Niño occurrence, the wet season generally starts later, around December, and presents a different pattern of incidence and frequency (GRIMM, 2010).

The global circulation pattern influences rain occurrence in the Amazon Basin, as in the entire of South America. Near the zero-latitude line, the convergent air from both hemispheres is also associated with low equatorial pressure. This is the region with the highest precipitation frequency and intensity, due to movement of the trade winds. High levels of rainfall occur in the Amazon Basin area, a region with a high evapotranspiration rate, which helps to retain the humidity over the forest. In South America, the ITCZ influence and the west topography are important for the spread of humidity along the continent, modulating the rain distribution. Thus, the dry and rainy seasons, according to humidity at the northern region, have a fundamental role in the continent climate (GRIMM, 2003; GRIMM, 2010; TEDESCHI; CAVALCANTI; GRIMM, 2012).

Regardless of the season, about 90% of the atmospheric particulate matter in the region is organic material (ANDREAE and CRUTZEN, 1997; MARTIN et al., 2010; ANDREAE et al., 2015). Also, the Amazon Basin receives annually about 28 million tons of African dust (YU et al., 2015), as well as Atlantic sea spray and smoke from African biomass burning (TALBOT et al., 1990; MARTIN et al., 2010; BAARS et al., 2011; ANDREAE et al., 2015).

During the dry season, the smoke from forest fires and the predominant northeastern wind transport (due to the trade winds) may explain the abundance of carbonaceous organic particles (potassium-containing). At this period, surrounding anthropogenic activity affects the properties of the PM and biomass burning

contributes to high sulfur levels, in addition to chloride and potassium, to the fine particulate fraction composition (GUNTHER et al., 2009; MARTIN et al., 2010).

During the rainy season, the Amazon region is known as pristine, with very low trace gases and PM concentrations consisting mostly of biogenic elements (ARTAXO et al., 2013). During this period, increased concentrations of crustal elements is due to the intercontinental transport of dust from Africa, enabled by the global circulation pattern (BEN-AMI et al., 2010; BAARS et al., 2011; RIZZOLO et al., 2017). There is also the observation of new particle formation in the range of 10 to 20 μm in intervals of less than 24 h (MARTIN et al., 2010).

Studies indicate that fine particles, which serve as cloud condensation nuclei in pristine forests, such as the Amazon, are predominantly composed of organic secondary aerosol, formed by oxidation of volatile organic compounds and condensation of oxidation of semi-volatile products. The results support the hypothesis that the Amazon forest ecosystem can be considered as a biogeochemical reactor, in which cloud formation and precipitation in the atmosphere are driven by particles emitted from the biosphere (ARTAXO et al., 2006; PÖHLKER et al., 2012).

According to the IPCC simulations, the Amazon Basin should experience an average increase of 3°C, with a reduction of about 20% in the average precipitation in this century. Such climate change would reduce the water availability of plants and thus increase water stress for many species because these areas tend to be more vulnerable to increased drought and heat. Each species varies in tolerance to environmental stress, and it is difficult to predict the overall response to this environmental change (IPPC, 2013).

In the formulation of future scenarios, there are high uncertainties about changes in biomass, and significant rearrangement of plant species within communities in response to such changes. Plant growth rates have increased in tropical forests over the past three decades, related to increased CO_{2eq} (carbon dioxide equivalent) and incident radiation (LEWIS et al., 2004; PHILLIPS et al., 2009; HASHIMOTO et al., 2010).

Interactions between CO_{2eq} and the water cycle can be very important for tropical forests in a future with high carbon dioxide concentrations. By increasing photosynthesis and/or reducing water usage via reduced stomatal conductance, water use efficiency generally rises in response to CO_{2eq} addition, and that could increase drought tolerance (NORBY; ZAK, 2011; CERNUSAK; WINTER; DALLING, 2013).

In some localities, recent global climate changes may be associated with increases in the length of the season of certain types of pollen (SINGER et al., 2005; ROGERS et al., 2006; ZISKA et al., 2011). The effect on production varies according to several factors, whereby some areas showed increased pollen concentrations, others had a decrease, as observed in European studies after 1992 (FREI; GASSNER, 2008) where grass pollen decreased with a reduction in precipitation (JATO et al., 2009).

Air sampling in a forest clearing near Manaus (Amazonas state) at ground level in 2004 showed consistent high level emissions of both pollen and fungal spores each day and throughout the day/night cycle with clear variations in species abundance in wet and dry weather. Previous published work at forest canopy level at Balbina, Amazonas state, was consistent with these observations (GRAHAM et al., 2003). In pristine tropical rainforest air, fungal spores account for a major fraction of coarse particulate matter (ELBERT et al., 2007).

Around the globe, pollen and fungal spores are continuously monitored, usually in large and dense populated areas, due to its harm effect regarding public health. The daily concentration of the allergen species is a parameter for public policies. In Japan, Italy, USA, France, Spain and Germany are installed the major number of monitoring stations in urban areas (BUTERS et al., 2018). The present project is responsible for the first monitoring station installed in the Amazon area.

3 METHODS

3.1 SAMPLING SITE

The sampling site is a natural forest area located in the Uatumã Sustainable Development Reserve (RDS Uatumã), at the Amazonas state, in Brazil, designated as the ATTO site elsewhere (FIGURE 9). For the present project two towers were used to install the samplers at different heights according to the sampling strategy: the INSTANT tower (walk-up) with 80 m above ground level (S 2° 8.647' W 58° 59.992') and the ATTO tower, 320 m height (S 2° 8.752' W 59° 0.335') illustrated on FIGURE 10.

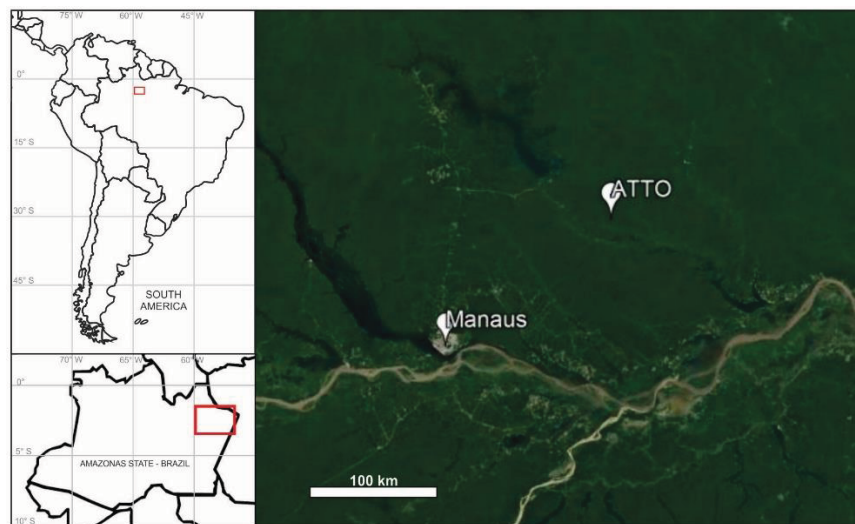


FIGURE 9: Sampling site location: Amazon Tall Tower Observatory (ATTO) almost 200 km northeast of Manaus, the capital of Amazonas state in Brazil.



FIGURE 10: Image of the tall towers at the research site where the sampler(s) were installed: INSTANT tower: 80 m height (left) and ATTO tower: 320 m height (right).

Vertical measurements were made possible through towers that have been developed by national and international research institutes to measure the relationship between climate change, land use and biological, chemical and physical functions (OMETTO et al., 2005). The focus includes meteorological and micrometeorological measurements, trace gases, physical/chemical and optical measurements of particulate matter and vegetation cover profiles, all at different heights (ANDREAE et al., 2015).

Following the same principle of vertical measurement of carbon dioxide fluxes as the ZOTTO observatory tall tower project, installed in Siberia in the last decade (MIKHAILOV et al., 2015; TIMOKHINA et al., 2015), the ATTO project (Amazon Tall Tower Observatory) was designed to monitor fluxes, particles and trace gases in the rainforest region with great potential for fauna and flora still unexplored.

The site location for the ATTO project was defined based on the importance of the tropical rainforest in the climate change global context, the specific circulation pattern, the extent influence in humidity for the continent, the high emission rate of aerosol to the atmosphere and the system of carbon generation and consumption. Thus, it is a remote site in the Amazon Basin, without direct urban influence and far from urban areas.

Since 2012, two 80 m height towers have been operating on the site, which serves as a basis for continuous measurement equipment. In 2015, the main tower with 320 m height was completed. The towers were installed to establish long-term profiles of variables that could elucidate the biosphere-atmosphere interaction and assist in climate predictions. The project was developed to operate continuously for at least 20 years (ANDREAE et al., 2015).

The following variables are continuously measured above the canopy: CO/CO₂ flux, CH₄/CO₂ flux, CO₂ concentration, O₃ concentration, Black Carbon concentration, Aerosol scattering, Aerosol number and size distribution (0.3 to 10 µm), Aerosol mass and chemical speciation, and Visibility. There is also a vertical meteorological profile with data from 4 cm to 80 m above ground level, distributed in seven different heights: air temperature, air relative humidity, short and long wave radiation, ultraviolet radiation, net radiation, air pressure, rainfall, CO₂ flux, sensible/latent heat flux, humidity absorption, wind speed and direction, soil water volume content and soil temperature/heat flux.

The meteorological sensors, installed at the Instant tower, are periodically calibrated and maintained by LBA's Micrometeorology Department, that provides data each minute for all the ongoing researches. Air Temperature and RH were monitored by Rotronic CS215 and Vaisala HMP45C sensors at 0.4, 1.5, 4, 12, 26, 36, 40, 55, 73 and 81 m. Air Pressure is monitored by LICOR LI-7200 and LI7500A sensors. Rainfall measured by TB4 sensor at 81 m. Wind Speed/Direction measured by EC and Gill WindSonic at 19, 26, 42, 50, 65 and 73 m.

3.2 SAMPLING EQUIPMENT

The sampling of biological particles can be performed with passive equipment that collects the particles by sedimentation, or active traps known as Hirst-type volumetric trap, which forces the impaction using a vacuum pump. The last one is the most widely used due to its robustness and reproducibility, allowing data collection and comparison (FRENZ, 1999; FRENZ; JOHANN, 2001; LACEY; WEST, 2006; FERNÁNDEZ-RODRÍGUEZ et al., 2014). From the almost 900 active pollen monitoring stations around the globe, densely installed in North American, European and Japanese territories, 70 % are Hirst-type (BUTERS et al., 2018).

At the ATTO site, the first biological particle collecting station used a Hirst-type volumetric equipment consisting of a Sporewatch spore sampler. This is a Burkard 7-Day Recording Volumetric Spore Sampler (Burkard Scientific Ltd., Uxbridge, UK). The sampler was installed with a metallic arm support allowing the main body to be placed outside the tower and freely rotate according to the wind direction.

The impactor (FIGURE 11), called pollen sampler elsewhere, has a wind vane that always directs the intake orifice into the wind and a rain shield that protects the air inlet from direct rain droplets. The inlet (2 x 14 mm) allows the entrance of particles into the 2 mm slot with inertia from the 10 L min⁻¹ air flow provided by a vacuum pump. The interior design enables the impaction of particles larger than 3.7 µm (diameter) onto a tape fixed around a rotating drum, but smaller particles can remain in the airflow. The drum rotates 2 mm per hour allowing up to seven days of continuous sampling, permitting the time-discriminate analysis according to the set up chosen on the electronic panel.

The tape was prepared for sampling with a translucent adhesive mixture of gelatine, glycerol, phenol and water, developed for this purpose (see recipe in APPENDIX A). The adhesive has the following properties: stickiness, weather resistance, compatible with mountant and clean and transparent structure. It holds the particles on the tape surface, maintains moisture and prevents biological particles from germinating after the sampling.

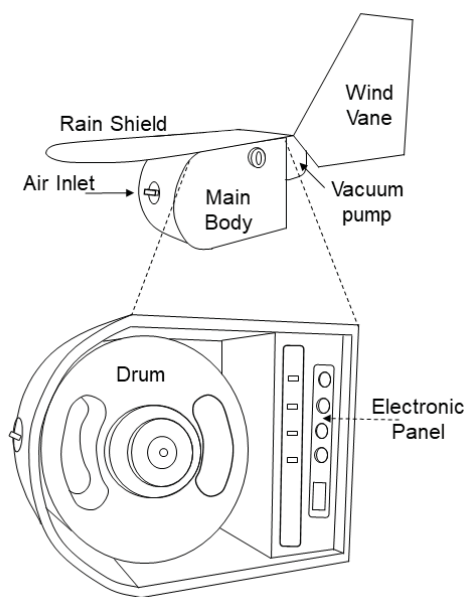


FIGURE 11: The Sporewatch spore sampler: Scheme of the external view describing the parts attached to the main body, with the internal view in detail showing the rotating drum (left), and image of the sampler installed at the tower (right).

After the exposure period, that varied from 3 to 7 days for each tape, the sampled tape was removed and mounted onto microscope slides (26 x 76 mm) using the mountant media consisting of Mowiol, glycerol, phenol and water (see recipe in APPENDIX A). A piece of tape up to 48 mm of length that corresponds to 24 hours of sampling was attached to each slide (FIGURE 12) with a coverslip placed using a glycerol (40%) / water (60%) solution. After the mounting, they were stored for further optical scanning.

The samples followed a pattern of preparation according to the International Association for Aerobiology, so any biological material collected was prevented from growing or reproducing (IAA, 2015). Therefore, no special authorization for collection or transportation applied. All the sampled material was stored in slide boxes under room conditions for further optical microscopic analysis.

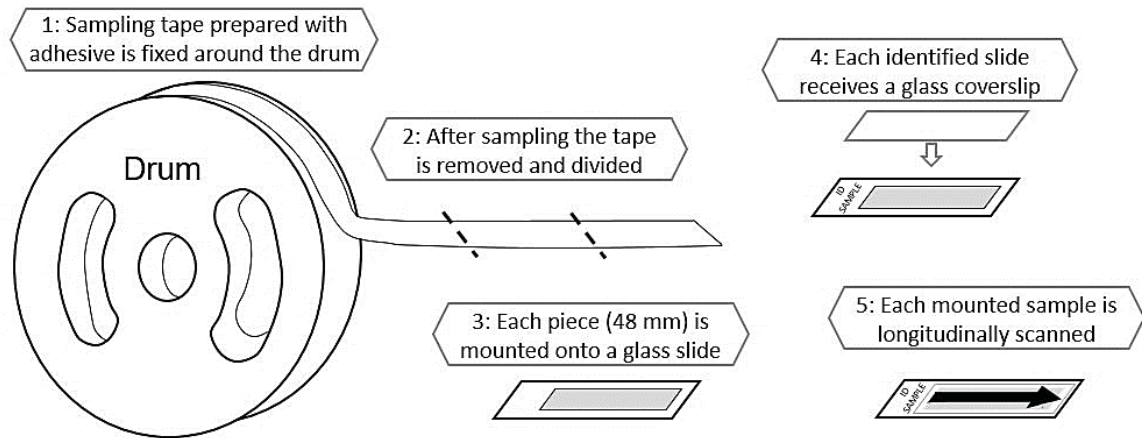


FIGURE 12: Scheme of the steps followed during sampling: (1) tape preparation with adhesive for sampling, (2) after sampling the tape was divided, (3) mounted onto glass slides (4) with a coverslip, (5) and then stored for longitudinal optical scanning.

3.3 SAMPLING PERIODS

The towers INSTANT (80 m height) and ATTO (320 m height) installed in the Amazon forest, municipality of São Sebastião do Uatumã, 130 m above sea level and located approximately 200 km northeast of Manaus (TOLLEFSON, 2010; ANDREAE et al., 2015), were used for sampling following the chronogram presented in TABLE 1. The primary goal was to use different heights along the sampling period, and those were chosen based on the spot availability and access allowance at the towers.

TABLE 1: Description of sampling periods with pollen trap, according to the height, with total sampled hours. Periods of simultaneous sampling at different heights are specified.

HEIGHT	PERIOD	TOTAL SAMPLING	COMMENTS
25 m	08 OCT to 12 OCT 2017	96 h	
40 m	15 SEP to 07 OCT 2016 29 NOV to 16 DEC 2016	904 h	Simultaneous with 80 m Simultaneous with 300 m
60 m	16 SEP to 20 NOV 2015	1328 h	
80 m	09 to 24 JAN 2015 28 MAR to 25 APR 2015 15 SEP to 07 OCT 2016	1546 h	Simultaneous with 40 m
300 m	29 NOV to 16 DEC 2016 12 MAR to 25 APR 2017	1250 h	Simultaneous with 40 m

The first sampling was performed in January 2015, after an initial field test of the system structure: sampler, tape, adhesive, time of exposure, storage and laboratory preparation. One Sporewatch sampler was installed at 80 m height on the INSTANT tower, during 09th and 24th January. Another sampling was performed from

28th March to 25th April 2015, also at 80 m height. After new tests with the adhesive substance, the third sampling was executed from September to November 2015, at 60 m height at the INSTANT tower.

The fourth sampling took place for 20 days, with two samplers installed at the INSTANT tower: 40 m and 80 m height. During the same period, particulate matter was also sampled into different size stages using a PIXE impactor only at 80 m height, from 17th September to 07th October 2016.

Another simultaneous sampling took place in November/ December 2016 at 40 m (INSTANT tower) and 300 m (ATTO tower) over 3 weeks. The tapes were exposed from 3 to 7 days and during rainy days the drums were replaced more often. The same occurred only at 300 m, over 7 weeks during March and April 2017. So, from 2015 to the middle of 2017 all the samplings took place above the forest canopy. With this lack of data below the canopy, another sampling was executed during October 2017, only for a week at 25 m height.

The samplings performed so far were not designed for the pollen seasonality, the seasons for this project concern only for the dry and wet periods at the region. The CHART 1 illustrates the periods described in TABLE 1 with most samples collected on March, April, September, October and November among the sampled years.

CHART 1: Monthly distribution of the sampling periods by height, regardless the year of the sampling. Months with sampling for each height are marked in green.

	Jan	Feb	Mar	Apr	May	Jun	Jul	Aug	Sep	Oct	Nov	Dec
300												
80												
60												
40												
25												

Due to the unique characteristics of the field, and as it was the first time a sampling like this was performed in that region, some adjustments in the adhesive substance were necessary along the entire project period due to the influence of high temperature and humidity on the sampling substrate surface. Laboratory tests (simulating the field conditions) to optimize the adhesive substance, were carried out

during the 3 years of sampling in order to respond to the challenges faced along the way (details can be found in APPENDIX A).

3.4 MICROSCOPY ANALYSIS

During the last half-century, optical microscopy has been used to identify biological particles based on morphology (LACEY; WEST, 2006). New techniques for identifying species are starting to become available nowadays, but there are some considerations regarding their use: particle concentrations may not be enough to be detected and quantified, sample preparation can degrade the particles, and the range of biological particles present in an environmental sample can interfere with the identification method (HOSPODSKY et al., 2010; CROUZY et al., 2016; LEONTIDOU et al., 2017).

The optical microscope allows the visual observation of mounted specimens, usually in the micrometer scale. Using a lens system to produce a virtual image, the eyepiece and objectives can achieve up to 3000x of magnification. The equipment includes a tungsten halogen lamp as a source to transmit the light through the condenser, the observed specimen, and the lens, what classifies the ensemble as brightfield optical microscope.

Therefore, tapes from the Pollen trap were analysed by optical microscopy using an Olympus BX50 light microscope installed in the NeuroAllergy Laboratory (Deakin University – Australia). The brightfield optics equipment has Olympus UPlanApo lens (40x) allowing a 400x image magnification. A Canon EOS 1100D camera coupled to the microscope by a phototube was used to capture the images.

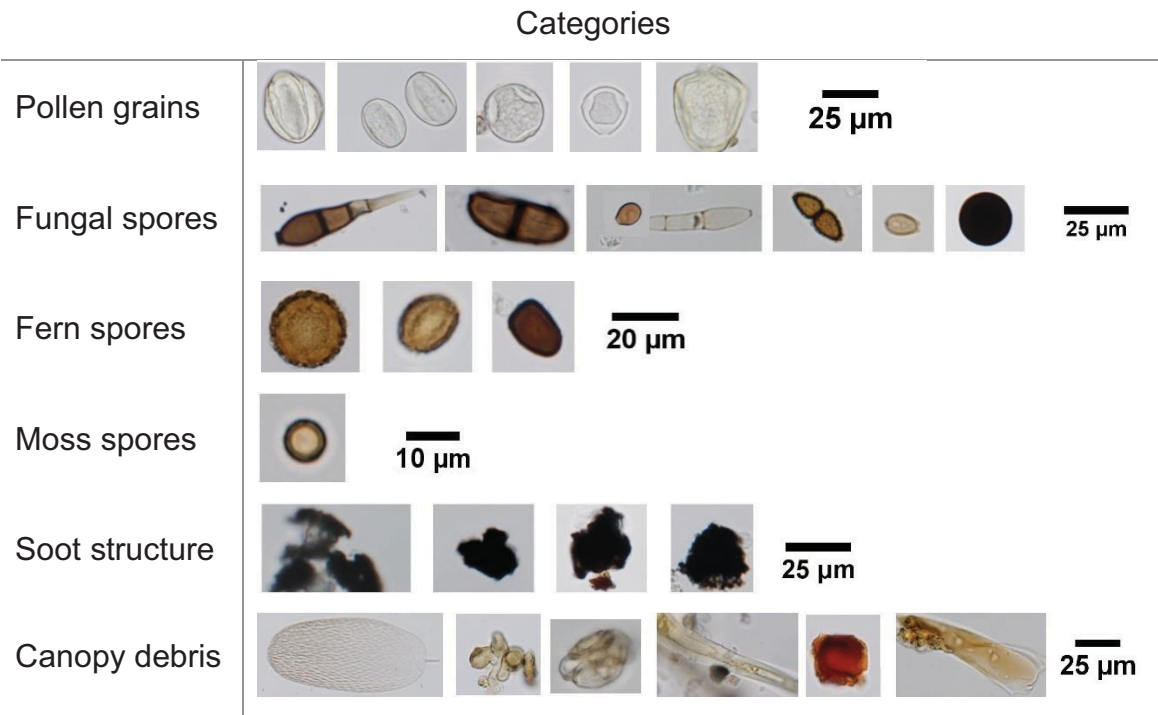
The set up for the microscope followed the Koehler alignment (MORTIMER, 2004). The halogen's lamp voltage was set in 9 V and no neutral density filters were used. The condenser aperture was set at 85% of the lens description. The microscope was dedicated to the samples analysis so there was no change in the set up during analysis.

All mounted slides were prepared with a temporary coverslip (25 x 50 mm) using a mixture 40 % glycerol and 60 % water (FIGURE 12). After placing the coverslip, the slide was linear scanned and photographed through its longitudinal dimension. Particles were morphologically identified in 200 fields of view for each sample and with the assistance of a certified pollen and spore counter with the US National Allergy

Bureau, following the guidelines from the International Association for Aerobiology (ELBERT et al., 2007; IAA, 2015). Identification and counting were performed manually, for each particle, and by an open source software: Image J (NIH - USA, version 1.51j8).

The bioaerosols found in the samples were separated into the following categories (CHART 2): pollen grains, fungal spores, fern spores, moss spores, soot (black amorphous structures), unknown particles (bioaerosols that could not be related with one of the previous categories) and canopy debris including all sorts of leaf/wood pieces, plant waxes, leaf glands, leaf trichomes, insect fragments, hyphae parts, mineral grains and amorphous particles.

CHART 2: Examples of bioaerosols categorized for this project: pollen, fungal, fern, moss, soot and debris. The particles were redimensioned and the scale for each category is shown.



After identification, particles were counted and the Feret's diameter¹ was measured using Image J software (FERREIRA; RASBAND, 2012) through the pictures using 400x magnification. Overlapping particles were counted as one and categorized based on the top particle, the only one that could be completely visualized for identification, i.e., hidden particles were not counted. The concentration was

¹ The longest distance between any two points along the selection boundary (FERREIRA; RASBAND, 2012).

determined for all the different types of particles through raw counts, averaged over one-hour sampling period and expressed per cubic meter of air.

3.5 SAMPLE VALIDATION AND DATA TREATMENT

All the sampled tapes were visually inspected after sampling to ensure the quality of the data. The samples were considered valid regarding the adhesive surface if there were no visual damage, wrinkles, or breaks. The amount of valid samples considered for the present project, according to the height above ground level, is described in TABLE 2. Periods with alterations on the sampling substrate surface were considered invalid, likewise periods with technical problems regarding the sampler and/or transport conditions.

TABLE 2: Total and valid sampled hours according to the height.

HEIGHT	TOTAL SAMPLING	VALID SAMPLES
25 m	96 h	1 h (1%)
40 m	904 h	228 h (25%)
60 m	1328 h	1320 h (99%)
80 m	1546 h	1392 h (90%)
300 m	1250 h	1214 h (97%)

The sampling at 300, 80 and 60 m was executed with minimal failures and the sampling conditions allowed high-quality tapes for analysis. The sampling at 40 m height was interrupted several times due to technical issues. Only 25% of the samples were considered for the valid results, as the rest of the data might not be reliable.

The sampling at 25 m, the last one executed, presented minimal technical failures but the high temperature and high humidity on the site caused damage to the tape surface, a mix of melting, wrinkles, and breaks, hindering and/or preventing the visualization and identification of the particles in 99% of the samples. Thus, all the samples from this height were excluded from the results, as showed in CHART 3.

Every sampling and analysis process was susceptible to random and systematic errors related to equipment functioning and human operation. As this is a singular project regarding particles counting, the accuracy and precision of the data

were equally important. Therefore, the error of the valid data presented on the following section was calculated considering:

- sampler efficiency regarding the wind speed range during sampling,
- sampler efficiency considering the size range of the collected particles,
- flow deviation of the sampler during all the sampling periods,
- deviation between the manual particle's identification by:
 - the author and
 - the certified pollen/spore counter (co supervisor on this project),
- particles counting deviation among the counts executed by:
 - the ImageJ software,
 - the author and
 - the certified pollen/spore counter,
- conversion factor from raw counts to concentration in the air.

For those items, the expanded uncertainty at the 95% level of confidence (BIPM, 2008) is 18.5% for the sampled tapes. So, this uncertainty must be considered for each value presented in the Results section.

CHART 3: Monthly sampling calendar with the periods marked in green: valid samples and results, or red: invalid samples, results not used.

2015											
JAN 80 m	FEB	MAR 80 m	APR 80 m	MAY	JUN	JUL	AUG	SEP 60 m	OCT 60 m	NOV	DEC
2016											
JAN	FEB	MAR	APR	MAY	JUN	JUL	AUG	SEP 40 / 80 m	OCT 40 / 80 m	NOV 40 / 300 m	DEC 40 / 300 m
2017											
JAN	FEB	MAR 300 m	APR 300 m	MAY	JUN	JUL	AUG	SEP	OCT 25 m	NOV	DEC

The meteorological data set received had a 1 min resolution, up to 80 m, and were pooled to obtain hourly resolution (the same of the biological data). The Pearson's correlation among maximum, minimum, average, median and mode values defined the variables for temperature, wind speed, and humidity. No meteorological data was available for 300 m.

The complete data set for the biological data has the concentration values from the results and also zeros recording the absence of that particle during the period,

then, the distribution function is Poisson-like. As the data set failed the tests for normal distribution, shown in FIGURE 13, where the sample quantiles should follow the pattern of the theoretical quantiles for a normal distribution using the same parameters; and no normalization procedure such as logarithm, square root or cubic square root was successful, the results were statistically processed with non-parametric tests using the R software (The R Project - Austria, version 3.3.3).

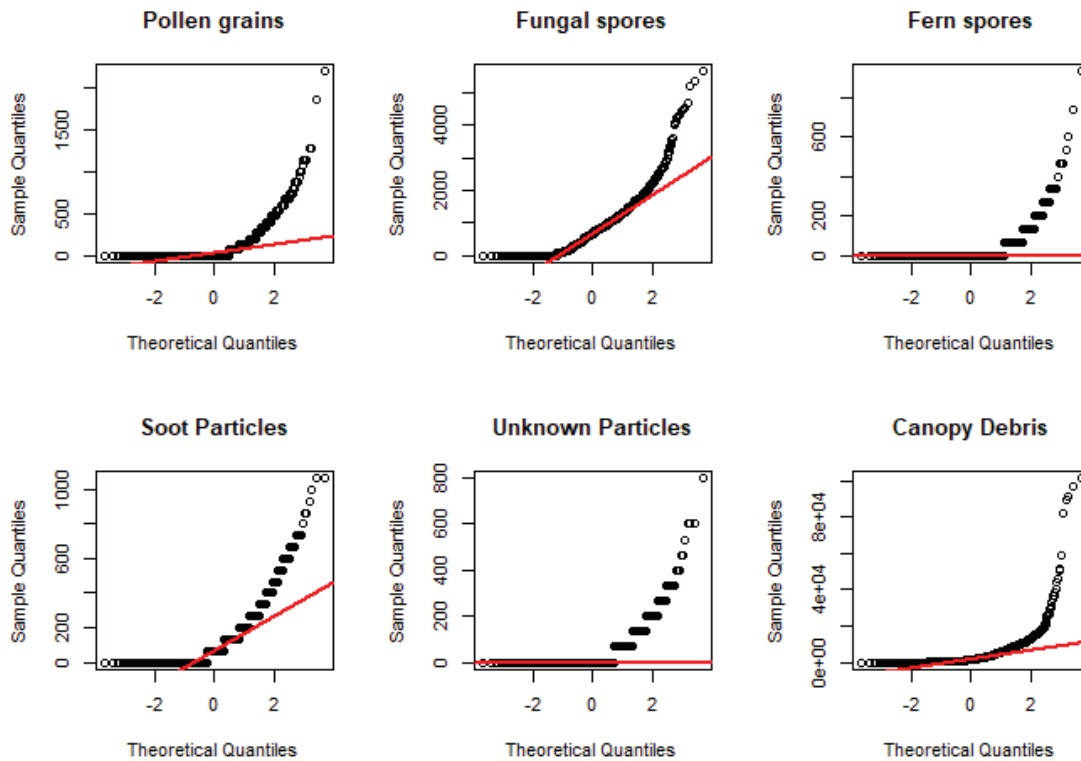


FIGURE 13: Normal Q-Q plot for each category with the respective distribution in dots (vertical axis) and the Normal Quantiles line marked in red (horizontal axis).

The next section will describe both results: the complete data set with the absence data and only the concentrations for each measured category, without the zeros. All the concentration results (number of particles per cubic meter of air) were hourly averaged.

4 RESULTS AND DISCUSSION

4.1 MORPHOLOGY AND VERTICAL DISTRIBUTION OF BIOLOGICAL PARTICLES

Optical identification of bioaerosols was performed using the morphological characters, such as format (general shape), colour, structure (cell wall and content), size and surface texture, as referenced in the literature (KAPP, 1975; BFA, 1995; FRENZ, 1999; FRENZ; JOHANN, 2001; KAGEN; LEWIS; LEVETIN, 2005; LACEY; WEST, 2006).

Pollen grains are hyaline structures, generally with a thick wall and granular content. The fungal spores observed were comprised of two major classes: ascospores and basidiospores. The ferns collected were less morphologically diverse, having a circular to semi-circular shape and brown colour. Soot was identified as amorphous shaped, black structures. Debris believed to be sourced from the canopy appeared as a wide range of leaf and insect fragments, wax-like particles and hyphae, as pictured in FIGURE 14.

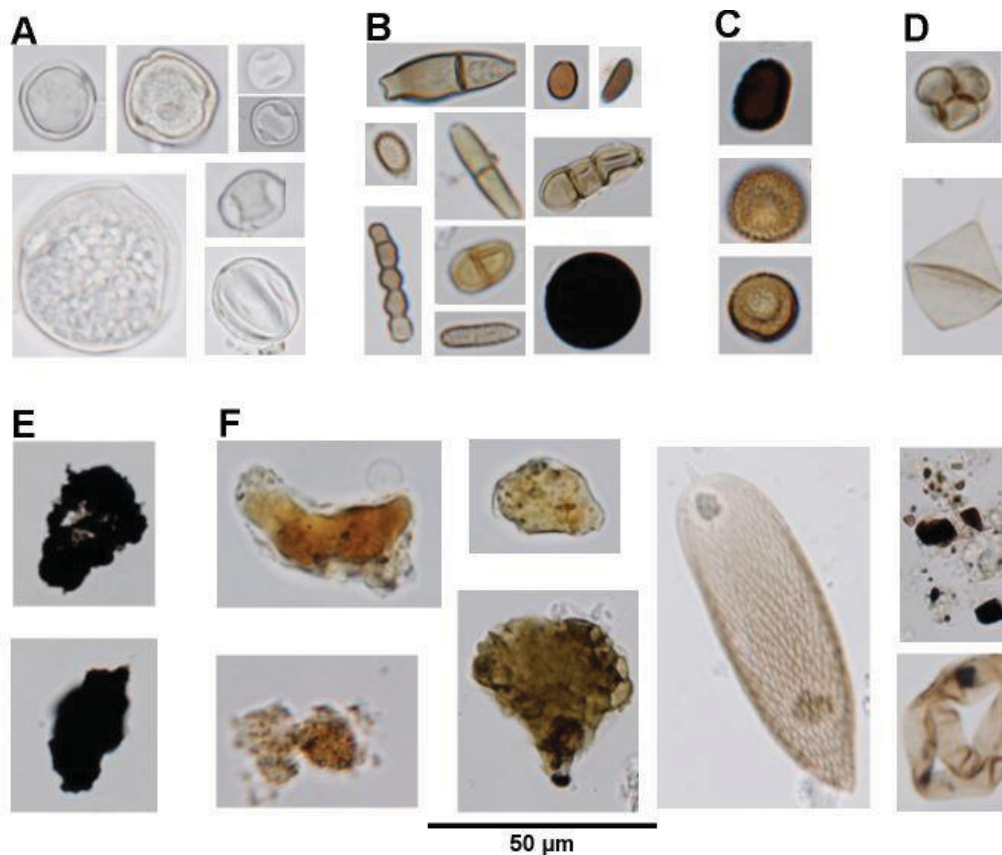


FIGURE 14: Pictures of biological particles sampled showing the morphology of the selected categories: (A) Pollen grains, (B) Fungal spores, (C) Fern spores, (D) Unknown particles, (E) Soot particles and (F) Canopy debris. Scale: 50 µm.

All the valid samples were scanned and the total of 491,745 were counted, thereby distributed: 67,236 particles counted and identified for the 40 m height, 236,898 particles for 60 m height, 61,598 for 80 m and 126,013 for 300 m height. No representative value for moss spores were found among the samples, so the particles were classified in: pollen, fungi (fungal spores), fern, soot, debris and unknown, as illustrated in the FIGURE 14.

The concentration for each category, FIGURE 15, regardless the sampled height, presents the general pattern for counted samples, high frequency for lower concentrations and the opposite for high concentrations. These results show similar distribution ratio of bioaerosols across all heights, whereas canopy debris is dominant. Canopy debris, or just debris, is the category with the wider range, and represents approximately 70% of all sampled particles in each height (see APPENDIX B). Fern spores represent less than 1% and is the group with lower variety of particles. Among the biological particles, fungal spores are the group with higher variety and number of particles (only individual particles were considered, hyphae parts, for example were categorized as debris), followed by pollen grains and fern spores (see APPENDIX C).

Pollen represents only a small fraction of all the airborne particles, similar to fern spores. Among the biological particles that were identified, fungal spores are the dominant group. Particles that could not be classified into the groups above, the unknown category, are less than 1% of the total for all the measured heights.

Particles varied in size, mostly from 5 to 100 μm in diameter. Soot and canopy debris categories had 5% of their particles larger than 100 μm in diameter. The total size distribution, up to 100 μm , can be viewed in FIGURE 16. Across all four sampling heights, the highest abundance occurs in the size range of 3 to 20 μm , integrating all the categories. Once canopy debris correspond to the major fraction at each height, this is the size range where dust particles peaked. The elemental composition for total PM was investigated to elucidate this category, details presented in APPENDIX B.

A decrease in particle size with increased height occurred along each level, with a difference in the number of particles. The 60 m height presented the higher values for all the categories, in absolute number and concentration, followed by 300, 40 and 80 m. This can also be a result of the sampling period length and season.

So, a decreasing pattern dominates all the data set regarding each category, as well, each height, as shown in FIGURE 15 and FIGURE 16 for both seasons integrated.

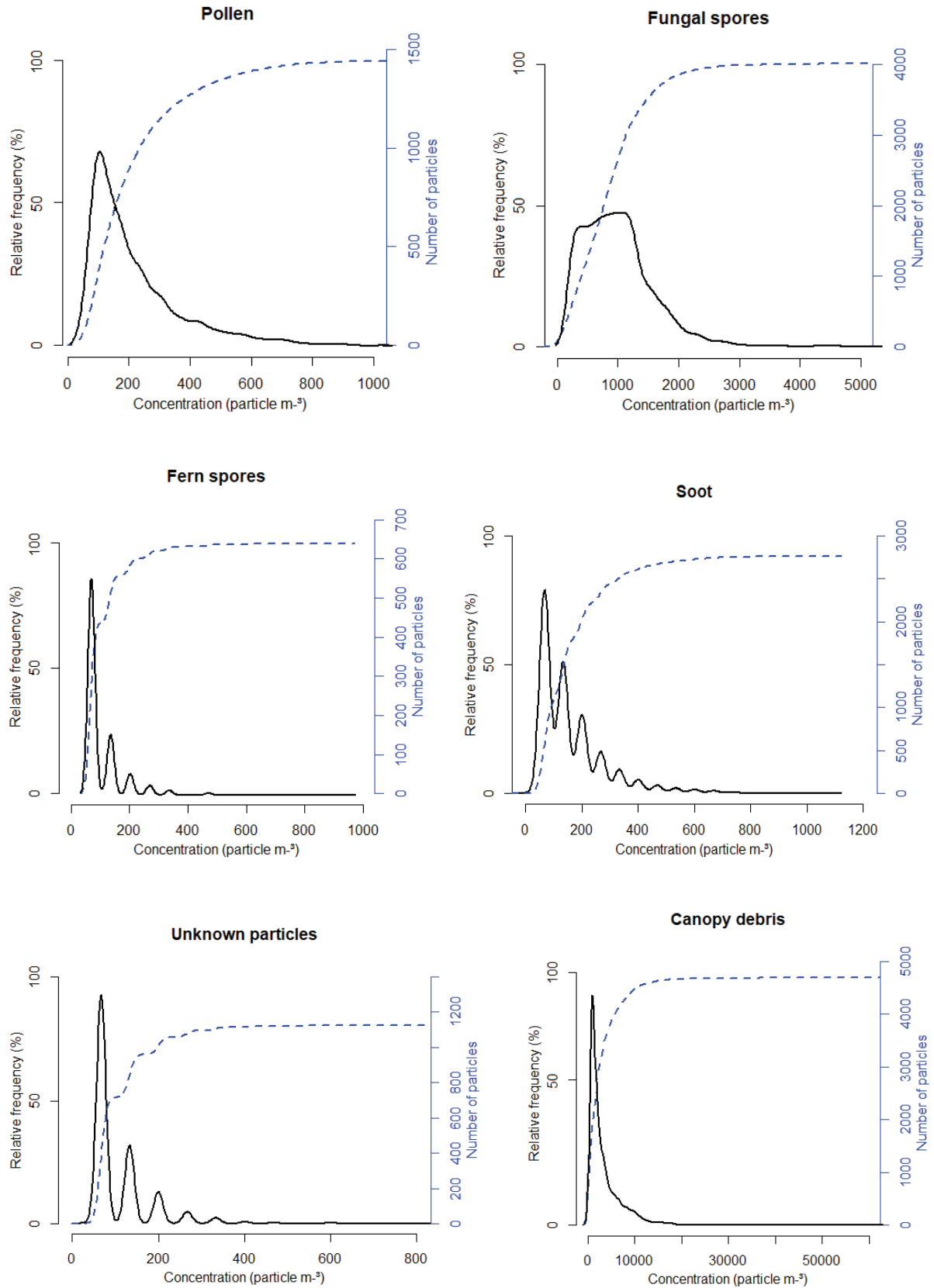


FIGURE 15: Density distribution (black line) and accumulated distribution (dotted blue line) for each category with all sampled heights integrated. All the horizontal axis are in concentration unit (particles m⁻³): Pollen (top left), Fungal spores (top right), Fern spores (center left), Soot (center right), Unknown particles (bottom left) and Debris canopy (bottom right).

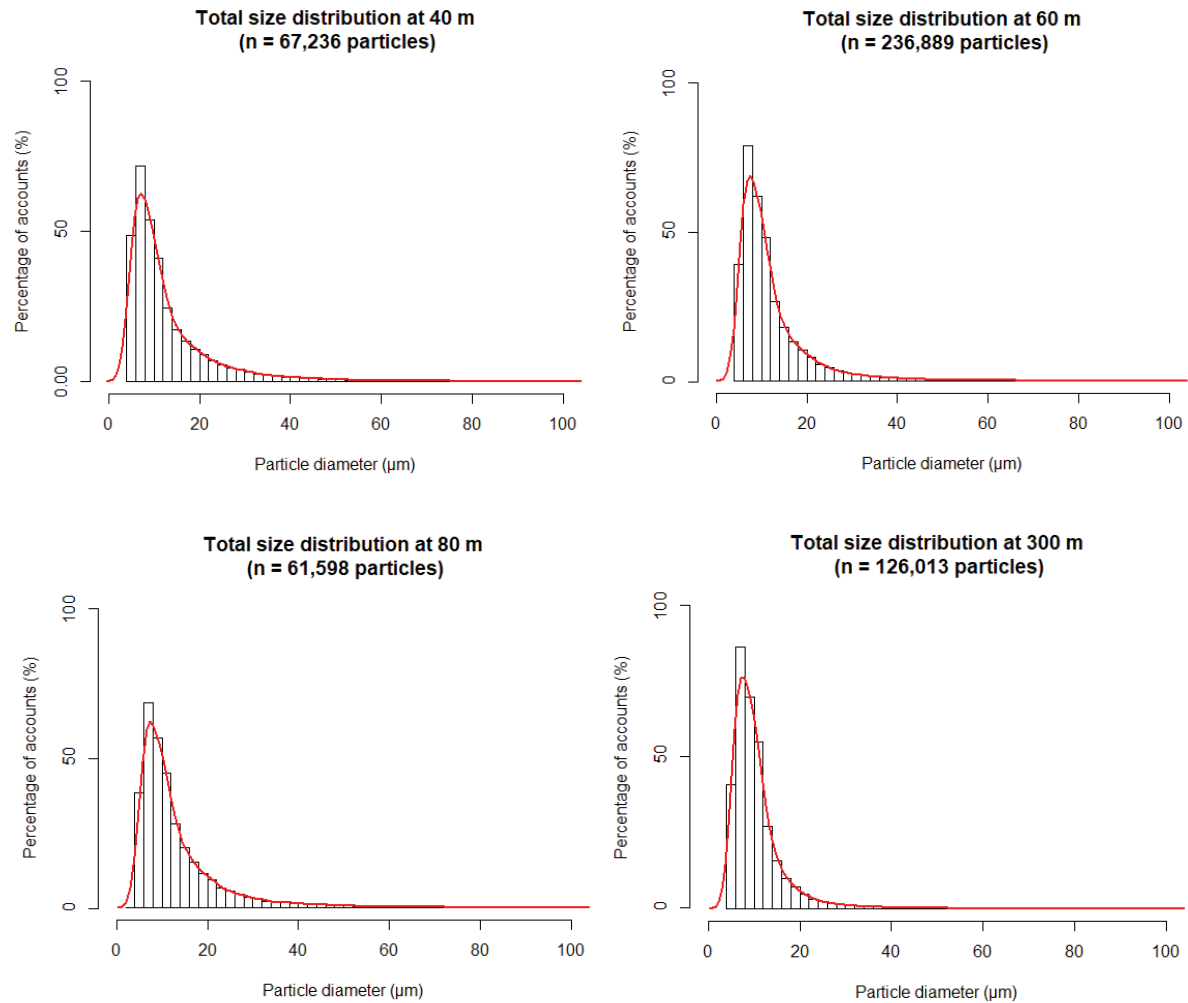


FIGURE 16: Relative histogram (black lines) and log-normal distribution (red line) for the size (from 3 to 100 μm) of all particles sampled, integrating all the categories and seasons at each sampled height: 40 m (top left), 60 m (top right), 80 m (bottom left) and 300 m (bottom right).

Across the various heights, many different types of pollen were identified, in sizes varying from 10 to 95 μm (details in APPENDIX C.1). In all measurements a deviation of $\pm 2.5 \mu\text{m}$ for the particle diameter was considered. The most common sizes were 10 to 20 μm for all the heights, showed on the left in FIGURE 17. Only two grains with 95 μm were collected, a unique event, one at 60 m and another at 80 m during a storm event. Even with the sampling height variation, the 10 μm size peaked in all the measured levels, illustrated in FIGURE 18.

The 40 m was the only height with no pollen larger than 50 μm diameter. The frequency of observations follows the sequence: 60 m had the higher frequency with 3,520 grains collected, followed by 300 m with 294 pollen grains, 80 m with 202 and 40 m with 130 units. At 40 m, around 5 to 15 m above the canopy, there were less valid samples available, so, the total sampling period might influence comparisons between

counts. The 60 m height is the only one with frequency in a different magnitude scale, see FIGURE 18.

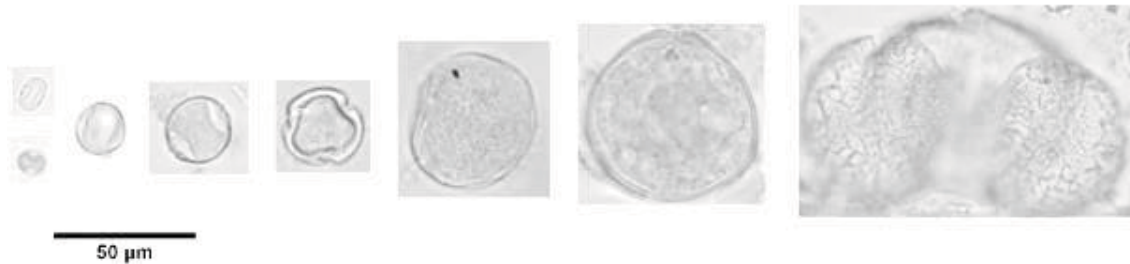


FIGURE 17: Examples of the size difference for pollen grains collected across all heights. The scale bar is marked.

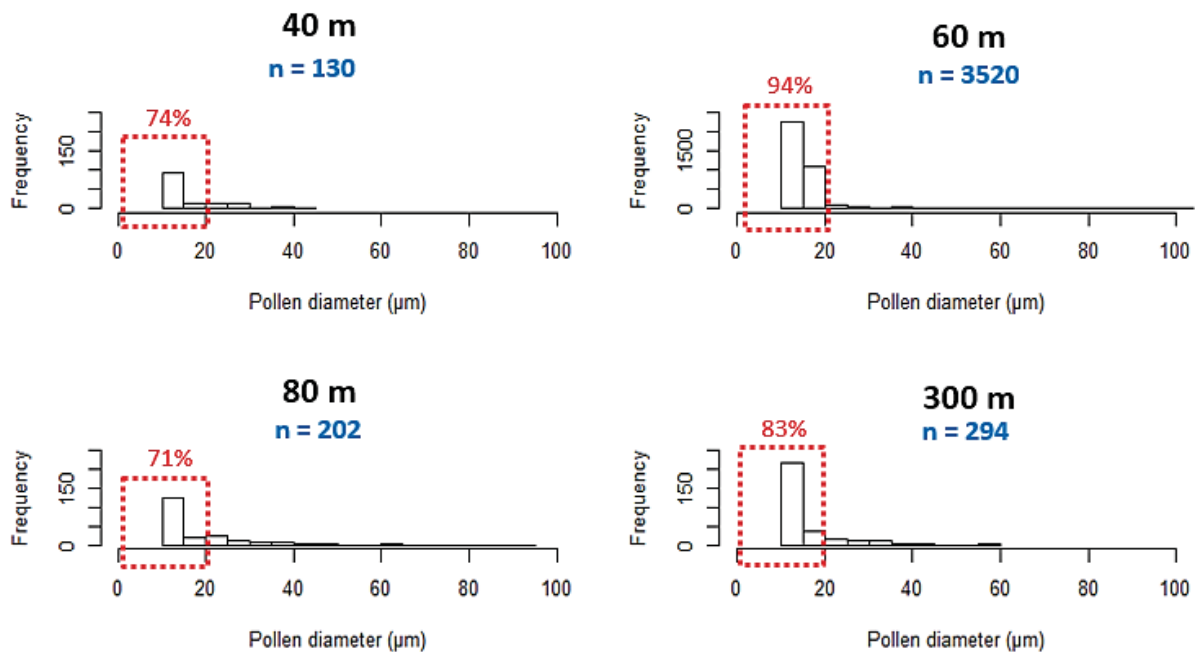


FIGURE 18: Histogram of absolute frequency for size distribution of pollen grains at each sampled height, with both seasons integrated for 40 and 80 m: 40 m (top left), 60 m (top right), 80 m (bottom left) and 300 m (bottom right). The total number of pollen sampled is detailed in blue and the percentage up to 20 μm is marked in red.

At 40 m height, 130 pollen grains were observed with diameters ranging between 10 and 45 μm, and with 48 % of the pollen having a 10 μm diameter. At 60 m, 3,519 pollen grains up to 60 μm were observed with 39 % having 10 μm diameter, 24 % with 15 μm and 31 % with 20 μm. Just one particle with 95 μm was collected. At 80 m, a distribution similar to 60 m was observed: 201 pollen grains up to 65 μm in a frequency inversely proportional to size (45 % with 10 μm, 17 % with 15 μm, 9 % with 20 μm) and just one grain with 95 μm. Grains up to 50 μm were evenly collected at

300 m, and just one with 60 μm . The diameter of 10 and 15 μm respond to 70 % of the collected grains at that height.

The fungal spore category, the larger biological fraction collected, has 95 % of the particles up to 15 μm . This kingdom can be separated into different divisions or phyla, and the most frequent found were: Ascomycota and Basidiomycota, according to FIGURE 19.

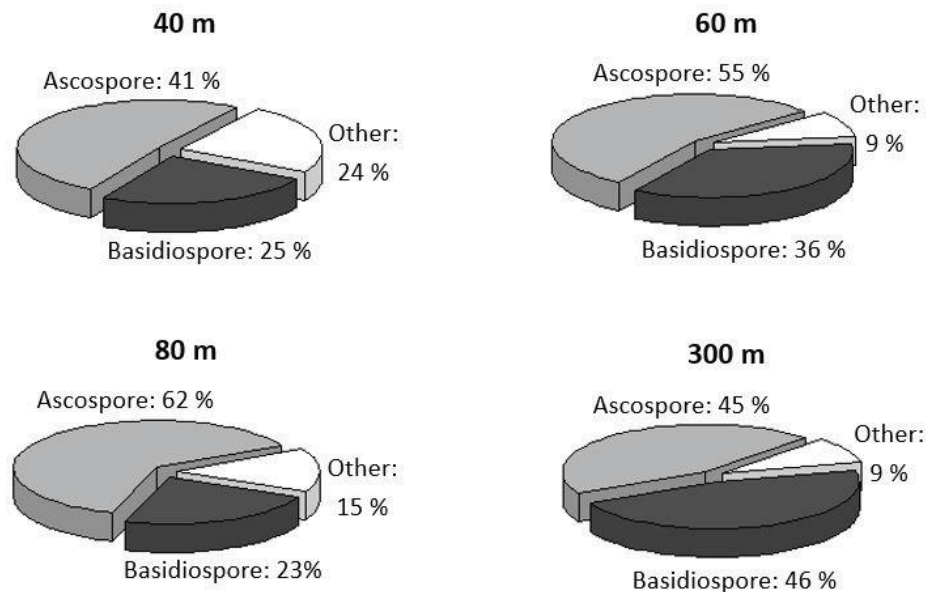


FIGURE 19: Fungal spores major division at each height, with integrated seasons: 40 m (top left), 60 m (top right), 80 m (bottom left) and 300 m (bottom right).

The Ascomycota and Basidiomycota phyla respond to more than 70 % of the particles collected at the four heights. The pattern is the same for the heights: Ascospores had the higher frequency, followed by Basidiospores and Other phyla. The pictures, regarding each phylum, of all the sampled fungal spores can be found in APPENDIX C.2.

4.2 METEOROLOGICAL PATTERN AND SEASONAL DISTRIBUTION

For the Amazon Basin, seasonality is well delimited according to precipitation amounts and convection activity. The characteristic period of the year varying from rainy/wet season to dry season (low precipitation) is an important issue due to the washout that removes particles from the atmosphere. The average precipitation for a 30-year historical series (INMET) reveals monthly values higher than 200 mm for January, February, March, April, May and December, and below 200 mm from June to November, a drier period. So, according to the rainfall, the months can be classified as wet, dry or transition period (dry-to-wet or wet-to-dry).

All the meteorological data presented were provided by LBA's Micrometeorology Department. The sensors are installed at the same tower used for sampling, at different heights from 4 cm up to 80 m above ground level, and the sensor selected was the closest to the sampling spot. For the present analysis, the precipitation during the sampled period was evaluated and the seasonality defined according to the monthly precipitation trend line. The rain levels reached the minimum value in August and the peak in March for the three years (FIGURE 20).

An accentuated dry season took place in 2015, from July to December, as a result of an El Niño system, and that was the main difference among the sampling periods. Whilst for 2016 and 2017 November can be considered as a transition period between the dry and wet, whereas December is already a rainy month. Low precipitation amount persisted from July 2015 to January 2016. Therefore, for 2015, the rainy season was defined from January to May and the dry season from July to December. In the period covering 2016 to April 2017 the dry season ranged from June to October, and December was already a wet period.

The most obvious differences among the sampled years are the precipitation events. The relative humidity can reach 100% in every month, and the lower values, around 40%, are associated with drier months at the dry season (FIGURE 20). For a rainforest, the relative humidity is expected to remain high across the year, with some reductions observed during the dry season, consistent with the observed median values for the sampling period of around 80 %. Monthly values for temperature and wind speed are illustrated in FIGURE 21.

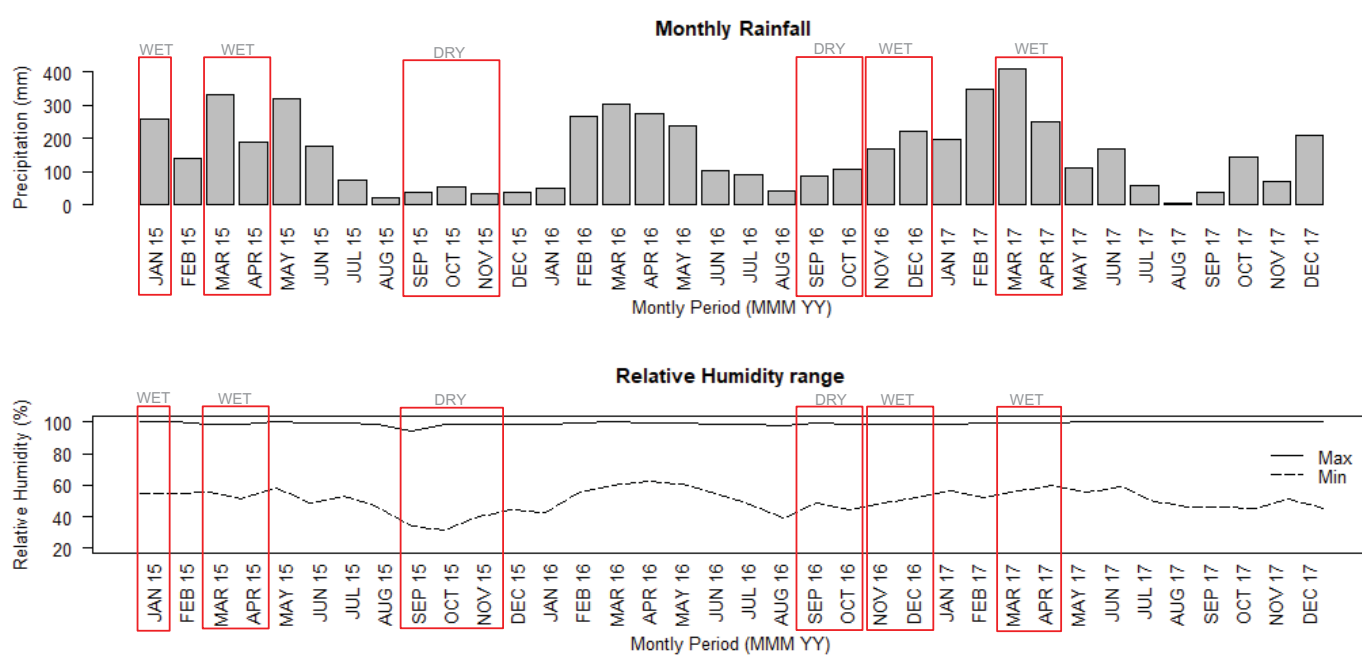


FIGURE 20: Accumulated monthly Precipitation (top) for the site and monthly Relative humidity range (bottom): minimum and maximum values measured at 80 m height, from 2015 to 2017. All the sampling periods with valid results are highlighted in red with the considered season specified.

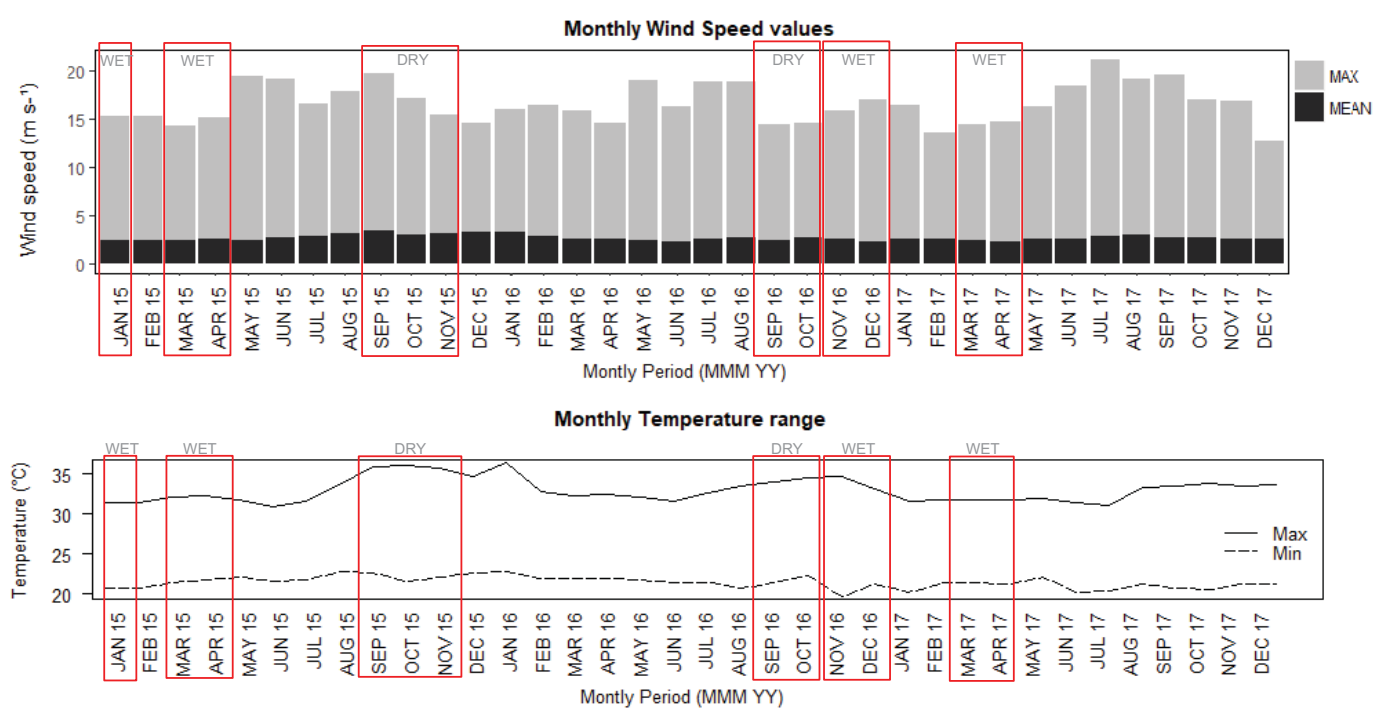


FIGURE 21: Mean and maximum monthly Wind Speed values (top) and monthly Temperature range with minimum and maximum values (bottom), from 2015 to 2017. Sampling periods with valid results highlighted in red. All the values correspond to the height of 80 m.

Temperatures ranged from 20.7 to 36.1 °C for 2015, 19.8 to 36.4 °C for 2016, and 20.2 to 33.6 °C for 2017. Higher values are observed at the end of 2015 and the beginning of 2016, consistent with the lack of precipitation. Mean wind speeds values, shown in FIGURE 21, were almost constant across the years, around 3 m s⁻¹, with frequent gusts above 11 m s⁻¹, but reaching 20 m s⁻¹ on occasions.

Gusts higher than 5 m s⁻¹ occurred on 86 % of the sampled days, and more than 40 events per day on average. The recorded wind speed for each sampled height can exceed 16 m s⁻¹, but gusts higher than 10 m s⁻¹ represent 0.5 % of the events.

Regarding the seasonality, specific meteorological conditions drive pollen emission: lack of precipitation, low relative humidity, temperatures above 21 °C, and high wind speed. Absence of precipitation is necessary for pollen emission, i. e. to exit the anther, so a higher amount of pollen in the 2015 dry season is coherent with that scenario. During the dry season, three heights were sampled: 40, 60 and 80 m, and the concentration for each category is shown in FIGURE 22.

As also illustrated in FIGURE 15, fungal spores reached the highest values among the biological data, not considering the canopy debris. Pollen abundance was greatest at 60 m during the extreme dry season of 2015. The higher values for 60 m might be due the low precipitation amount, and less washout effect. The dry season is less likely to immediately influence overall pollen production, but more likely to influence day to day pollen emission. This is consistent with the data collected from the air samples.

For the fungal spores during the dry season, there was little diversity of abundance across the different heights. Fern spores showed a pattern similar to pollen grains, with higher concentrations for 60 m. Unlike most pollen, fern spores are actively released from the fern plant with a drop in relative humidity, and thus the absence of precipitation is necessary for their emission in the atmosphere.

Large black soot structures decreased in abundance with increased height, which suggests a ground source. For the 2015 dry season, concentrations were highest, likely from the entrainment of brown carbon particles from biomass burning sites distant from the study area. Particles classified as unknown also had a similar pattern of abundance across the sampled heights.

During the wet season, the sampled heights were 40, 80 and 300 m, as pictured in FIGURE 23. As occurred during the dry season, the fungal spores have the highest abundance. Pollen grains peaked at 133 particles per cubic meter of air near

the canopy at 40 m and presented higher variability at 80 m related with storms occurrence.

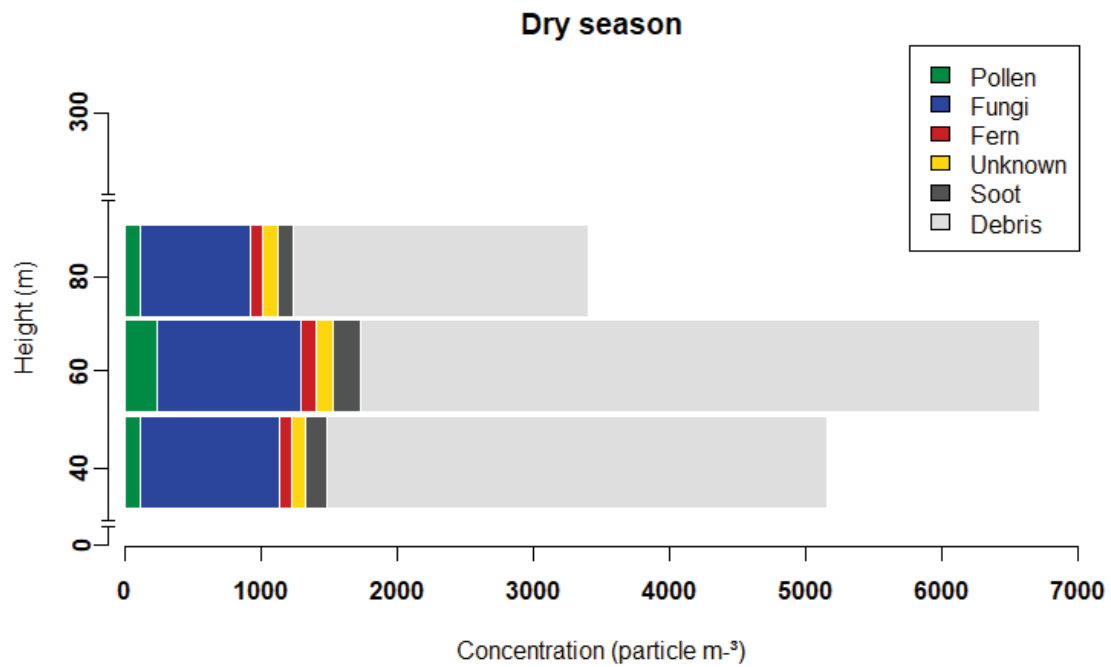


FIGURE 22: Bar plot of particles concentration by category: pollen, fungal spores, fern spores, unknown particles, soot and canopy debris, sampled during dry season periods from 2015 to 2017 at 40, 60 and 80 m (vertical axis out of scale).

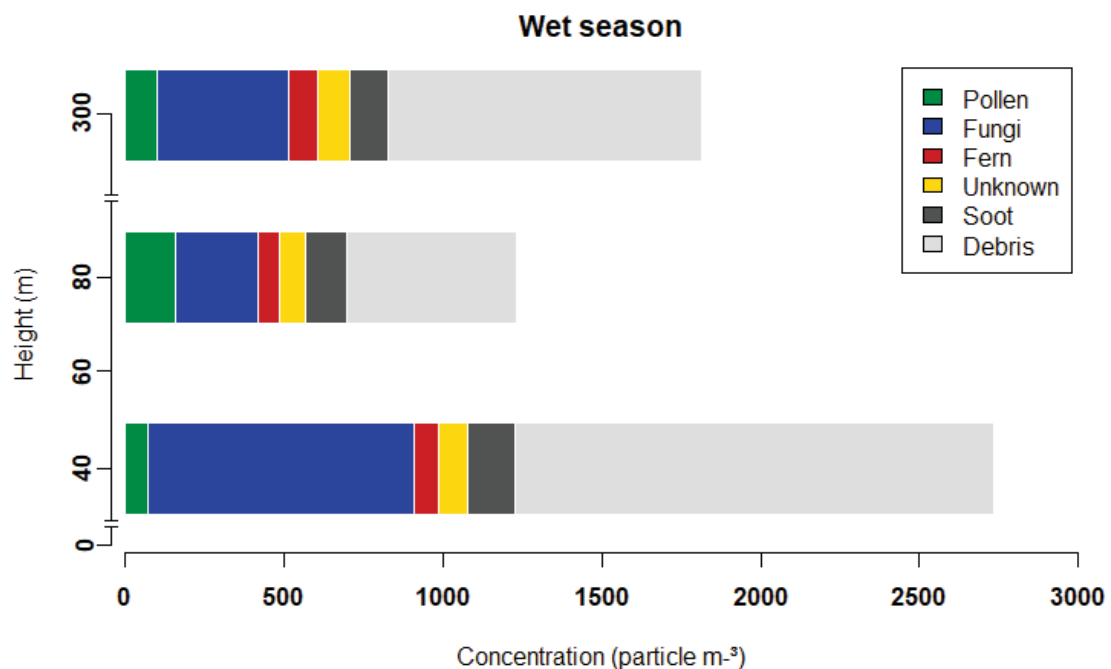


FIGURE 23: Bar plot of particles concentration by category: pollen, fungal spores, fern spores, unknown particles, soot and canopy debris, sampled during wet season periods at 40, 80 and 300 m, from 2015 to 2017 (vertical axis out of scale).

The heights of 40 and 80 m were the ones simultaneous sampled during the dry and wet seasons, and the season comparison by height is illustrated in FIGURE 24 and FIGURE 25, respectively.

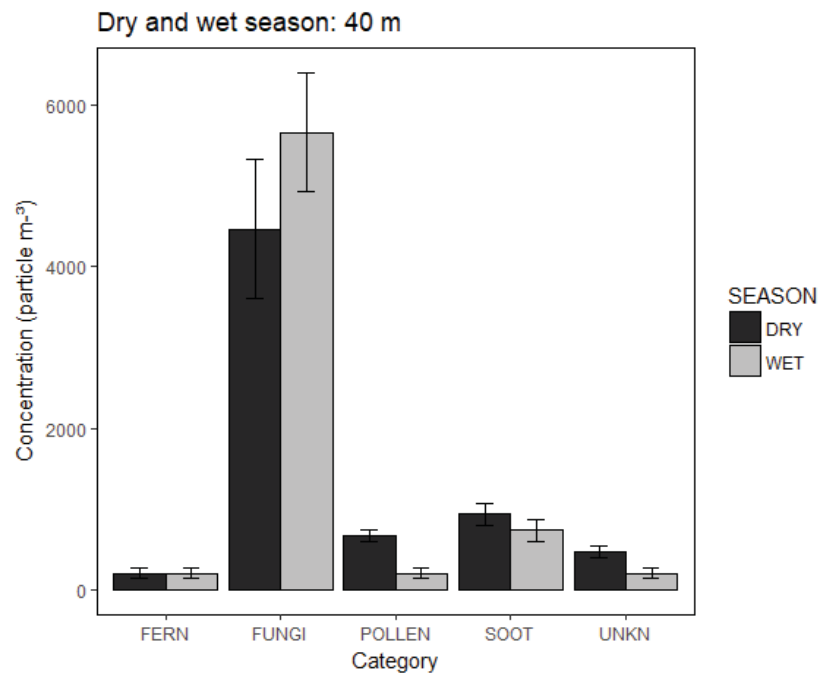


FIGURE 24: Seasonal median concentration of fern, fungal spores, pollen, soot and unknown particles for 40 m height. Interquartile ranges are represented on the top of each columns.

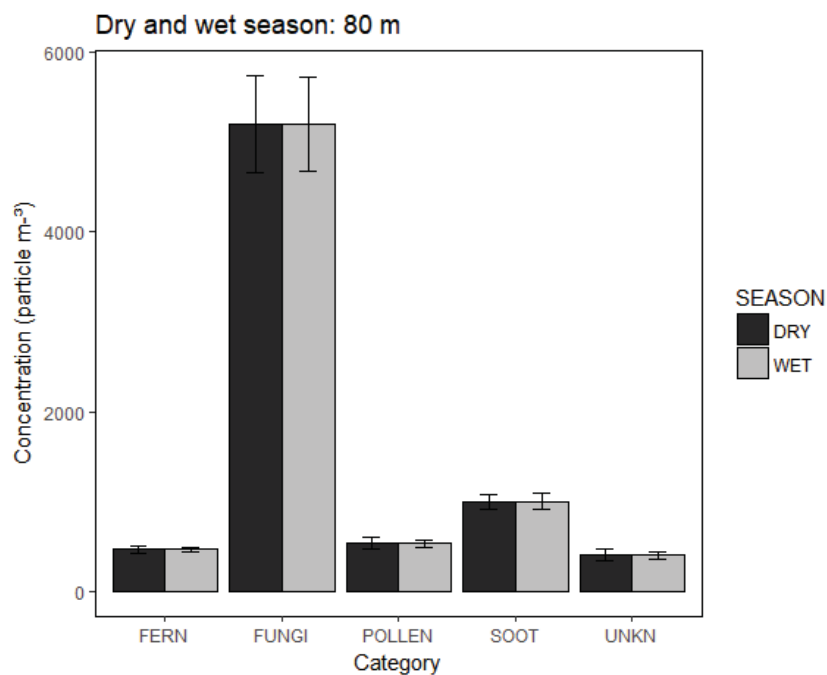


FIGURE 25: Seasonal median concentration of fern, fungal spores, pollen, soot and unknown particles for 80 m height. Interquartile ranges are represented on the top of each columns.

The FIGURE 24 shows the concentrations for fern, fungal, pollen, soot and unknown particles for all the valid samples at 40 m. All of the categories, except fern, have median statistical differences (Kruskal-Wallis test, 99 % level of confidence, p-value < 0.01). Only fern spores do not have a significative difference between the seasons (p-value = 0.8) at 40 m height.

For the 80 m height, besides the apparent similarity between the seasons for the entire data set (FIGURE 25), pollen, fungi, fern and unknown particles have median statistical differences (Kruskal-Wallis test, p-value < 0.01). For that height, only soot have a similar pattern across the seasons (p-value = 0.1).

The tropical zone has almost equal day/night duration throughout the year, according to the solar radiation data received. Thus, all sampled days were separated into periods with and without sunlight. The concentrations separated into day and night periods of sampling for pollen, fungi, fern and soot, during both seasons do not showed any statistical difference.

All the sampled heights had particles throughout the day and night for all the measured groups. Regarding only the categories, the day/night concentration showed no statistic difference (Kruskal-Wallis test, 95 % level of confidence) for pollen grains (p-value = 0.14), fungal spores (p-value = 0.13), fern spores (p-value = 0.75) or soot particles (p-value = 0.84). For each category and considering the height differences, just 40 and 300 m showed similar day/night concentration distribution for pollen, fungi and fern. For all the other heights and categories, a statistic difference is observed (p-value < 0.05).

Soot were present in the samples even during the night period and throughout wet and dry periods (FIGURE 24 and FIGURE 25). On average, the organic debris from the canopy made up 70 % of the collected material, with no statistic differences observed between day and night emissions (p-value = 0.37). This pattern was very consistent across the different heights.

The hourly resolution enabled the visualization of the emission pattern across the entire day. The pollen results can be viewed in FIGURE 26. The concentration of pollen grains was highest at 60 m during the 2015 dry season. From the day/night distribution, the 60 m sampler showed the highest number of pollens grains per cubic meter of air. The meteorological conditions were consistent with an increased pollen dispersion and/or less particles rain-related scavenging, as was subsequently observed. Only during this period values higher than 700 particles m^{-3} were found, as

can be seen in FIGURE 26 (top right). The concentrations during sunlight periods were slightly higher (p-value = 0.04) than during the night.

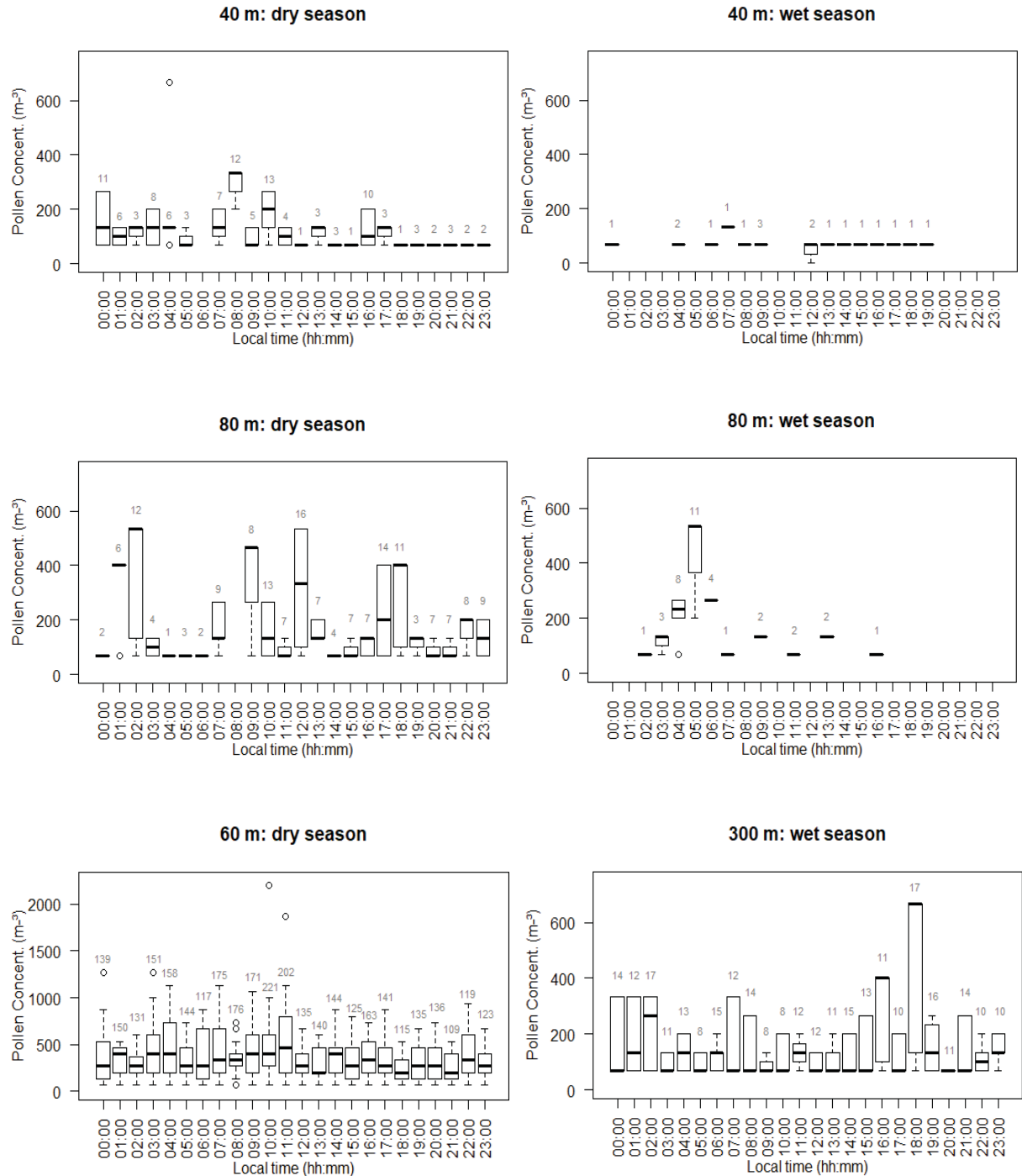


FIGURE 26: Boxplot of pollen concentrations (particle m^{-3}) for each hour interval (in local time): dry season at 40 m (top left), wet season at 40 m (top right), dry season at 80 m (center left), wet season at 80 m (center right), 60 m (bottom left), and 300 m (bottom right). Number of events recorded during each hour interval is in gray above each boxplot.

For the pollen concentration at 300 m, FIGURE 26, a peak around 18 h (local time) is due to a peak in just as few types of pollen, possibly correlated with a change in wind speed. The pollen concentration presented no specific correlation with the time of the day (FIGURE 26), and higher values were found during dry season. There is no evidence or statistical significance among the sampled hours for each height. Instead, there are correlation with meteorological conditions.

At 40 m height, the maximum and minimum relative humidity values and the maximum wind speed were the most significant parameters for the pollen concentration distribution (p -value < 0.05 , Generalized Linear Model (GLM) and Generalized Additive Model (GAM) with consecutive iterations for each parameter). At 60 m, the association with pollen concentration is significant for maximum and minimum relative humidity values, maximum and minimum wind speed and rain amount (p -value < 0.01 for the cited parameters).

At 80 m height, for dry and wet seasons, there was significant correlation between pollen abundance and minimum relative humidity, maximum and minimum temperatures, maximum and minimum wind speed and rain occurrence (p -value < 0.01 for the cited parameters).

For the precipitation variable, two parameters were investigated: the occurrence of, and the amount of rain. The precipitation occurrence influenced all the categories (p -value < 0.01) at every height. These were the only parameters analysed for 300 m height. The wind direction, considered as the mode of all the directions recorded during the hour period was relevant only for fern spores at 40 m and 80 m, and fungal spores at 60 m and at 80 m (p -value < 0.01). The recurrent significant parameters for each category at each height were: maximum and minimum relative humidity, wind speed, temperature and rain occurrence (p -value ≤ 0.01 , GLM and GAM tests, 95 % level of confidence).

In summary, the concentrations found varied up to 2200 particles m^{-3} for pollen grains throughout the entire sampling period. Maximum values for fungal spore values were in the range of 2,733 to 5,200 particles m^{-3} and for fern spores from 67 to 933 particles m^{-3} , as detailed in TABLE 3. The time resolution for the concentration values follows the sampler resolution: one-hour interval.

TABLE 3: Summary of pollen, fungi and fern results with median and maximum values for each height at each sampled season. All values are in one-hour time resolution.

HEIGHT/ SEASON	POLLEN (particle m ⁻³)		FUNGI (particle m ⁻³)		FERN (particle m ⁻³)	
Dry/Wet	MED	MAX	MED	MAX	MED	MAX
40 m (D)	133	667	1200	4467	67	200
40 m (W)	67	133	333	2733	67	200
60 m (D)	333	2200	1067	5333	200	933
80 m (D)	200	533	600	5200	67	467
80 m (W)	200	533	400	4667	67	67
300 m (W)	267	667	600	4267	67	333

Pollen monitoring around the globe follows the pattern of concentration averaged over 24-hour time period. With this time resolution is known the daily concentration for each location, used as an indicator for public health purposes. Pollen concentration overcomes 1000 of pollen particles m⁻³ averaged over 24 hours in Melbourne, Australia, during grass season (SILVER et al., 2017). Peaks higher than 4000 particles m⁻³ were recorded in Aomori and Hirosaki, Japan, as a consequence of a meteorological front (TAKAHASHI et al, 2018). In Sydney (Australia) values from 2008 to 2012 show pollen concentrations up to 300 particles m⁻³ averaged over 24 hours. In France the following values were observed, around 800 particles m⁻³ (24 h) in Montlucon, and up to 500 in Lyon and 300 in Amiens during the season peak considering a 11-year period (DEVADAS et al., 2018).

The present study was designed for morphological characterization and is not related to public health issues, so, it is complex to directly correlate the forest environment with urban sites due to the differences on vegetation distribution and emission pattern. The top value for the forest just overcomes 600 pollen particles m⁻³ averaged over 24 hours, with median values around 150 particles m⁻³ for 60 m, during the driest period, and below 50 particles m⁻³ for the other heights, considering daily values. Regarding just that, the values measured over the Amazon rainforest, even near the canopy, are considerably low compared to urban sites under crops and ornamental grass influence. However, the seasonality of the particles emission must be considered for a direct comparison approach.

4.3 BIOGENIC PARTICLE VERTICAL DISTRIBUTION

Chronologically, the first sampler was installed at 80 m in January 2015 during the wet season. With the washout effect, just a few particles suspended in the atmosphere were sampled, as illustrated in FIGURE 28 - top left. This period showed few pollen events, with the lowest pollen concentrations observed. The concentration reached 533 pollen particles m^{-3} during the night, and 267 particles m^{-3} during daylight.

Only two pollen events occurred during that period, with the presence of the biggest pollen grains yet observed (FIGURE 27). These events were associated with peaks in wind speeds, as registered for each hour period and were the only pollen grains collected during that month. Apart from those grains, there was no other pollen observed during January 2015.

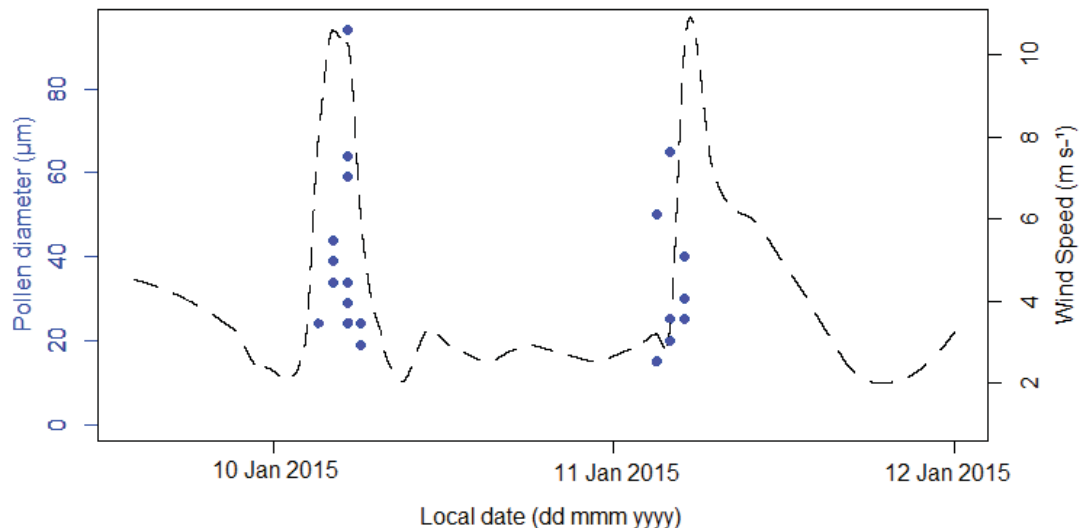


FIGURE 27: Each pollen occurrence (with size diameter marked in blue dots) and maximum wind speed (black dotted line), in hourly resolution during thunderstorms in January 2015, for 80 m height.

No pollen grains nor other giant particles were present, except for two peaks correlated with thunderstorm occurrences when horizontal wind speeds reached more than 10 m s^{-1} . The two thunderstorm events coincided with the observation of giant particles, larger than $50 \mu\text{m}$ (FIGURE 28 – top right, bottom left and right), and within a temporal resolution of less than 1 hour (the minimum temporal resolution of the sampler). Most of the pollen grains were from trees, but some were from ground-based weeds as well as bamboo (APPENDIX C.1). The samples were consistent with pollen grains sourced from both the local canopy plus long-distance transport from regions likely including cleared forest openings or river banks.

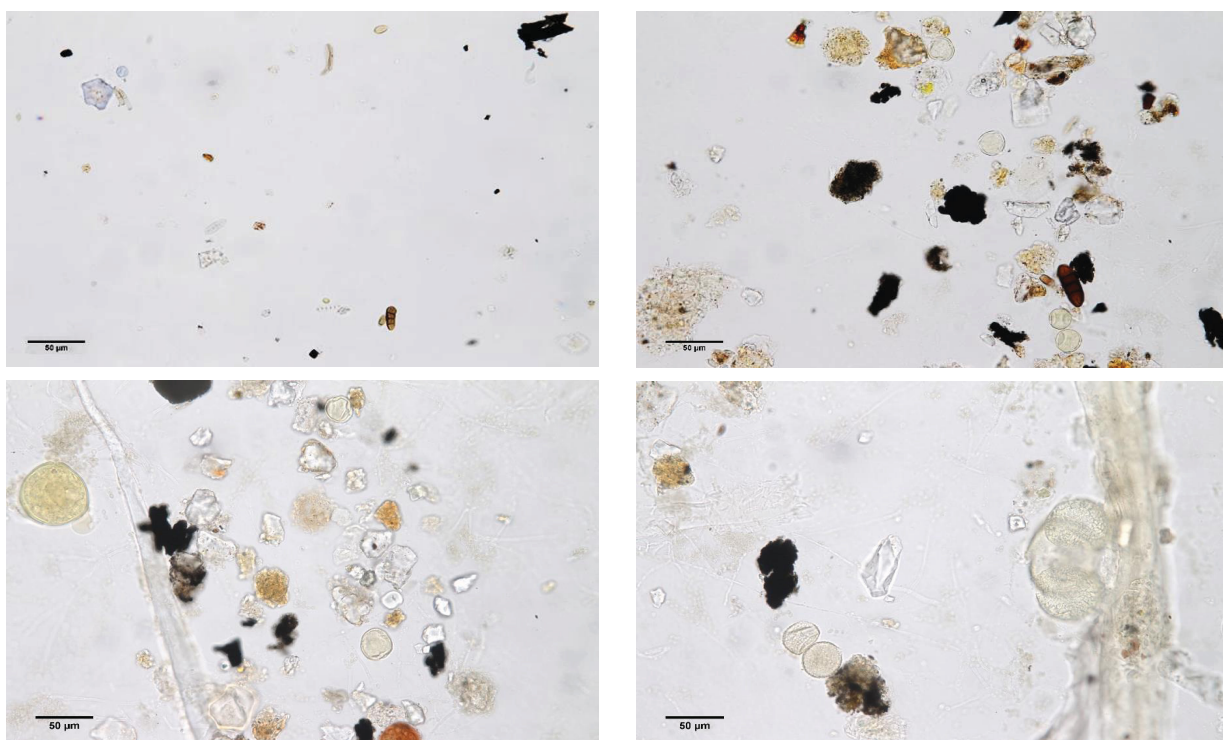


FIGURE 28: Samples from 80 m height, 10th January 2015: only a few particles observed for long hours (top left), a large variety of particles sampled during thunderstorm event around 6 am (top right and bottom right/left), and larger size of pollen particle sampled at 80 m height (bottom right) also during a thunderstorm, probably from *Podocarpaceae* family (giant hyaline particle on the left).

The following March and April again showed an absence of any giant particles at 80 m except during the peak of the Saharan dust transport over the ATTO site in early April. During the 2 days of this dust event, high concentrations of giant particles were observed and these included small fungal spores and a few pollen grains (RIZZOLO et al., 2017).

During this sampling, very few coarse particles ($> 2 \mu\text{m}$ diameter) occurred in the atmosphere until the beginning of April. On 3rd April at 13 h (local time), coarse particles (2 to 10 μm) peaked in number and were black, hyaline or variously coloured and of irregular shape, as shown in FIGURE 29. The amorphous particles were interspersed with a large diversity of small fungal particles. Several small pollen grains apparently from ground growing herbs were also observed. No moss nor fern spores were found. All primary biological particles in the sample had a diameter less than 12 μm , similar to adjacent coarse dust particles.

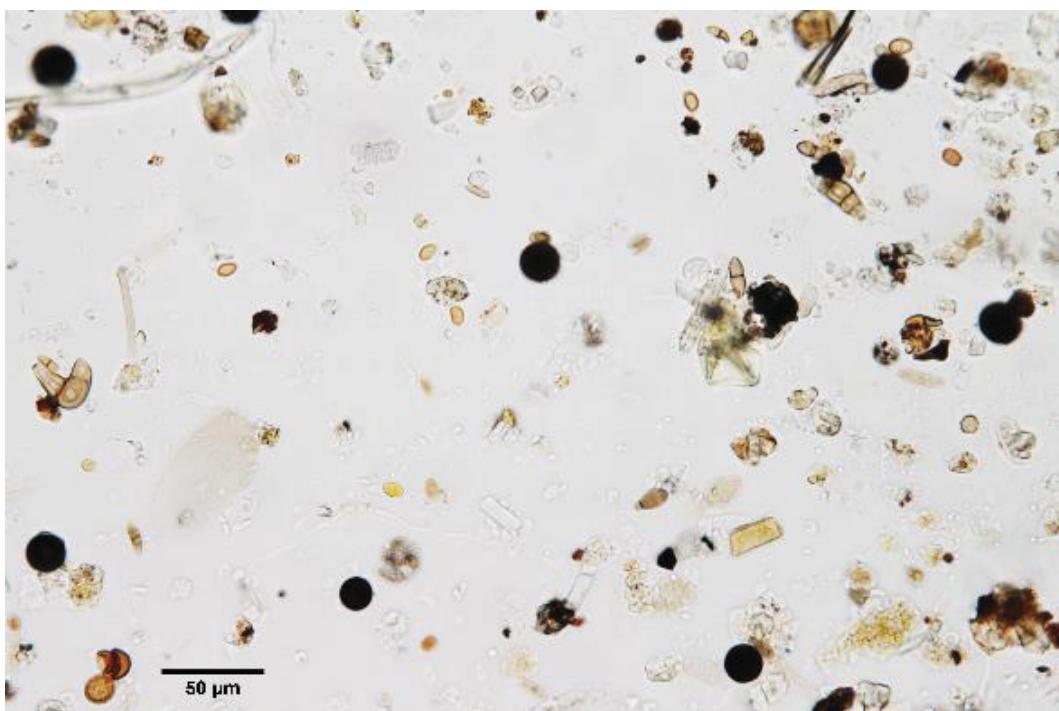


FIGURE 29: High density of particles sampled during a wind gust event at 80 m, on 3rd April at 1pm during the 2015 wet season. Larger concentration of canopy debris and fungal spores.

At 80 m height, the total fungal count was 1,587 spores per cubic meter of air, averaged over 24 h (on 2 to 3 April). High concentrations of fungi and other coarse particles persisted in the samples for several days in the first days of April, then, once again very few particles and only the occasional spore was observed, as shown in

FIGURE 28 – top left. The variety of particles that could be identified are more common at ground level across arid and temperate zones, consistent with an African source. (MIMS; MIMS, 2004; PROSPERO et al., 2014; WOMACK et al., 2015). However, genetic analysis of the samples is needed to confirm this assumption, as well as confirmation from genetic analysis of diverse plant types at the source and destination of the dust plume, a huge challenge.

The wind rose chart (FIGURE 30) for the period shows a predominant easterly air mass reaching the site, with some influences from northeast and southeast (inner continent). Some pollen grains were identified as ground based weeds, which could not be emitted from the forest canopy. Winds speeds at ATTO were quite low other than during the Saharan dust event. During most of the time, calm winds prevailed, with just a few episodes presenting gusts higher than 8 m s^{-1} . Those episodes were responsible for the movement of the few pollen grains collected.

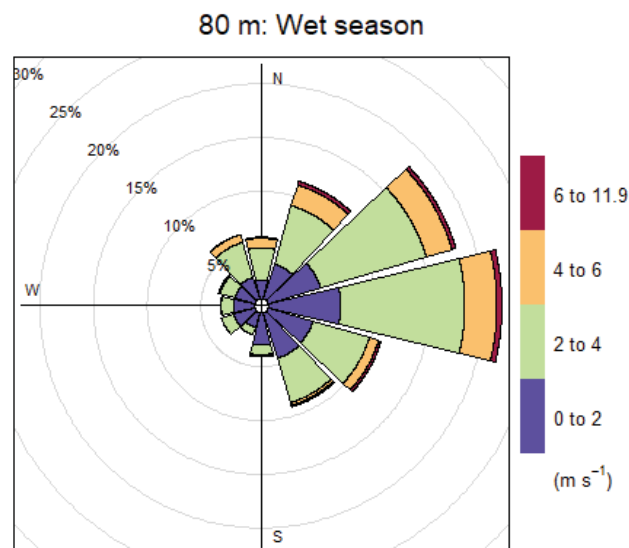


FIGURE 30: Wind rose chart for the wet season sampling period at 80 m height from 9th to 24th January 2015.

One type of pollen identified above the canopy 80 m at ATTO was bamboo (*Parianaceae* family), see APPENDIX C.1. This short growing, understory species has been observed at rivers edge approximately 15 km away. As one source location is known, this is an interesting pollen type for its potential as a marker to record horizontal transport of pollen.

It is not possible to fully compare the bioaerosol to determine an African source because previous studies cultured air samples of viable spores only and analyzed them with high throughput sequencing. Only a few types of particles were detected at the species level in these studies. It is unknown whether any of the PBAP observed in the dust above the Amazon are still viable upon sedimentation onto the forest. Other than during the formation of a Saharan dust plume, smoke plumes are also known to entrain fungi over long distances (MIMS; MIMS, 2004), so that some of the airborne material could have been introduced by burning in west Africa.

During the dry season of September to November 2015, samples were collected at 60 m. Consistently high levels of fungi and pollen grains were observed each day, as pictured in FIGURE 31, compatible with a local canopy source, highly dense from 25 to approximately 35 m height. The black amorphous particles are soot derived. The spherical shaped structures with hyaline content are pollen grains. The long, narrow shaped particles are fungal spores and other small amorphous particles were classified as debris.

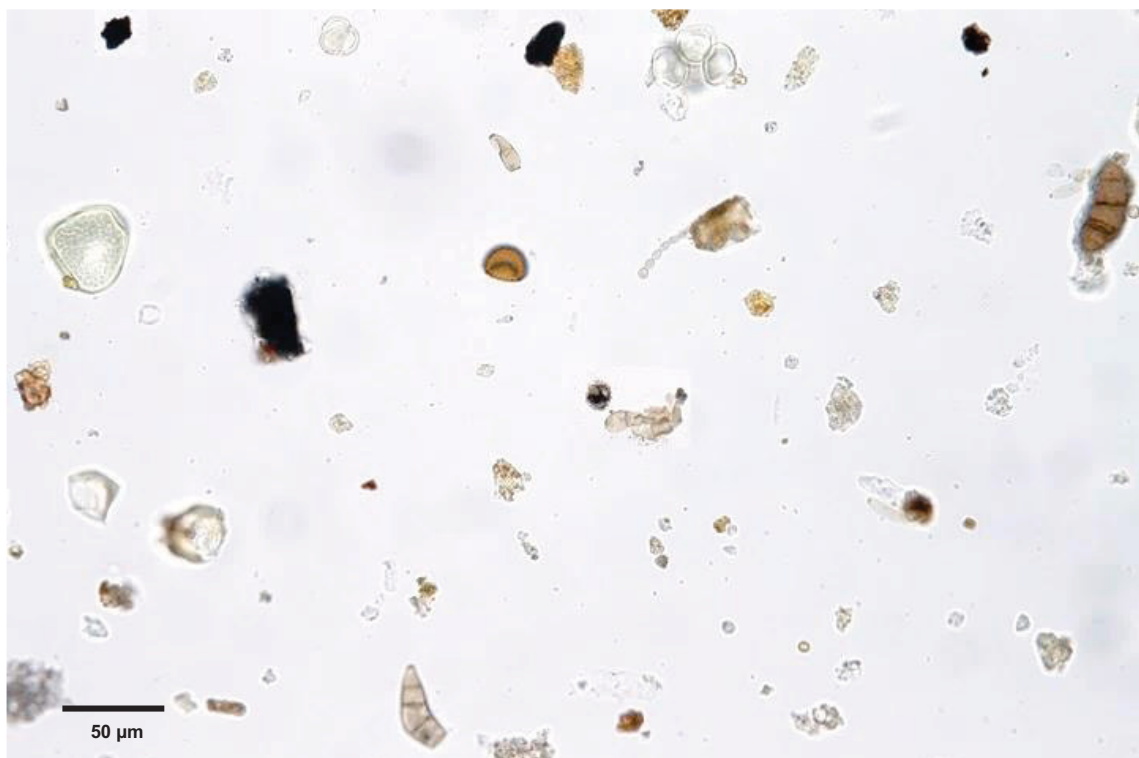


FIGURE 31: High variety of particles sampled at 60 m, on 19th September 2015 at 6 am, local time. All the categories are evenly represented during the sampling period.

This 2015 sampling was the only one with all the values one order of magnitude higher than the others. Unfortunately, this height was only sampled during the period of the El Niño effect at the dry season, and it is not possible to compare with a wet season at the same height. As shown in FIGURE 26, the pollen concentration reached $2,200 \text{ particles m}^{-3}$, and during the concentration peaks only small grains were found (10, 15 and $20 \mu\text{m}$ in diameter).

The larger particles ($50 - 95 \mu\text{m}$) are related to high wind speeds above 8 m s^{-1} . During that period easterly/northeasterly air masses reached the site with that velocity, as observed in FIGURE 32. Maximum wind speeds just reached 10 m s^{-1} in 0.5% of the sampling time and they are not specific correlated with the larger particles. The pollen concentration at that height is associated with the relative humidity and also wind speed range.

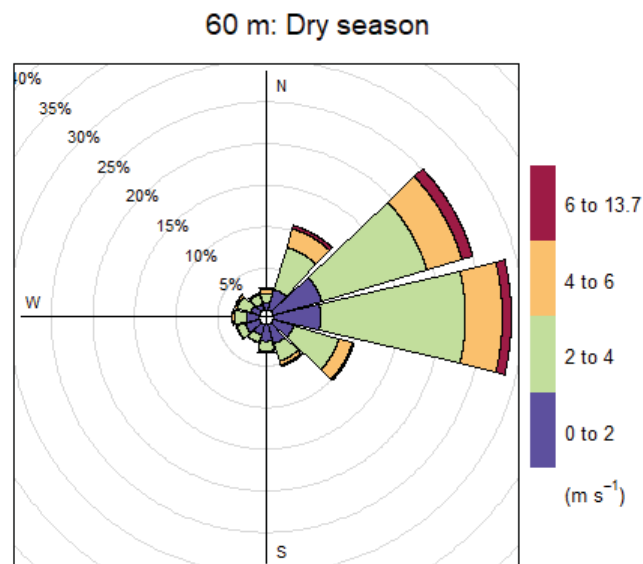


FIGURE 32: Wind rose chart for the dry season period sampled at 60 m height, from 16th September to 20th November 2015.

During the extreme dry season recorded in the Amazon in 2015, an opposite pattern was observed: an increase in the concentration of pollen in the atmosphere, with the same size distribution as observed in other seasons (FIGURE 18), but with higher frequency of the small pollen types. This could be a result of the reduction on the washout effect, with less precipitation events and even less intensity of the scarce rainfall.

The entire dry season showed high concentrations of small and medium pollen grains, very different from the previous wet season when pollen occurred in many size

ranges and types and peaks in PBAP were associated with specific meteorological conditions, such as storms. No tendency is highlighted in the 60 m data set, and perhaps this is also an effect of the drastic change in the weather for the period and the reduction of wash out events.

The only large-sized pollen found at 60 m (FIGURE 33) was collected two days after a small shower and with the wind direction from the northeast reaching a maximum velocity of 7 m s^{-1} . After the event several particles of debris and small pollen grains were also observed. Those conditions are different from the ones at 80 m, during the other big pollen sampling events, when a thunderstorm was necessary to take the particle up to 80 m height.

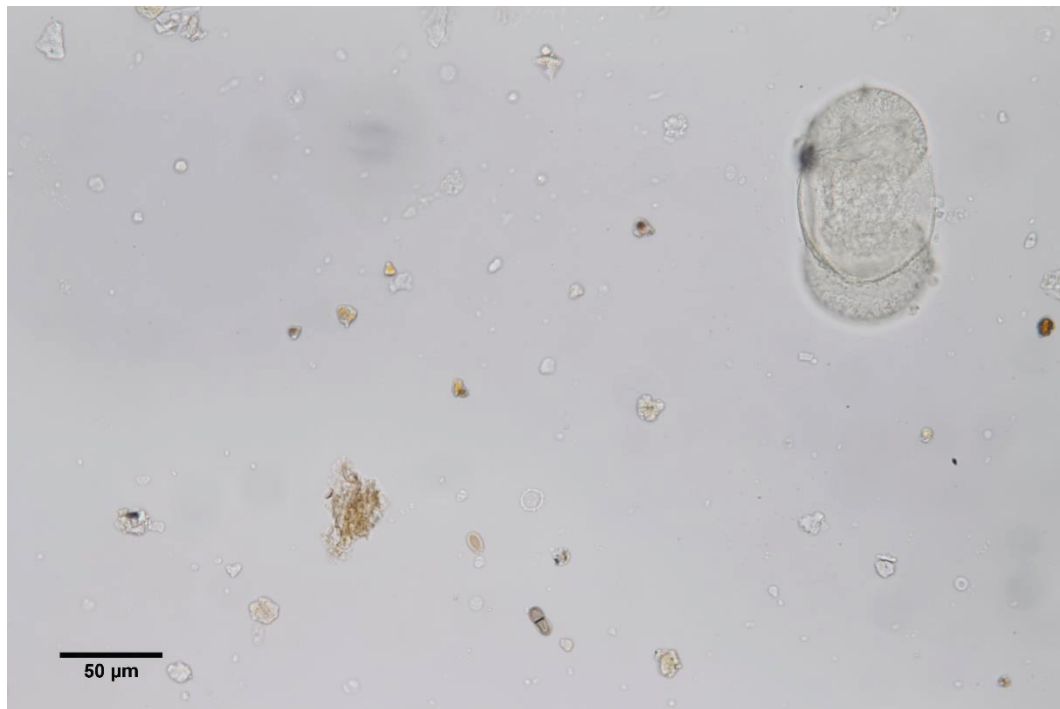


FIGURE 33: Unique larger pollen grain collected at 60 m during 2015 dry season, on 14th October 2015 at 8 pm.

During 2016, simultaneous samplings were carried out at the end of the dry season and the beginning of the wet season. At 40 m height, more pollen grains were collected during the dry season. Pollen collected during the wet season varied from 10 to 35 μm in diameter and peaked mainly during the day with wind speeds in the range of 1.0 to 7.5 m s^{-1} . During September and October, 2016, the air masses that reached the site came mainly from east and southeast, and for late November and December period the easterly and northeasterly winds were more frequent.

Total pollen concentration was $133 \text{ particle m}^{-3}$ for the wet season and $667 \text{ particle m}^{-3}$ for the dry season and with diameters up to $45 \mu\text{m}$. The majority of the grains were collected when wind speeds were up to 6 m s^{-1} . Most ambient pollen sampling is performed in temperate parts of the world at 15 m above ground level, and in open areas where grasses dominate. This height range is planned to minimize influence of emissions from the immediate vegetation. At 40 m in the Amazon forest, just above the canopy, the PBA sampled were more likely biased towards emissions from the tree canopy immediately below the sampler than occurs at 60 m.

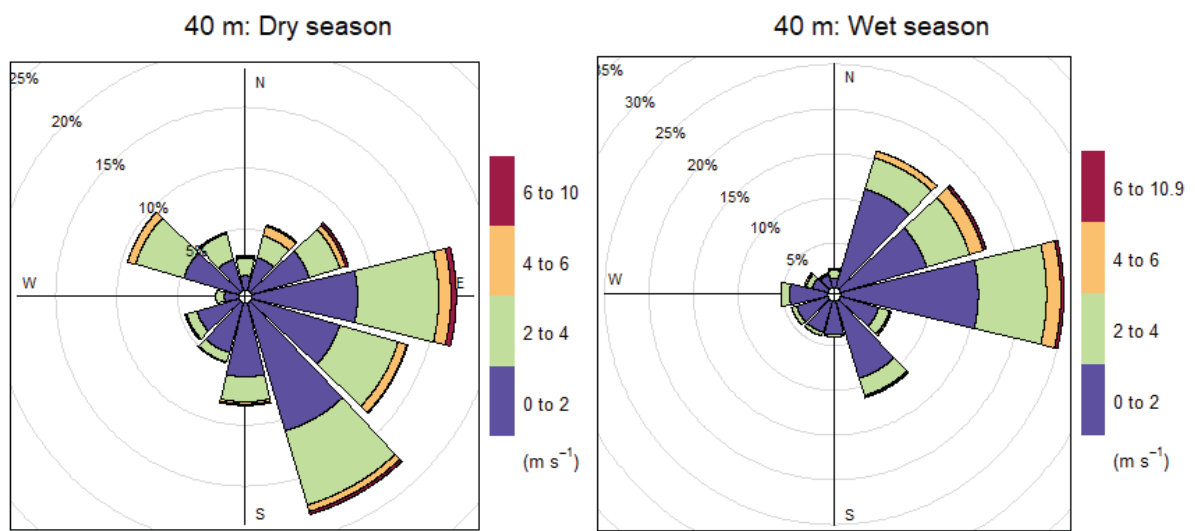


FIGURE 34: Wind rose for 40 m height during dry season (left), for 15th September to 7th October 2016 and wet season (right), from 29th November to 16th December 2016.

The other stages from the simultaneous samplings occurred at 80 and 300 m. At 80 m, the pollen concentration reached 533 m^{-3} with the larger pollen being $50 \mu\text{m}$ in diameter. Wind speed reached 7.6 m s^{-1} and the predominant direction was mainly southeast, FIGURE 35 (inner continent).

At 300 m, the pollen peaked at 667 m^{-3} with the largest at $50 \mu\text{m}$ in diameter. There is no information about wind speed, but the direction was mainly northeast, as illustrated by the backward trajectory from FIGURE 36.

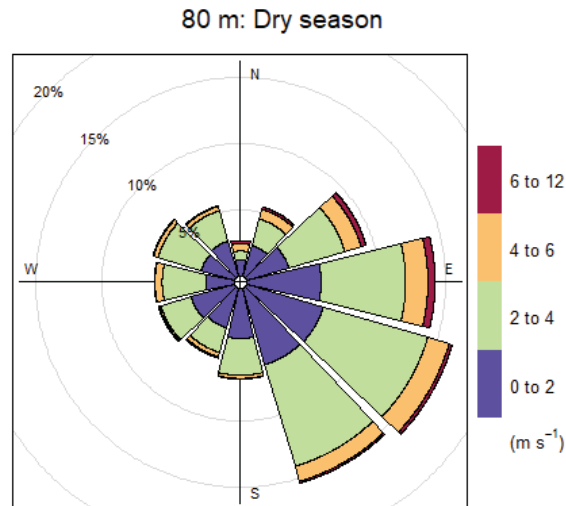


FIGURE 35: Wind rose chart for the dry season period sampled at 80 m height, from 15th September to 7th October 2016.

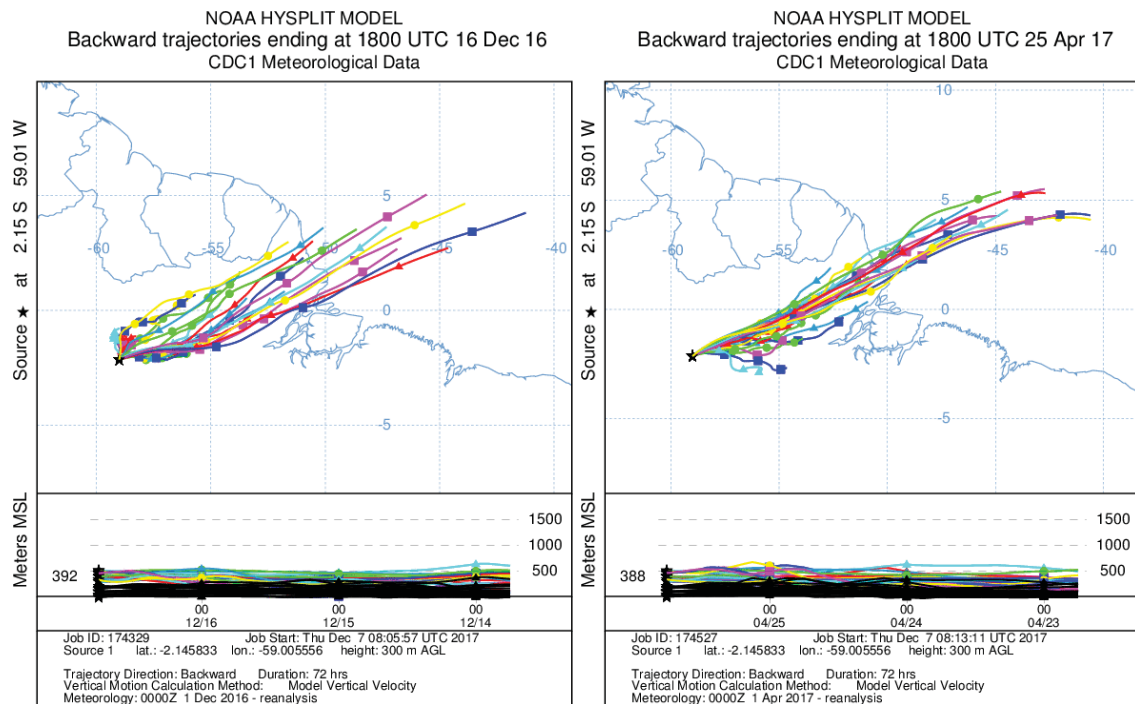


FIGURE 36: Backward trajectories reaching the site by the end of the sampling period on December 2016 (left) and April 2017 (right) at 300 m, showing the dominance of northeasterly air masses for the period.

At 300 m height, two sampling campaigns during the wet season were executed. December 2016 was the beginning of the wet season, with higher concentrations ($667 \text{ particles m}^{-3}$), while March and April 2017 were the middle/end of the wet season with few suspended particles (FIGURE 37). This period had a peak of

333 particles m^{-3} that are likely contributed from a distant area. The concentrations are quite similar with no pronounced day or night pattern.

At 80 and 300 m, samples followed similar pattern of low concentration and similar day/night abundance, and with a few peaks correlated with high wind speeds. A typical sample from the mid wet season (2016) can be viewed in FIGURE 37. A sample, likely during a wind gust or long-distance transport event, is shown in FIGURE 38. The high density was mainly formed from small particles with amorphous/irregular shape. There was no wind speed data available for that height.

Since low amounts of pollen are present at 300 m and, given the generally low wind velocities in and above the canopy (mean wind speed is below 3 m s^{-1} , as shown in FIGURE 21), most pollen grains released into the atmosphere from the rainforest are expected to quickly settle out the atmosphere and thus not travel far. This is different for storms, such as Saharan dust storms, and squall line thunderstorms with strong outflows.

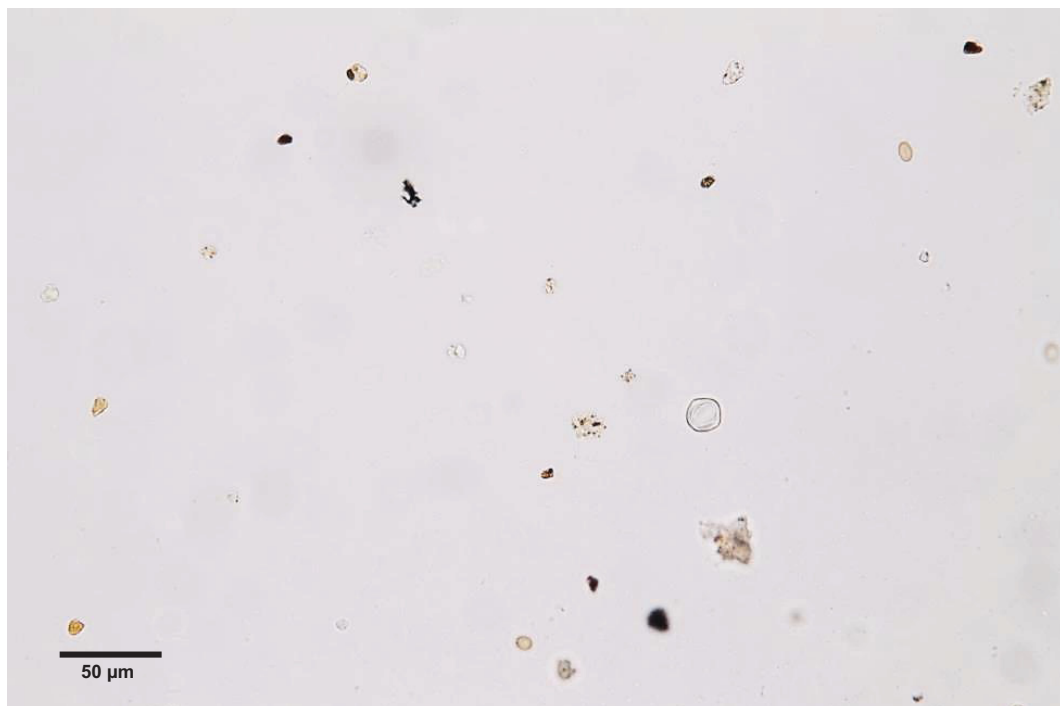


FIGURE 37: Example of a typical sample from 300 m during the wet season with a clear background and few collected particles, including biological ones, on 30th March 2017 at 11am.

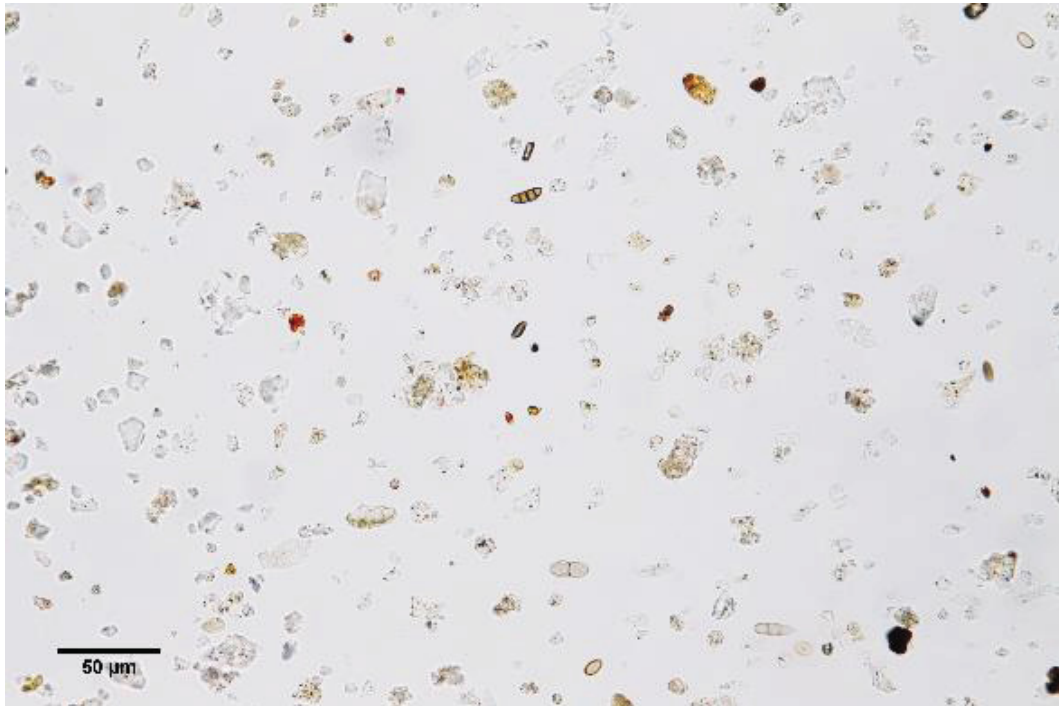


FIGURE 38: Example of an atypical observation during the mid wet season at 300 m, showing high density of small particles, up to 15 μm , on 3rd April 2015 at 6 pm.

It appears likely that the modeled vertical and long-distance transport of pollen might be over-estimated using only surface and low levels measurements. Current models used to estimate pollen levels in the air (ZHANG et al., 2014) need to re-assess the existing premise of regular vertical transport of pollen to 2,000 m. Instead, the majority of pollen and fungal spores are likely to be restricted to as little as 60 m above ground level or surface structures except for the duration of high speed winds found in thunderstorms, and at the source of dust storms.

In a general overview of all sampling heights and across both wet and dry seasons, pollen size and abundance were more diverse at 60 m and below. The 60 m samples in 2015 correlated with the unique meteorological scenario of an extreme dry season caused by an El Niño event. Pollen abundance exceeded all the previous measured ranges from 80 m. Coarse particle diversity was also high across all sampled heights and seasons.

Only under specific types of thunderstorm conditions large pollen grains were observed at 300 m. The detected high wind speeds were consistent with the passage of a storm front. Many of these pollen grains were likely transported in downdrafts and outflows from higher in the atmosphere near the cloud base. A similar pattern was observed by Ryder et al. (2015) during aircraft measurements of dust particles and

associated dust storms in the Saharan atmospheric boundary layer. At ATTO, the strong winds associated with the storm are likely to mix with updrafts that may also have driven large pollen grains to 300 m from the canopy. However, pollen was only identified to family level, and thus does not allow us to determine the potential for a local versus distant source. Data on the identification and position of trees around the tower might provide a valuable data source for comparison.

4.4 INCIDENCE OF POLLEN RUPTURE AT THE AMAZON REGION

Thunderstorm and lightning events are common at the sampling region (REHBEIN et al., 2018). Therefore, the high frequency of these events should have a substantial influence on the dispersion and transport of pollen, but also on the quality of pollen grains.

Pollen grains have a robust external layer, with the role of protection for the enclosed male gametophyte in order to survive transport and succeed at reproduction (MOORE et al., 1991; HESSE et al., 2009). So, under normal conditions, pollen has an unbreakable wall but, this can be damaged under specific meteorological conditions, e.g., high humidity with or without electric fields (GROTE et al., 2000; VAIDYANATHAN et al., 2006). This can occur on the anther of the flower, and winds can then subsequently release the pollen contents into the atmosphere (TAYLOR et al., 2002). These pollen cytoplasmic fragments disperse into thousands of smaller (nano, micro) particles that could have cloud nucleation properties (PÖSCHL et al., 2010; PÖHLKER et al., 2012).

At 80 m height and assessing the type of the storm defined by lightning and wind speed, the second storm occurrence was the Saharan dust storm (RIZZOLO et al., 2017). So, lightning plus high wind is consistent with a downdraft from a thunderstorm with a squall front, and many of the storms in the Amazon are mesoscale convective systems as confirmed by REHBEIN and others (2018). The thick band of large pollen (FIGURE 27) was sampled during high wind speed plus lightning (FIGURE 39) prior to rain and was a unique occurrence across a period of weeks when no other pollen was entrained to 80 m.

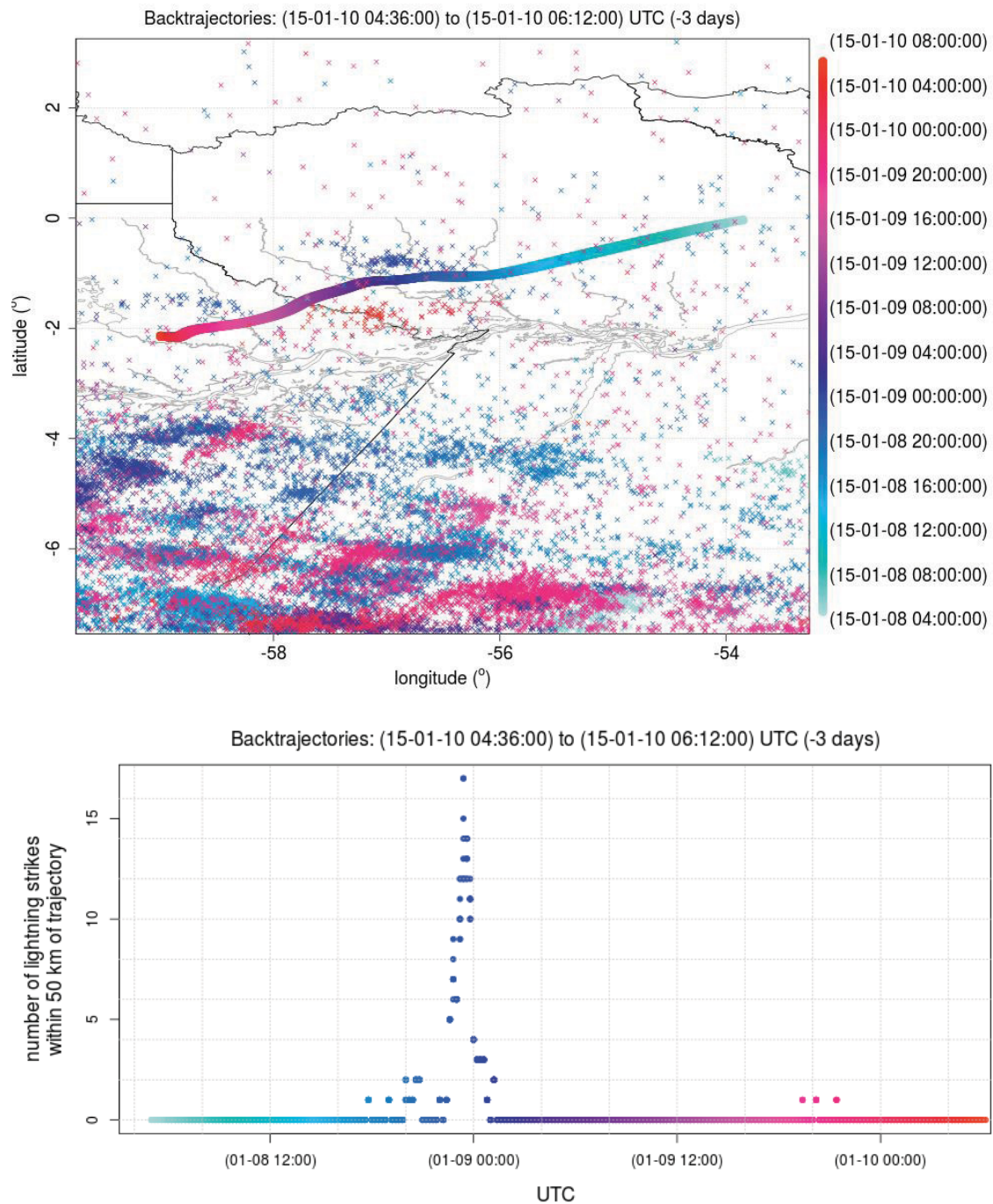


FIGURE 39: Air mass backtrajectories 3 days prior to the sampling with lightning occurrence highlighted in a map (top) and an electric field profile with number of strikes (bottom). Dark blue dots are the highest frequency of strikes reaching the air mass.

Source: provided by Dr. Rachel Albrecht (IAG/USP).

These storm conditions were present when ruptured pollen grain were observed at 80 m: more than 15 lightning strikes, 95 % relative humidity and wind speed reaching 10 m s^{-1} .

Pollen of most temperate plants have been shown to rupture in high humidity whilst still on the flower, and subsequently release pollen fragments into the airstream

(GLOVSKY et al., 2007). Laboratory experiments were performed for this project in order to determine if pollen can rupture in the atmosphere and disperse its contents. Preliminary experiments were done to test the minimum conditions required to rupture pollen. Past experiments relied only on immersion in water for direct observations. Under an optical microscope, pollen was placed on a glass slide inside a small chamber with controlled increases in relative humidity, as well as the application of different voltages to create an electric field, while recording the temperature.

Using 30 μm diameter, freshly collected pollen grains of ryegrass (*Lolium perenne*), each variable was tested for the effect on pollen rupture (FIGURE 40). Upon the relative humidity exceeding 92 %, pollen grains condensed moisture from the air. Within 10 min, a microdroplet of about 100 μm diameter formed around each pollen grain. The pollen subsequently ruptured and released the contents into the liquid meniscus external to the wall. Electric fields of up to 5kV per meter sped up the rate and percent of pollen grains that ruptured.

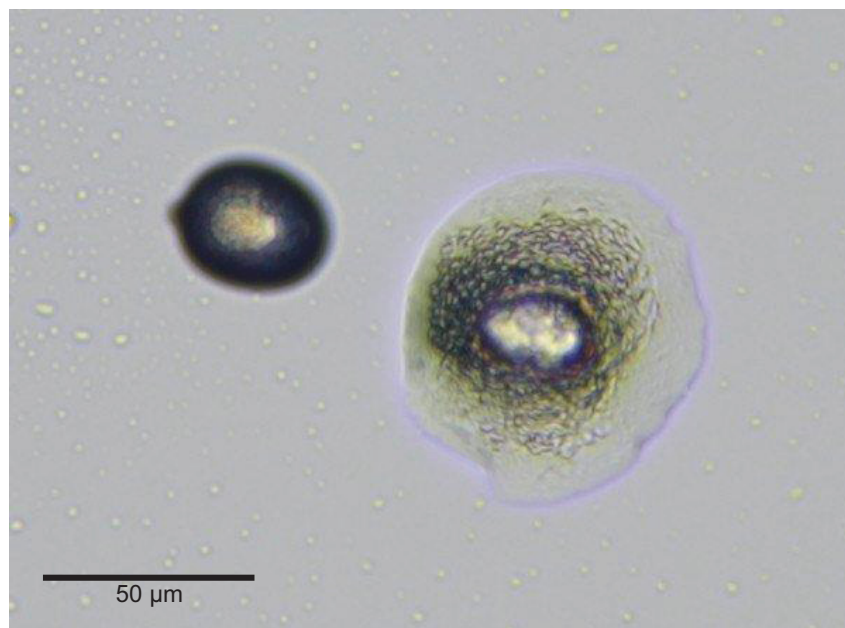


FIGURE 40: Image of a pollen rupture experiment. The particle on the left is still intact and the one on the right released the contents into the microdroplet of liquid that condensed around each pollen grain. Experiments performed in a controlled environment with up to 94 % relative humidity.

Because these experiments were performed on glass we did not observe dispersion of the fragments into the air upon drying. However, this is likely to occur in the atmosphere during a thunderstorm and under specific conditions, but this final observation remains to be performed. The mechanism of thunderstorm asthma as

proposed by Taylor and Johsson (2004) appears valid, and the detailed description of the process can now be further refined.

The natural appearance of the pollen looks like collapsed, but all the sampling was executed in order to moisturize the grain when collected. Damage pollen, observed as completely empty pollen shells, was observed in samples from above the rainforest (FIGURE 41). This suggest that even though they are adapted to high humidity environments, pollen of tropical plants is also susceptible to rupture.

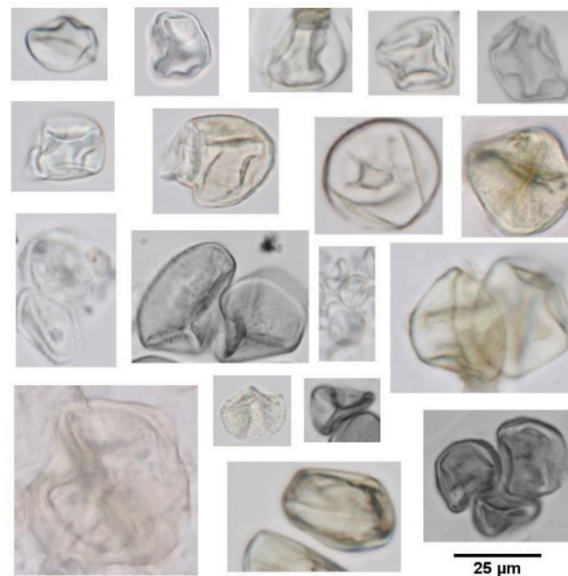


FIGURE 41: Pictures of damaged pollen grains sampled from 2015 to 2017, occurred at all sampled heights. Different types and sizes of particles can be observed. All the images are in the same scale: 25 μm .

Ruptured pollen was also observed during thunderstorm events at 60, 80 and 300 m heights. The rupture was recorded only when pollen grains had clearly lost their contents and the pollen shell was observed to be collapsed. However, there was no peak in, nor substantial amounts of, ruptured pollen. From all the pollen grains collected, only 0.3% were observed to be empty and obviously collapsed, i.e., just a small fraction of grains was damaged.

This amount of pollen contents released into the atmosphere would have no measurable influence on weather patterns, even at the scale of the rainforest. There does appear to be an emission of pollen fragments into the atmosphere above the Amazon, especially in thunderstorm squall lines, but, unlike temperate pastures and forests, pollen rupture does not appear to be a particularly large source of sub-micron sized particle mass nor number.

Ruptured pollen grains occurred associated high humidity and lightning, but again, they represent only a small amount total pollen present. Ruptured pollen grains were more readily observed during the dry season at 60 m height, during El Niño effects. This highlights that little is known about the consequences of climate change on the production, emission and viability of particles such as pollen.

5 CONCLUSION

The present project was designed to analyse the seasonal and vertical distribution of PBAP using towers installed in a pristine area of the Amazon rainforest. Four different heights were selected above the canopy: 40 m, 60 m, 80 m and 300 m (above ground level) at the maximum height of the tallest tower. In order to assess the relative amounts of the various types of bioaerosols, all the coarse particles were classified into different categories, labeled as: pollen grains, fungal spores, fern spores, moss spores, soot structures and canopy debris.

No significative value for moss spores was identified in the samples, and this might be a result of the sampling strategy executed for the project. Regarding the sampling height results, particles were abundant up to 60 m. The 80 m height samples, obtained mostly during the wet season, presented the lowest values for all the categories. For 80 m and upwards, bioaerosol abundance was considerably lower than near the canopy, consistent with a pattern of exponential decrease with height.

Seasonal distribution of bioaerosols confirmed the tendency of higher values during the dry season. For the wet season, even with a strong rainfall scavenging effect, all the categories were observed across all the sampled heights, but in lower concentrations. Although sampling occurred over a large PBAP source area, the largest tropical rainforest, bioaerosol abundance was relatively low compared to urban environments, at least by a magnitude order. This is an important result to be considered regarding IPCC estimates for bioaerosols. A large data set from forested areas should be considered for forthcoming investigations on future scenarios and estimated emission values.

The vertical analysis indicated that the most abundant region for bioaerosols is not immediately above the canopy, dominated by local tree canopy emissions, but about 25 m above (60 m), even though this sampling was performed during an El Niño year with the most low-rainfall dry season yet recorded. Those results could be just a consequence of the meteorological conditions, so, a future monitoring would be interesting to verify the pattern found. The pollen counts at 60 m in and out of lightning events did not show any distinct peaks but were well distributed across the entire sampling period. Bioaerosols concentrations were similar for 80 and 300 m, with occasional peaks correlated to specific storm events.

The majority of pollen and fungal spores appear to be restricted to the canopy area or surface structures, up to 60 m, except for the duration of high speed winds exceeding 10 m s^{-1} as found in thunderstorm outflows and at the source of dust storms. These storm like conditions appear to be the driving force for the suspension of the largest pollen grains that otherwise were rarely sampled at 80 and 300 m. Pollen emitted from the canopy appear to be restricted to approximately the surface roughness sub-layer of the atmospheric boundary layer, and seldom exceed 80 m above the canopy. So, giant particles such as pollen and large fungal spores are not evenly distributed across the entire atmospheric boundary layer, and therefore, it appears to have less influence on atmospheric processes.

Contradicting some existing models that estimate pollen levels in the air with a regular vertical transport up to 2 km, apart from a strong air mass and during high wind speed, it is unlikely for giant-sized pollen grains to remain suspension for a substantial period of time. As vertical transport is necessary for horizontal and long-distance transport, turbulent motions are needed to resuspend particles and entrain them to higher levels. With a continuous sampling at different heights above the canopy it would be possible to acquire accurate data on the vertical transport of coarse and giant particles and estimate their long-distance transport.

The high diversity of the sampled biological material above the canopy was categorized and illustrated in an atlas specifying the family level (when identified) and the collected height (APPENDIX C). The sampling period during the El Niño effect correlated with the highest diversity for all the categories. This was also the longest continuous sampling period and the results highlight the importance of frequent airborne biological particle measurements for the region. More than a hundred different types of pollen were collected from 2015 to 2017 across the various heights, and more than 200 types of fungal spores were also sampled. Almost half of the material was identified to the family level, and a multidisciplinary study should be considered for a future work in order to execute a continuous measurement as well. That would enable the identification of all the sampled particles, including the ones categorized as unknown for this project.

Even with the diversity of pollen types sampled at different heights and under varied meteorological conditions, only 0.3 % of the total pollen collected were obviously empty, notably showing a collapsed shell. The particle structure was intact on practically all the bioaerosols sampled. At temperate latitudes, a relatively large

amount of grass pollen can be found damaged and ruptured. Yet under the harsh conditions and frequent lightning events in the Amazon, tropical pollen types seem well adapted with a hard thick wall to protect their contents.

Aerosols studies agree that over the rainforest environment more than 90 % of atmospheric particles have organic source. The results presented here are in agreement with previous research from the region. Up to 70 % of the sampled material is accounted for as organic material from the canopy, followed by fungal spores, pollen grains and fern spores. Unknown recurrent particles are, in general, less than 1 % across all the sampled heights. High levels of mineral particles and dust are only present during specific storm events.

From 2015 to 2017, across both dry and wet seasons, the general relative composition and abundance of particles were similar despite weather conditions and height differences. Wet and dry seasons presented the same composition with differences in concentration. All the categorized PBAP for this work were observed up to 300 m regarding the concentration proportions, and events out of the ordinary occurred just during a few number of extreme meteorological conditions. So, as an indication for forthcoming monitoring two stages are essential: one not close to the canopy line and another as high as possible. These first results on airborne bioaerosols above a tropical rainforest open a wide range of possibilities for future investigations into biological emissions and dispersal.

REFERENCES

- AGASHE, S. N.; CAULTON, E. **Pollen and Spores: Applications with special emphasis on aerobiology and allergy**. Science Publishers, New Hampshire, USA. 399 p., 2009.
- ANDRADE, M. F.; MIRANDA, R. M.; FORNARO, A.; KERR, A.; OYAMA, B.; ANDRE, P. A.; SALDIVA, P. Vehicle emissions and PM_{2.5} mass concentration in six Brazilian Cities. **Air Quality Atmospheric Health**, 5, 79-88, 2012.
- ANDREAE, M. O.; ACEVEDO, O. C.; ARAÚJO, A.; ARTAXO, P.; BARBOSA, C. G. G.; BARBOSA, H. M. J.; BRITO, J.; CARBONE, S.; CHI, X.; CINTRA, B. B. L.; SILVA, N. F.; et al. The Amazon Tall Tower Observatory (ATTO): overview of pilot measurements on ecosystem ecology, meteorology, trace gases, and aerosols. **Atmospheric Chemistry and Physics**, 15, 10723-10776, 2015.
- ANDREAE, M. O.; BERRESHEIM, H.; BINGEMER, H.; JACOB, D. J.; LEWIS, B. L.; LI, S. M.; TALBOT, R. W. The atmospheric sulfur cycle over the Amazon Basin: 2. Wet season. **Journal of Geophysical Research**, 95, 16813 – 16824, 1990.
- ANDREAE, M. O.; CRUTZEN, P. J. Atmospheric Aerosols: Biogeochemical Sources and Role in Atmospheric Chemistry. **Science**, 276, 1052-1058, 1997.
- ANDREAE, M. O.; GELENCSE, A. Black carbon or brown carbon? The nature of light-absorbing carbonaceous aerosols. **Atmospheric Chemistry and Physics**, 6, 3131-3148, 2006.
- ANDREAE, M. O.; ROSENFELD, D. Aerosol-cloud-precipitation interactions. Part 1. The nature and sources of cloud-active aerosols. **Earth-Science Reviews**, 89, 13-41, 2008.
- ARAGÃO, L. E. O. C. The rainforest's water pump. **Nature**, 489, 7415, 217-218, 2012.
- ARIYA, P. A.; SUN, J.; ELTOUNY, N. A.; HUDSON, E. D.; HAYES, C. T.; KOS, G. Physical and chemical characterization of bioaerosols – Implications for nucleation processes. **International Reviews in Physical Chemistry**, 28, 1-32, 2009.
- ARTAXO, P.; OLIVEIRA, P. H.; LARA, L. L.; PAULIQUEVIS, T. M.; RIZZO, L. V.; PIRES JUNIOR, C.; PAIXÃO, M. A.; LONG, K. M.; FREITAS, S.; CORREIA, A. L. Efeitos climáticos de partículas de aerossóis biogênicos e emitidos em queimadas na Amazônia. **Revista Brasileira de Meteorologia**, 21, 168-189, 2006.
- ARTAXO, P.; RIZZO, L. V.; BRITO, J. F.; BARBOSA, H. M. J.; ARANA, A.; SENA, E. T.; CIRINO, G. G.; BASTOS, W.; MARTIN, S. T.; ANDREAE, M. O. Atmospheric aerosols in Amazonia and land use change: from natural biogenic to biomass burning conditions. **Faraday Discussions**, 2013.
- BAARS, H.; ANSMANN, A.; ALTHAUSEN, D.; ENGELMANN, R.; ARTAXO, P.; PAULIQUEVIS, T.; SOUZA, R. Further evidence for significant smoke transport from Africa to Amazonia. **Geophysical Research Letters**, 38, 2011.
- BEN-AMI, Y.; KOREN, I.; RUDICH, Y.; ARTAXO, P.; MARTIN, S. T.; ANDREAE, M. O. Transport of North African dust from the Bodélé depression to the Amazon Basin: a case study. **Atmospheric Chemistry and Physics**, 10, 7533-7544, 2010.
- BFA - British Aerobiology Federation. **Airborne pollen and spores: a guide to trapping and counting**. Larksfield: Kimberly Clark Ltd., 1995.

BIPM. Evaluation of measurement data – **Guide to the expression of uncertainty in measurement JCGM 100:2008** (GUM 1995 with minor corrections), Paris: BIPM Joint Committee for Guides in Metrology, 2008.

BOND, T. C.; DOHERTY, S. J.; FAHEY, D. W.; FORSTER, P. M.; BERNTSEN, T.; DEANGELO, B. J.; FLANNER, M. G.; GHAN, S.; KARSHER, B.; KOCH, D.; KINNE, S.; KONDO, Y. Bounding the role of black carbon in the climate system: A scientific assessment. **American Geophysical Union**, 118, 5380-5552, 2013.

BURKARD. User's manual for the 7-day volumetric spore trap, Uxbridge, UK, 2003.

BUSECK, P. R.; ADACHI, K.; GELENCSE, A.; TOMPA, E.; POSFAI, M. Are black carbon and soot the same? **Atmospheric Chemistry and Physics Discussions**, 12, 24821-24846, 2012.

BUSECK, P. R.; ADACHI, K. Nanoparticles in the atmosphere. **Elements**, 4, 389-394, 2008.

BUTERS, J. T. M.; ANTUNES, C.; GALVEIAS, A.; BERGMANN, K. C.; THIBAUDON, M.; GALÁN, C.; SCHMIDT-WEBER, C.; OTEROS, J. Pollen and spore monitoring in the world. **Clinical and Translational Allergy**, 8 (9), 1-5, 2018.

CERNUSAK, L. A.; WINTER, K.; DALLING, J. W. Tropical forest responses to increasing atmospheric CO₂: current knowledge and opportunities for future research. **Functional Plant Biology**, 40, 531-551, 2013.

CHINA, S.; WANG, B.; WEIS, J.; RIZZO, L.; BRITO, J.; CIRINO, G. G.; KOVARIK, L.; ARTAXO, P.; GILLES, M. K.; LASKIN, A. Rupturing of biological spores as a source of secondary particles in Amazonia. **Environmental Science and Technology**, 50 (22), 12179-12186, 2016.

COLINVAUX, P.; OLIVEIRA, P. E. De; PATINO, J. E. M. **Amazon pollen manual and atlas**. 413 p. Taylor & Francis, Amsterdam, The Netherlands, 2005.

CROUZY, B.; STELLA, M.; KONZELMANN, T.; CALPINI, B.; CLOT, B. All-optical automatic pollen identification: Towards an operational system. **Atmospheric Environment**, 140, 202-212, 2016.

DEMERS, I. Les pollens allergènes au Québec. **Institut National de Santé Publique**, Bulletin d'Information en Santé Environnementale, Novembre, 2013.

DESPRES, V. R.; HUFFMAN, J. A.; BURROWS, S. M.; HOOSE, C.; SAFATOV, A. S.; BURYAK, G.; FROHLICH, J.; ELBERT, W.; ANDREAE, M. O.; POSCHL, U.; JAENICKE, R. Primary biological particles in the atmosphere: a review. **Tellus B**, 64, 15598, 2012.

DEVADAS, R.; HUETE, A. R.; VICENDESE, D.; ERBAS, B.; BEGGS, P. J.; MEDEK, D.; HABERLE, S. G.; NEWNHAM, R. M.; JOHNSTON, F. H.; JAGGARD, A. K.; CAMPBELL, B. et al. Dynamic ecological observations from satellites inform aerobiology of allergenic grass pollen. **Science of Total Environment**, 6333, 441 – 451, 2018.

DINGLE, A. N. Pollens as condensation nuclei. **Journal de Recherches Atmospheriques**, 2, 231-237, 1966.

DOUGHTY, C. E.; METCALFE, D. B.; GIRARDIN, C. A. J.; AMÉZQUITA, F. F.; CABRERA, D. G.; HUARACA HUASCO, W.; SILVA-ESPEJO, J. E.; ARAUJO-MURAKAMI, A.; et al. Drought impact on forest carbon dynamics and fluxes in Amazonia. **Nature**, 519, 78-82, 2015.

ELBERT, W.; TAYLOR, P. E.; ANDREAE, M. O.; PÖSCHL, U. Contribution of fungi to primary biogenic aerosols in the atmosphere: wet and dry discharged spores, carbohydrates, and inorganic ions. **Atmospheric Chemistry and Physics**, 7, 4569-88, 2007.

EPA. Air Quality Guide for Particle Pollution. United States: Environmental Protection Agency, 2013. Available online: <http://www.epa.gov/airnow/air-quality-guide_pm_2013.pdf>. Accessed in 21 sept 2014.

EPA. National Ambient Air Quality Standards. United States: Environmental Protection Agency, 2011.

FAVET, J.; LAPANJE, A.; GIONGO, A.; KENNEDY, S.; AUNG, Y.; CATTANEO, A.; DAVIS-RICHARDSON, A. G.; BROWN, C. T.; KORT, R.; BRUMSACK, H.; SCHNETGER, B.; et al. Microbial hitchhikers on intercontinental dust: catching a lift in Chad. **The ISME Journal**, 7, 850-867, 2013.

FERNÁNDEZ-RODRÍGUEZ, S.; TORMO-MOLINA, R.; MAYA-MANZANO, J. M.; SILVA-PALACIOS, I.; GONZALO-GARIJO, A. A comparative study on the effects of altitude on daily and hourly airborne pollen counts. **Aerobiologia**, 30 (3), 257-268, 2014.

FERREIRA, T.; RASBAND, W. Image J User Guide, 2012. Available online: <<https://imagej.nih.gov/ij/docs/guide/user-guide.pdf>>. Accessed in 15 nov 2017.

FISCH, G.; MARENGO, J. A.; NOBRE, C. A. Clima da Amazônia. **Climanálise**, edição comemorativa de 10 anos, seção 3, 1996.

FRAUND, M.; PHAM, D. Q.; BONANNO, D.; HARDER, T. H.; WANG, B.; BRITO, J.; SÁ, S. S.; CARBONE, S.; CHINA, S.; ARTAXO, P.; MARTIN, S. T.; POHLKER, C.; et al. Elemental Mixing State of Aerosol Particles Collected in Central Amazonia during GoAmazon2014/15. **Atmosphere**, 8 (173), 1-28, 2017.

FREI, T.; GASSNER, E. Climate change and its impact on birch pollen quantities and the start of the pollen season an example from Switzerland for the period 1969-2006. **International Journal of Biometeorology**. 52:667–74, 2008.

FRENZ, D. A. Comparing pollen and spore counts collected with the Rotorod Sampler and Burkard spore trap. **Annual Allergy Asthma Immunology**, 83, 341-349, 1999.

FRENZ D.; JOHANN J. **An introduction to sampling and identifying airborne pollen and fungus spores**, Multidata LLC, USA, 2001.

FRÖHLICH-NOWOISKY, J.; PICKERSGILL, D. A.; DESPRÉS, V. R.; PÖSCHL, U., High diversity of fungi in air particulate matter. **PNAS**, 106 (31), 12814 – 12819, 2009.

FUENTES, J. D.; CHAMECKI, M.; NASCIMENTO DOS SANTOS, R.; VON RANDOW, C.; STOY, P.; KATUL, G.; FITZJARRALD, D.; MANZI, A.; GERKEN, T.; TROWBRIDGE, A.; et al. Linking meteorology, turbulence, and air, chemistry in the Amazon rainforest. **Bulletin of American Meteorology Society**, 2329-2342, 2016.

GABEY, A. M.; GALLAGHER, M. W.; WHITEHEAD, J.; DORSEY, J. R.; KAYE, P. H.; STANLEY, W. R., Measurements and comparison of primary biological aerosol above and below a tropical forest canopy using a dual channel fluorescence spectrometer. **Atmospheric Chemistry and Physics**, 10, (10), 4453-4466, 2010.

GARSTANG, M.; SCALA, J.; GRECO, S.; HARRIS, R.; BECK, S.; BROWELL, E.; SACUSE, G.; GREGORY, G.; HILL, G.; SIMPSON, J.; TAO, W.; TORRE, A. Trace gas exchange and

convective transports over the Amazonian rainforest. **Journal of Geophysical Research**, 93, 1528-1550, 1988.

GINOUX, P.; PROSPERO, J. M.; GILL, T. E.; HSU, N. C.; ZHAO, M. Global-scale attribution of anthropogenic and natural dust sources and their emission rates based on MODIS Deep Blue aerosol products. **Reviews of Geophysics**, 50, RG3005, 2012.

GLOVSKY, M. M.; JACOBSON, K.; ZAKARIAN, S.; JENSEN, J.; MORAN, J.; TAYLOR, P.E. Meteorological Effects May Alter the Incidence of Rye-grass Pollen Related Asthma. **Journal of Allergy and Clinical Immunology**, 119 (1), 742, 2007.

GOUDIE, A. S. and MIDDLETON, N. J. Saharan dust storms: nature and consequences. **Earth-Science Reviews**, 56, 179-204, 2001.

GRAHAM, B.; GUYON, P.; TAYLOR, P. E.; ARTAXO, P.; MAENHAUT, W.; GLOVSKY, M. M.; FLAGAN, R. C.; ANDREAE, M. O. Organic compounds present in the natural Amazonian aerosol: Characterization by gas chromatography-mass spectrometry. **Journal of Geophysical Research**, 108, 4766, 2003.

GRIMM, A. M. Interannual climate variability in South America: impacts on seasonal precipitation, extreme events, and possible effects of climate change. **Stochastic Environmental Research and Risk Assessment**, 25, 537–554, 2010.

GRIMM, A. M. The El Niño Impact on the Summer Monsoon in Brazil: Regional Processes versus Remote Influences. **Journal of Climate**, 16, 263-280, 2003.

GRIMM, A. M.; TEDESCHI, R. G. ENSO and Extreme Rainfall Events in South America. **Journal of Climate**, 22, 1589 – 1609, 2009.

GRIPST. Aerobiology Research Laboratories. Manual Rotation Impaction Sampler, 2009.

GROTE, M.; VRTALA, S.; NIEDERBERGER, V.; VALENTA, R.; REICHELT, R. Expulsion of allergen-containing materials from hydrated rye grass (*Lolium perenne*) pollen revealed by using immunogold field emission scanning and transmission electron microscopy. **Journal of Allergy and Clinical Immunology**, 105 (6), part 1, 2000.

GUNTHER, S. S.; KING, S. M.; ROSE, D.; CHEN, Q.; ROLDIN, P.; FARMER, D. K.; JIMENEZ, J. L.; ARTAXO, P.; ANDREAE, M. O.; MARTIN, S. T.; POSCHL, U. Cloud condensation nuclei in pristine tropical rainforest air of Amazonia: size resolved measurements and modeling of atmospheric aerosol composition and CNN activity. **Atmospheric Chemistry and Physics**, 9, 7551-7575, 2009.

HART, M.; WENTWORTH, J.; BAILEY, J.: The effects of trap height and weather variables on recorded pollen concentration at Leicester. **Grana**, 33, 100–103, 1994.

HASHIMOTO, H.; MELTON, F.; ICHII, K.; MILESI, C.; WANG, W.; NEMANI, R. R. Evaluating the impacts of climate and elevated carbon dioxide on tropical rainforests of the western Amazon basin using ecosystem models and satellite data. **Global Change Biology**, 16, 255-271, 2010.

HESSE, M.; HALBRITTER, H.; ZETTER, R.; WEBER, M.; BUCHNER, R.; FROSCH-RADIVO, A.; ULRICH, S. **Pollen Terminology: An illustrated handbook**. Springer Wien New York. University of Viena, Austria. 266p., 2009.

HOORNAERT, S.; GODOI, R. H. M.; GRIEKEN, R. V. Single particle characterization of aerosol in the marine boundary layer and free troposphere over Tenerife, NE Atlantic, during ACE-2. **Journal of Atmospheric Chemistry**, 46, 271-293, 2003.

HOOSE, C.; KRISTJANSSON, J. E.; BURROWS, S. M. How important is biological ice nucleation in clouds on a global scale? **Environmental Research Letters**, 5, 2010.

HOSPODSKY, D.; YAMAMOTO, N.; PECCIA, J. Accuracy, Precision, and Method Detection Limits of Quantitative PCR for Airborne Bacteria and Fungi. **Applied Environmental Microbiology**, 76(21), 7004–7012, 2010.

HUFFMAN, J. A.; PÖHLKER, C.; PRENNI, A. J.; DEMOTT, P. J.; MASON, R. H.; ROBINSON, N. H.; FRÖHLICH-NOWOISKY, J.; TOBO, Y.; DESPRÉS, V. R.; GARCIA, E.; et al. High concentrations of biological aerosol particles and ice nuclei during and after rain. **Atmospheric Chemistry and Physics Discussions**, 13: 1767-1793, 2013.

HUSSEIN, T.; NORROS, V.; HAKALA, J.; PETAJA, T.; AALTO, P. P.; RANNIK, U.; VESALA, T.; OVASKAINEN, O., Species traits and inertial deposition of fungal spores. **Journal of Aerosol Science**, 61, 81-98, 2013.

IAA. Manual for Aerobiology. 12th European course on basic aerobiology. International Association for Aerobiology. July 2015.

IPCC. Summary for Policymakers. In SOLOMON, S.; QIN, D.; MANNING, M.; CHEN, Z.; MARQUIS, M.; AVERYT, K. B.; TIGNOR M., MILLER, H. L. (Eds.), **Climate Change 2007: The Physical Science Basis**. Contribution of Working Group I to the Fourth Assessment Report of the Intergovernmental Panel on Climate Change, Cambridge, 2007.

IPPC. Climate Change 2013: The Physical Science Basis. 2013.

JAENICKE, R. Abundance of cellular material and proteins in the atmosphere. **Science**, 308, 73, 2005.

JATO, V.; RODRIGUEZ-RAJO, F. J.; SEIJO, M. C.; AIRA, M. J. Poaceae pollen in Galicia (N.W. Spain): characterization and recent trends in atmospheric pollen season. **International Journal of Biometeorology**, 2009.

JEOL. User's Manual for Scanning Electron Microscope. 2017.

KAGEN, S.; LEWIS, W.; LEVETIN, E. **Aeroallergen Photo Library**: The classic collection transcribed. 2005.

KAPP, R. O. **How to know Pollen and Spores**, 3rd ed., Brown Company Publishers, Washington, 250 p., 1975.

KOEHLER, K. A.; DEMOTT, P. J.; KREIDENWEIS, S. M.; POPOVICHEVA, O. B.; PETTERS, M. D.; CARRICO, C. M.; KIREEVA, E. D.; KHOKHLOVA, T. D.; SHONIJA, N. K. Cloud condensation nuclei and ice nucleation activity of hydrophobic and hydrophilic soot particles. **Physical Chemistry Chemical Physics**, 11, 7906-7920, 2009.

KRUPINSKA, B.; WOROBIEC, A.; ROTONDO, G. G.; NOVAKOVIC, V.; KONTOZOVA, V.; RO, C.; VAN GRIEKEN, R.; DE WAEL, K. Assessment of the air quality (NO₂, SO₂, O₃ and particulate matter) in the Plantin-Moretus Museum/Print Room in Antwerp, Belgium, in different seasons of the year. **Microchemical Journal**, 102, 49–53, 2012.

LACEY, M. E.; WEST, J. S. **The air Spora: A manual for catching and identifying airborne biological particles**. Springer, Dordrecht, The Netherlands, 156p., 2006.

LEONTIDOU, K.; VERNESI, C.; GROEVE, J. De; CRISTOFOLINI, F.; VOKOU, D.; CRISTOFORI, A. Taxonomic identification of airborne pollen from complex environmental

samples by DNA metabarcoding: a methodological study for optimizing protocols. **Bio R xiv**, 2017.

LEWIS, S. L.; MALHI, Y.; PHILLIPS, O. L. Fingerprinting the impacts of global change on tropical forests. *Philosophical Transactions of the Royal Society of London, Series B. Biological Sciences*, 359, 437-462, 2004.

LONGO, A. F.; FENG, Y.; LAI, B.; LANDING, W. M.; SHELLEY, R. U.; NENES, A.; MIHALOPOU-LOS, N.; VIOLAKI, K.; INGALL, E. D. Influence of Atmospheric Processes on the Sol-ubility and Composition of Iron in Saharan Dust. **Environmental Science Technol.**, 50 (13), 6912-6920, 2016.

LOWRY, G. V.; GREGORY, K. B.; APTE, S. C.; LEAD, J. R. Transformations of nanomaterials in the environment. **Environmental Science and Tecnology**, 46, 6893-6899, 2012.

MAENHAUT, W.; CORNILLE, P.; PACYNA, J. M.; VITOLS, V. Trace element composition and origin of the atmospheric aerosol in the Norwegian Arctic. **Atmospheric Environment**, 23, 2551 -2569, 1989.

MANDRIOLI, P.; NEGRINI, M. G.; CESARI, G.; MORGAN, G. Evidence for long-range transport of biological and anthropogenic aerosol particles in the atmosphere. **Grana**, 23, 43–53, 1984.

MAHOWALD, N. M.; ENGELSTAEDTER, S.; LUO, C.; SEALY, A.; ARTAXO, P.; BENITEZ-NELSON, C.; BONNET, S.; CHEN, Y.; CHUANG, P. Y.; COHEN, D. D.; et al. Atmospheric Iron Deposition: Global Distribution, Variability, and Human Perturbations. **Annual Review of Marine Science**, 1, 245-78, 2009.

MARTIN, S. T.; ANDREAE, M. O.; ARTAXO, P.; BAUMGARDNER, D.; CHEN, Q.; GOLDSTEIN, A. H.; GUENTHER, A.; HEALD, C. L.; MAYOL-BRACERO, O. L.; et al. Sources and properties of Amazonian aerosol particles. **Reviews of Geophysics**, 48, 2010.

MIKHAILOV, E. F.; MIRONOV, G. N.; POHLER, C.; CHI, X.; KRUGER, M. L.; SHIRAIWA, M.; FORSTER, J. D.; POSCHL, U.; VLASENKO, S. S.; RYSHKEVISH, T. I.; et al. Chemical composition, microstructure, and hygroscopic properties of aerosol particles at the Zotino Tall Tower Observatory (ZOTTO), Siberia, during a summer campaign. **Atmospheric Chemistry and Physics**, 15, 8847-8869, 2015.

MIMS, S. A.; MIMS, F. M. Fungal spores are transported long distances in smoke from biomass fires. **Atmospheric Environment**, 38, 5, 651-655, 2004.

MÖHLER, O.; DEMOTT, P. J.; VALI, G.; LEVIN, Z. Microbiology and atmospheric processes: the role of biological particles in cloud physics. **Biogeosciences**, 4, 1059-1071, 2007.

MOORE, P. D.; WEBB, J. A.; COLLINSON, M.E. **Pollen Analysis**. 2nd ed., Blackwell Scientific Publications, 216 p., 1991.

MORTIMER, A. Microscope basics and beyond - vol. 1. *Scanning*, 26(4), 204-206, 2004.

NOH, Y. M.; LEE, H.; MUELLER, D.; LEE, K.; SHIN, D.; SHIN, S.; CHOI, T. J.; CHOI, Y. J.; KIN, K. R. Investigation of the diurnal pattern of the vertical distribution of pollen in the lower troposphere using LIDAR. **Atmospheric Chemistry and Physics**, 13, 7619-7629, 2013.

NORBY, R. J.; ZAK, D. R. Ecological lessons from free-air CO₂ enrichment (FACE) experiments. **Annual Review of Ecology, Evolution, and Systematics**, 42, 181-203, 2011.

- OMETTO, J.; NOBRE, A.; ROCHA, H.; ARTAXO, P.; MARTINELLI, L. Amazonia and the modern carbon cycle: lessons learned. **Oecologia**, 143(4), 483-500, 2005.
- PAULIQUEVIS, T.; LARA, L. L.; ANTUNES, M. L.; ARTAXO, P. Aerosol and precipitation chemistry measurements in a remote site in Central Amazonia: the role of biogenic contribution. **Atmospheric Chemistry and Physics**, 12, 4987-5015, 2012.
- PENNER, J. E. Carbonaceous aerosols influencing atmospheric radiation: black and organic Carbon. In: **Aerosol Forcing of Climate**, John Wiley and Sons, Chichester, 108 p., 1995.
- PERRAUD, V.; BRUNS, E. A.; EZELL, M. J.; JOHNSON, S. N.; YU, Y.; ALEXANDER, M. L. ZELNYUK, A.; IRME, D.; CHANG, W. L.; DABDUB, D.; PANKOW, J. F.; FINLAYSON-PITTS, B. J. Nonequilibrium atmospheric secondary organic aerosol formation and growth. **PNAS**, 109 (8), 2836-2841, 2012.
- PETTERS, M. D.; KREIDENWEIS, S. M. A single parameter representation of hygroscopic growth and cloud condensation nucleus activity. **Atmospheric Chemistry and Physics**, 7, 1961-1971, 2007.
- PHILLIPS, O. L.; ARAGAO, L. E. O. C.; LEWIS, S. L. Drought sensitivity of the Amazon rainforest. **Science**, 323, 1344-1347, 2009.
- PÖHLKER, C.; WIEDEMANN, K. T.; SINHA, B.; SHIRAIWA, M.; GUNTHER, S. S.; SMITH, M.; SU, H.; ARTAXO, P.; CHEN, Q.; CHENG, Y.; ELBERT, W.; GILLES, M. K.; et al. Biogenic Potassium Salt Particles as Seeds for Secondary Organic Aerosol in the Amazon. **Science**, 337 (6098), 1075-1078, 2012.
- POPE, F. D. Pollen grains are efficient cloud condensation nuclei. **Environmental Research Letters**, 5, 1–6, 2010.
- PORSBJERG, C.; RASMUSSEN, A.; BACKER, V. Airborne pollen in Nuuk, Greenland, and the importance of meteorological parameters. **Aerobiologia**, 19, 29–37, 2003.
- PÖSCHL, U. Atmospheric aerosols: Composition, transformation, climate and health effects. **Angewandte Chemie - International Edition**, 44, 7520–7540, 2005.
- PÖSCHL, U.; MARTIN, S. T.; SINHA, B.; CHEN, Q.; GUNTHER, S. S.; HUFFMAN, J. A.; BORRMANN, S.; FARMER, D. K.; GARLAND, R. M.; HELAS, G.; JIMENEZ, J. L.; KING, S. M.; et al. Rainforest Aerosols as Biogenic Nuclei of Clouds and Precipitation in the Amazon. **Science**, 329, 1513-1516, 2010.
- PROSPERO, J. M.; COLLARD, F. X.; MOLINIE, J.; JEANNOT, A. Characterizing the annual cycle of African dust transport to the Caribbean Basin and South America and its impact on air quality and the environment. **Global Biogeochemistry Cycles**, 29, 757-773, 2014.
- RAVELO-PÉREZ, L. M.; RODRÍGUEZ, S.; GALINDO, L.; GARCÍA, M. I.; ALASTUEY, A.; LÓPEZ-SOLANO, J. Soluble iron dust export in the high altitude Saharan Air Layer. **Atmospheric Environment**, 133:49-59, 2016.
- RAO, Z.; HUA, D.; HE, T.; WANG, Q.; LE, J. Ultraviolet laser-induced fluorescence lidar for pollen detection. **Optik**, 136, 497-502, 2017.
- RAYNOR, G. S.; OGDEN, E. C.; HAYES, J. V. Variation in ragweed pollen concentration to a height of 108 meters, **Journal of Allergy and Clinical Immunology**, 51, 199–207, 1973.
- REHBEIN, A.; AMBRIZZI, T.; MECHOSO, C. R. Mesoscale convective systems over the Amazon basin. Part I: climatological aspects. **International Journal of Climatology**, 38, 215-229, 2018.

REMPE, H. Untersuchungen u"ber die Verbreitung des Blutenstaubes durch die Luftstr"omungen. **Planta**, 27, 93-147, 1937.

RIZZOLO, J. A.; BARBOSA, C. G. G.; BORILLO, G. C.; GODOI, A. F. L.; SOUZA, R. A. F.; ANDREOLI, R. V.; MANZI, A. O.; S"Á, M. O.; ALVES, E. G.; P"ÖHLKER, C.; ANGELIS, I. H.; et al. Soluble iron nutrients in Saharan dust over the central Amazon rainforest. **Atmospheric Chemistry and Physics**, 17, 2673-2687, 2017.

RYDER, C. L.; McQUAID, J. B.; FLAMANT, C.; ROSENBERG, P. D.; WASHINGTON, R.; BRINDLEY, H. E.; HIGHWOOD, E. J.; MARSHAM, J. H.; PARKER, D. J.; TODD, M. C.; et al. Advances in understanding mineral dust and boundary layer processes over the Sahara from Fennec aircraft observations. **Atmospheric Chemistry and Physics**, 15, 8479-8520, 2015.

ROGERS, C. A.; WAYNE, P. M.; MACKLIN, E. A.; MUILENBERG, M. L.; WAGNER, C. J.; EPSTEIN, P. R.; BAZZAZ, F. A. Interaction of the onset of spring and elevated atmospheric CO₂ on ragweed (*Ambrosia artemisiifolia* L.) pollen production. **Environmental Health Perspectives**. 114: 865–869, 2006.

SALVADOR, P., ALMEIDA, S. M., CARDOSO, J., ALMEIDA-SILVA, M., NUNES, T., CERQUEIRA, M., ALVES, C., REIS, M. A., CHAVES, P. C., ARTÍÑANO, B.; PIO, C. Composition and origin of PM₁₀ in Cape Verde: characterization of long-range transport episodes. **Atmospheric Environment**, 127, 326-339, 2016.

SANDRADEWI, J.; PREVOT, A. S. H.; SZIDAT, S.; PERRON, N.; ALFARRA, M. R.; LANZ, V. A.; WEINGARTNER, E.; BALTENSBERGER, U. Using Aerosol Light Absorption Measurements for the Quantitative Determination of Wood Burning and Traffic Emission Contributions to Particulate Matter. **Environmental Science and Technology**, 42, 3316-3323, 2008.

SICARD, M.; IZQUIERDO, R.; ALARCON, M.; BELMONTE, J.; COMERON, A.; BALDASANO, J. Near-surface and columnar measurements with a micro pulse lidar of atmospheric pollen in Barcelona, Spain. **Atmospheric Chemistry and Physics**, 16, 6805-6821, 2016.

SILVER, J. D.; SUTHERLAND, M. F.; JOHNSTON, F. H.; LAMPUGNANI, E. R.; MCCARTHY, M. A.; JACOBS, S. J.; PEZZA, A. B.; NEWBIGIN, E. J. Seasonal asthma in Melbourne, Australia, and some observations on the occurrence of thunderstorm asthma and its predictability. **Plos One**, 1 – 24, 2018.

SCHNEIDER, C.A.; RASBAND, W.S.; ELICEIRI, K.W. NIH Image to ImageJ: 25 years of image analysis. **Nature Methods**, 9, 671-675, 2012.

SOLDEVILLA, C. G.; TENO, P. C. G. P. A.; VILCHES, E. D. **Spanish Aerobiology Network (REA): Management and Quality Manual**. Servicio De Publicaciones De La Universidad de Córdoba, Campus de Rabanales, 2007.

STEINER, A. L.; BROOKS, S. D.; DENG, C.; THORNTON, D. C. O.; PENDLETON, M. W.; BRYANT, V. Pollen as atmospheric cloud condensation nuclei. **Geophysical Research Letters**, 42, 3596-3602, 2015.

STULL, R. B. **An introduction to boundary layer meteorology**. Kluwer Academic Publishers, Dordrecht, The Netherlands, 670p., 2003.

STULL, R. B. **Meteorology for Scientists and Engineers**, 3rd ed., Univ. of British Columbia, 938 p., 2011.

SUN, J.; ARIYA, P. A. Atmospheric organic and bio-aerosols as cloud condensation nuclei (CCN): A review. **Atmospheric Environment**, 40, 795–820, 2006.

TAKAHASHI, Y.; KAWASHIMA, S.; SUZUKI, Y.; OHTA, N.; KAKEHATA, S. Enrichment of airborne Japanese cedar pollen in mountain ranges when passing through a front accompanying temperate low pressure. **Aerobiologia**, 34, 105 – 110, 2018.

TALBOT, R. W.; ANDREAE, M. O.; BERRESHEIM, H.; ARTAXO, P.; GARSTANG, M.; HARRISS, R. C.; BEECHER, K. M.; LI, S. M. Aerosol chemistry during the wet season in Central Amazonia: The influence of long-range transport. **Journal of Geophysical Research**, 95, 16,955-16,969, 1990.

TAYLOR, P. E.; FLAGAN, R. C.; MIGUEL, A. G.; VALENTA, R.; GLOVSKY, M. M. Birch pollen rupture and the release of aerosols of reparable allergens. **Clinical and Experimental Allergy**, 34, 1591–1596, 2004.

TAYLOR, P. E.; JONSSON, H. Thunderstorm asthma. **Current Allergy and Asthma Reports**, 4, 409–413, 2004.

TAYLOR, G. E.; JOHNSON, D. W.; ANDERSEN, C. P. Air Pollution and Forest Ecosystems: A Regional to Global Perspective. **Ecological Applications**, 4: 662–689, 1994.

TEDESCHI, R. G.; CAVALCANTI, R. F. A.; GRIMM, A. M. Influences of two types of ENSO on South American precipitation. **International Journal of Climatology**, 2012.

TIMOKHINA, A. V.; PROKUSHKIN, A. S.; ONUCHIN, A. A.; PANOV, A. V.; KOFMAN, G. B.; VERKHOVETS, S. V.; HEIMANN, M. Long-term trend in CO₂ concentration in the surface atmosphere over Central Siberia. **Russian Meteorology and Hydrology**, 40, 186-190, 2015.

TOLLEFSON, J. A towering experiment. **Nature**, 467, 2010.

TRAIL, F.; XU, H.; LORANGER, R.; GADOURY, D. Physiological and environmental aspects of ascospore discharge in *Gibberella zeae* (anamorph *Fusarium graminearum*). **Mycologia**, 94, 181–189, 2002.

TRAPP, J. M.; MILLERO, F. J.; PROPERO, J. M. Trends in the solubility of iron in dust-dominated aerosol in the equatorial Atlantic trade winds: importance of iron speciation and sources. **Geochemistry Geophysics Geosystems**, 11(3), 2010.

VAIDYANATHAN, V.; MIGUEL, A. G.; TAYLOR, P. E.; FLAGAN, R. C.; GLOVSKY, M. M. Effects of electric fields on pollen rupture. **Journal of allergy and clinical immunology**, 117(2), S157-S157, 2006.

VÁZQUEZ, L.; GALAN, C.; DOMINGUEZ-VILCHES, E. Influence of meteorological parameters on olea pollen concentrations in Córdoba (South-western Spain). **International Journal of Biometeorology**, 48, 83–90, 2003.

WANG, J.; KREJCI, R.; GIANGRANDE, S.; KUANG, C.; BARBOSA, H. M. J.; BRITO, J.; CARBONE, S.; CHI, X.; COMSTOCK, J.; DITAS, F.; LAVRIC, J.; MANNINEN, H. E.; et al. Amazon boundary layer aerosol concentration sustained by vertical transport during rainfall. **Nature**, 539, 2016.

WINIWARTER, W.; BAUER, H.; CASEIRO, A.; PUXBAUM, H. Quantifying emissions of primary biological aerosol particle mass in Europe. **Atmospheric Environment**, 43, 1403-1409, 2009.

WOMACK, A. M.; ARTAXO, P. E.; ISHIDA, F. Y.; MUELLER, R. C.; SALESKA, S. R.; WIEDEMANN, K. T.; BOHANNAN, B. L. M.; GREEN, J. L. Characterization of active and total fungal communities in the atmosphere over the Amazon rainforest. **Biogeosciences**, 12, 6337-6349, 2015.

WOROBIEC, A.; SZALÓKI, I.; OSÁN, J.; MAENHAUT, W.; STEFANIAK, E. A.; GRIEKEN, R. V. Characterization of Amazon Basin aerosols at the individual particle level by X-ray microanalytical techniques. **Atmospheric Environment**, 41, 9217-9230, 2007.

YAMAGUCHI, N.; ICHIJO, T.; SAKOTANI, A.; BABA, T.; NASU, M. Global dispersion of bacterial cells on Asian dust. **Science Report**, 2, 525, 2012.

YAMASOE, M. A.; ARTAXO, P.; MIGUEL, A. H.; ALLEN, A. G. Chemical composition of aerosol particles from direct emissions of vegetation trees in the Amazon Basin: water-soluble species and trace elements. **Atmospheric Environment**, 34, 1641-1653, 2000.

YU, H.; CHIN, M.; YUAN, T.; BIAN, H.; REMER, L. A.; PROSPERO, J. M.; OMAR, A.; WINKER, D.; YANG, Y.; ZHANG, Y.; ZHANG, Z.; ZHAO, C. The fertilizing role of African dust in the Amazon rainforest: A first multiyear assessment based on data from Cloud-Aerosol Lidar and Infrared Pathfinder Satellite Observations. **Geophysical Research Letters**, 42, 1984-1991, 2015.

ZHANG, R.; DUHK, T.; SALAM, M. T.; HOUSE, J. M.; FLAGAN, R. C.; AVOL, E. L.; GILLILAND, F. D.; GUENTHER, A.; CHUNG, S. H.; LAMB, B. K.; VANREKEN, T. M. Development of a regional-scale pollen emission and transport modeling framework for investigating the impact of climate change on allergic airway disease. **Biogeosciences**, 11, 1461-1478, 2014.

ZHANG, Z.; ENGLING, G.; ZHANG, L.; KAWAMURA, K.; YANG, Y.; TAO, J.; ZHANG, R.; CHAN, C.; LI, Y. Significant influence of fungi on coarse carbonaceous and potassium aerosols in a tropical rainforest. **Environmental Research Letters**, 10, 034015, 2015.

ZHAO, H.; CHE, H.; ZHANG, X.; MA, Y.; WANG H.; WANG Y. Characteristics of visibility and particulate matter (PM) in an urban area of Northeast China. **Atmospheric Pollution Research**, 4, 427-434, 2013.

ZHOU, Q. Relative Humidity induced plant pollen grain rupture and conceptual model development. Master's dissertation. Washington State University. Department of Civil and Environmental Engineering, 2014.

ZISKA, L.; KNOWLTON, K.; ROGERS, C.; DALAN, D.; TIERNEY, N.; ELDER, M. A.; FILLEY, W.; SHROPSHIRE, J.; FORD, L. B.; HEDBERG, C.; FLEETWOOD, P. et al. Recent warming by latitude associated with increased length of ragweed pollen season in central North America. **Proceedings of the National Academy of Sciences**, 108, 4248-4251, 2011.

ZISKA, L. H.; EPSTEIN, P.R.; ROGERS, C. A. Climate change, aerobiology, and public health in the Northeast United States. **Mitigation and Adaptation Strategies for Global Change**, 13, 607-613, 2008.

APPENDIX A: ADHESIVE RECIPE AND PREPARATION

The adhesive substance responsible for fixing the particles onto the tape can be chosen from a wide range of chemicals with a gelatine, silicone or vaseline base (FRENZ, 1999; KAGEN, LEWIS and LEVETIN, 2005; SOLDEVILLA et al, 2007; GRIPST, 2009). The final substance must be clear, sticky and transmissible to bright light (BURKARD, 2003).

The recipe chosen for this project was gelatine based, using agar (adhesive), glycerol (moisture), phenol (preservative) and ultrapure water. The proportions suggested in the literature were executed during the last 20 years in mid-latitudes (20 to 40°): 5 % agar, 20 % glycerol, 0.5 % phenol in ultrapure water to complete 100 % (TAYLOR et al, 2002).

The adhesive preparation steps are as follows: heat 90% of the ultrapure water at 60 °C in a glass bottle (heatproof), add the agar stirring gently until dissolved, remove the bottle from the heater and add the glycerol and phenol stirring until complete homogeneity. This substance is stored in a sealed bottle at room temperature. For the tape preparation before the sampling the substance should be heated until it becomes liquid and a thin layer spread on the Mellinex tape (cellophane) surface, leaving the borders clean to handle the tape and fixing it around the drum.

The mountant media used to attach the sampled tape to the glass slide after the sampling is prepared with 15 % Mowiol or Gelvatol (water soluble plastic), 25 % glycerol and 0.5 % phenol in ultrapure water solution. The preparation is similar to that of the adhesive: warm water with the mowiol (60 °C) until complete dissolution, first the glycerol is added and then the phenol, the mixture is stirred until completely homogeneous. The solution can be placed into small glass or plastic inert containers and stored at – 4 °C. A small aliquot is kept at room temperature for immediate use.

Regarding the adhesive substance, some challenges were faced during this project, but the mountant media's recipe worked well throughout the whole period. During the preliminary tests and upon first sampling, the adhesive started melting on the tape with the natural warm temperature (30 to 40 °C), so it was not working properly as an adhesive. Protocols had been developed for temperate zones, and this is the first time this sampling method was used in a tropical rainforest. The sampling region has an unusual characteristic for sampling as shown by its location near zero latitude, with high temperatures plus very high relative humidity. The texture of the first adhesive

(plane, smooth and firm at room temperature) changed as soon as the tape exposure started at the tower. Also, the preserving chemical (phenol) was not enough to actually prevent fungi growth.

Thus, some tests were made in a controlled environment, inside a foam cupboard with known temperature and humidity simulating the field conditions, in order to find a better combination of the components to allow the capture of the particles during the sampling. First of all, only phenol was added to the original adhesive recipe: 5 % agar, 20 % glycerol and 1.5 % phenol, but during the second sampling it also started to melt.

Then, more agar and glycerol were added to the mixture: 10 % agar, 30 % glycerol and 5 % phenol. This resulted in an adhesive resistant to heat, but with high humidity some fungi started growing just after the third sampling.

Another adhesive recipe, used for the last samplings, more resistant to heat and humidity simultaneously, was composed of: 20 % agar, 35 % glycerol and 10 % phenol. As the tape remained exposed from 1 to 7 days (replaced with rain occurrence), after the sampling a mixture of ethanol and phenol (30 %) was also sprayed onto the tape to prevent any growth.

This last recipe was used for sampling during wet and dry seasons and worked very well during the dry season above the canopy. But during the wet season with constant rain and humidity frequent at 100 % or during the dry season below the canopy, where the humidity is continuously high, and there is a lack of evapotranspiration, some issues such as melting and wrinkles still appeared.

The vaseline and silicon base, due to its temperature resistance, also starts melting in the range of the field conditions, so more tests with other chemical substances are necessary to develop the ideal adhesive recipe for both seasons that can maintain the moisture at the sample.

APPENDIX B: TOTAL PARTICULATE MATTER AND BIOGENIC FRACTION

During the 2016 dry season, a simultaneous sampling with fractionated fine particulate matter was carried out to investigate the dust composition classified as canopy debris from the pollen sampling.

In order to separate specific fractions of the total particulate matter, a cascade impactor (PIXE, Model I-1L, Tallahassee, USA) was installed connected to a vacuum pump with 1 L min^{-1} flow. This cascade-type sampler allows size fractionation of all particles from the income air. The sampler was connected to an inlet of 20 cm and protected from direct rain, in order to prevent water droplets impinging into the filters.

Fiberfilm filters (Pallflex, 25 mm diameter) were used as substrates on the following stages: 8, 4 and $2 \mu\text{m}$. A Mellinex tape with adhesive (gelatine based), as used in the pollen sampler, was placed atop the first stage, to retain particles with an aerodynamic diameter larger than $16 \mu\text{m}$.

Two sets of filters were sampled, each with 10 days of exposure. Also, a blank filter was kept for each set. The collected samples from the first stage were analysed by optical microscopy, and the rest were analysed by scanning electron microscopy.

The fiberfilm filters were weighed before and after sampling using a Sartorius micro-balance (MSA2.7S-000- DF) from Laboratory of Analysis and Air Quality (UFPR - Brazil), and then coated with carbon and analysed by Scanning electron microscopy (JEOL JSM-IT300) at the Microscopy Laboratory (Deakin University - Australia).

The optical microscopy has a magnification limitation due to the lens system. In order to access the morphology and also the composition of smaller particles, another type of microscopy, electron-based, can be used. The Scanning Electron Microscopy (SEM/EDX) provides information on elemental composition, size, and shape of the particles. Its operation consists of an electron-emitting source (electron beam) finely scanning the specimen surface generating various continuous signals as secondary electrons, backscattered electrons, Auger electrons and characteristic X-rays. The different signals produced by the interaction of the energy on the sample are detected, converted, amplified and simultaneously displayed for chemical composition and morphology of a microscopic volume in one single particle (KRUPINSKA et al., 2012; JEOL, 2017).

For the fractionated total particles collected in fiberfilm filters, the Scanning electron microscopy(e) - SEM - was chosen. The filters were analysed with a SEM

(JEOL JSM-IT300, Peabody, USA) using a Tungsten secondary electron detector (SED) and giving a resolution of 4 nm. The filters were previously placed on an aluminium stage using a thick layer of carbon tape and were also coated with carbon (Leica EM ACE 600, Macquarie Park, Australia) to conduct the electron beam through the sample. They were stored in a sealed container with silica to maintain low humidity.

The samples were analysed with an acceleration voltage of 20 kV in high vacuum to increase the sensitivity in the analysis of low Z elements, allowing double scanning to verify the beam stability. The X-ray spectra were captured and integrated using the AZ Tech software.

For the fiberfilm filters only one stage in the range of 2 μm was damaged (by visual inspection), and because it could be caused by handling, leading to contamination, this one was not analysed. The fiberfilm filters, rather one, were scanned for morphology and composition. The expanded uncertainty (BIPM, 2008) for the results is 5.4%.

The amount of specific biological particles on the Mellinex tape in the pollen trap are presented as daily averaged concentration on TABLE 4. Those results are higher than the ones sampled during wet season, but quite low regarding urban sites.

TABLE 4: Particle concentration sampled with Pollen trap during the dry season of 2016. Median results in number of particle per cubic meter of air, averaged over 24 h.

PERIOD	Pollen	Fungi	Fern	Soot	Debris	Total
17 th Sep 07 th Oct	25	812	11	78	2183	3011

The samples from 80 m height for the period were very clear with low particles density, as shown in FIGURE 42. Canopy debris were predominant, as occurred during the entire sampling period, followed by fungal spores, soot particles, pollen grains and fern spores. The total amount of collected particles was around 3000 particles m^{-3} averaged over 24 h.

The 2014 wet season (ANDREAE et al., 2015) showed the total number of PM₁₀ as 282 particles cm^{-3} in a seven-day period, and more than 1000 particles cm^{-3} during the dry season. On a daily basis, this corresponded to almost 2×10^7 particles m^{-3} over 24 h compared with 3000 found with this sampling that covered the size range of 3 to 100 μm .

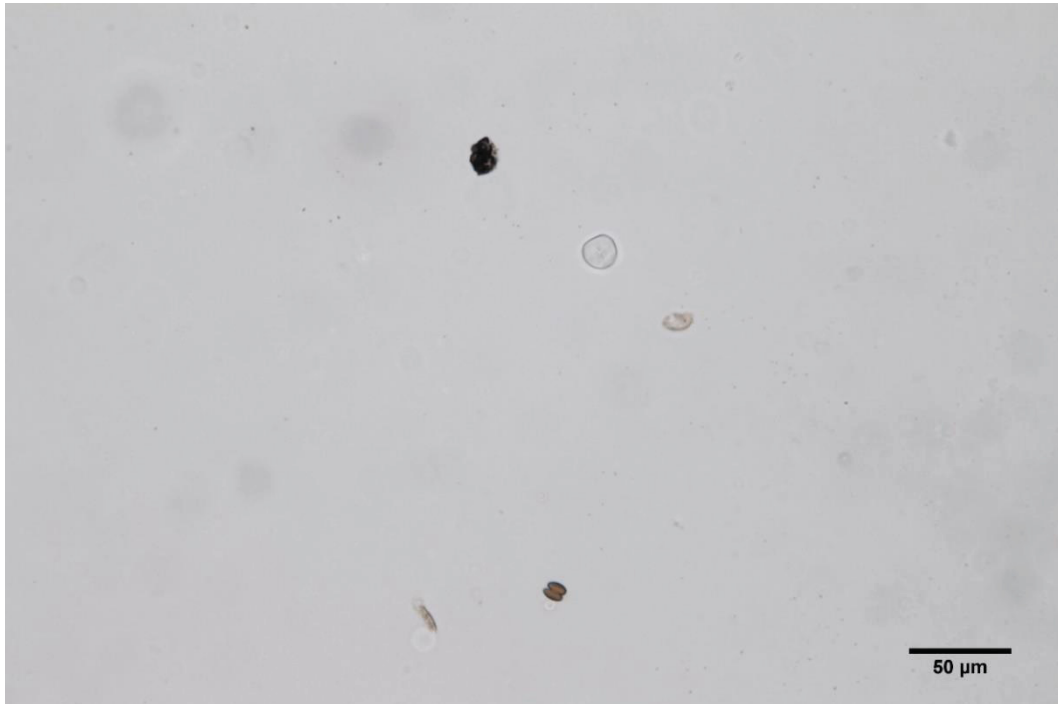


FIGURE 42: Example of a sample from 80 m height with the Pollen trap on the 26th of September 2016, 8h (local time).

The few particles observed could also have been influenced by marine and urban aerosols transported from the surroundings. The FIGURE 43 illustrates that during the 20-day period of sampling, the area received air masses from all directions, but mainly south-easterly, with wind speeds reaching 10 m s^{-1} .

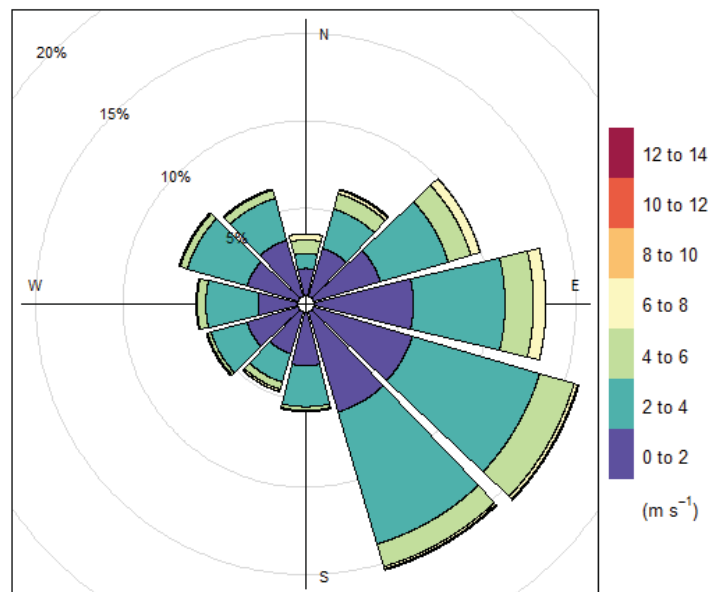


FIGURE 43: Wind rose from September 17th to October 7th 2016, at 80 m height.

The collected mass per cubic meter of air sampled in each period for the fractionated particulate matter in fiberfilm filter is shown in TABLE 5. Considering the sum of the last two stages as an approximation to PM₁₀, the results are quite low compared to a range from 500 to 2000 cm⁻³ (ANDREAE et al., 2015), previous recorded at the same site two years before, during September 2014. For that season, it is known that the PBAP dominates the coarse particle mode. (HUFFMAN et al., 2012; ANDREAE et al., 2015). Only particles in the range of 3.2 to 5.6 µm were measured by Fraund (et al, 2017), with a daily average count of 0.0011 particles m⁻³ and an organic fraction of 3.8 µg m⁻³.

From the first stage of tape and for both periods, the dominant particles observed were just canopy debris. Only around 4% (3.6% for the first period and 3.9% for the second period of sampling) were biological particles belonging to the fungi category. The number of pollen grains correspond to less than 1% of the particles collected at this first stage.

TABLE 5: Total particle concentration for fractionated particle sampling using the PIXE cascade impactor during the dry season of 2016.

Size range	Substrate	Particles Concentration	
		17 th Sep - 27 th Sep	27 th Sep - 07 th Oct
> 16 µm	Mellinex Tape	19 pollens m ⁻³	35 pollens m ⁻³
8 - 16 µm	Fiberfilm	0.6 µg m ⁻³	0.3 µg m ⁻³
4 - 8 µm	Fiberfilm	2.6 µg m ⁻³	2.8 µg m ⁻³
2 - 4 µm	Fiberfilm	-----*	2.9 µg m ⁻³
Blank	Fiberfilm	0.0 µg m ⁻³	0.0 µg m ⁻³

* filter excluded due to possible contamination.

Among the 5 samples, a total of 140 individual particles were analysed for elemental compounds. At the size range from 8 to 16 µm a total of 32 particles were analysed, 83 particles from 4 to 8 µm, and 25 particles from the lower stage. Elemental composition from the spectrum results will be presented as relative composition for all the samples.

The fiberfilm filter contained Fluorine (F) Silicon (Si) and oxygen compounds, with some minor elements, such as Sodium (Na), Barium (Ba), Zinc (Z), Aluminium (Al), Potassium (K) and Calcium (Ca). The filters were scanned in order to find particles with a composition different from the main ratio 2:1:1 for F, Si and O, the substrate

composition. C:O ratio could not be measured due to the coating of the samples with carbon.

Organic particles are mainly C O-containing, but as the samples were coated with carbon, all the results present some C fraction. Mineral particles can be identified when the elements O, Si and Al prevails. The biological ones show N, P, K, O, S and also C. Salt particles can be mainly Na or Mg-containing. Inorganic salts also can be present in fungal spores' fractions (PÖHLKER et al., 2012). Minor compounds as Fe, Mg, S, Ca can be present in almost all categories.

The filters from the stage 8 to 16 μm showed amorphous particles with mainly an oxygen element peak, FIGURE 44. The particles composition is mainly Si, Na, Zn, Ba, Ca or Al oxygen compounds, i.e., mainly organic and mineral particles were found at this stage. Al- and Si-containing (FIGURE 44 - right) are almost half of the analysed particles, followed salt particles (Na-containing). Two of the particles showed Potassium as the major element. Also, 6 % presented Iron as major compound ($> 15\%$ Fe), illustrated in FIGURE 44 (left).

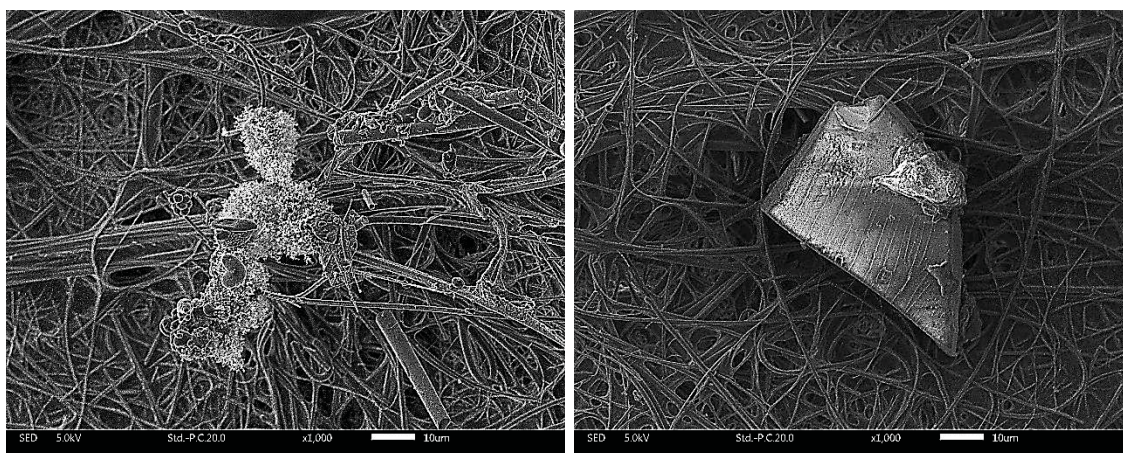


FIGURE 44: Images with 1000x magnification of particles from 8 to 16 μm sampled with fiberfilm filter, scale bar: 10 μm . Example of Iron-containing particles with minor oxygen compounds (left) and Si-, O-containing particle (right).

From the next stage, 4 to 8 μm , the particles peaked in O, N, Si and Na, with minor recurrent elements, such as Ba, Al, Zn, Ca, Cl, S and K. Organic and mineral elements prevails (FIGURE 45 – top left and right), also followed by salt elements with Na-, Mg- and Cl-compounds (FIGURE 45 –bottom left and right). Biological particles are present (FIGURE 45 – top left), Potassium and Iron containing particles were also sampled in this range (FIGURE 46).

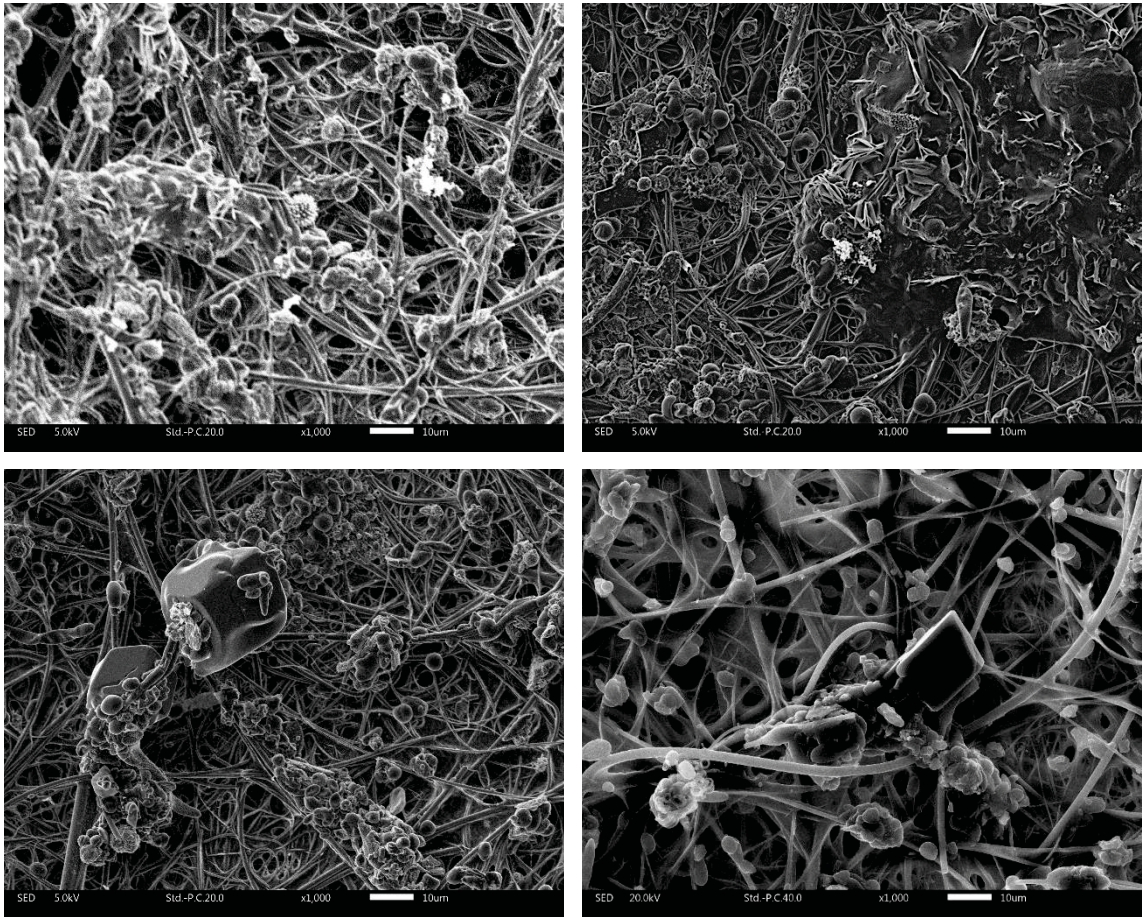


FIGURE 45: Images with 1000x magnification of particles from 4 to 8 μm sampled with fiberfilm filter, scale bar: 10 μm. Example of biological particles (top left), Si-, O-, N-containing particles (top right), salt and mineral particles (bottom left and right).

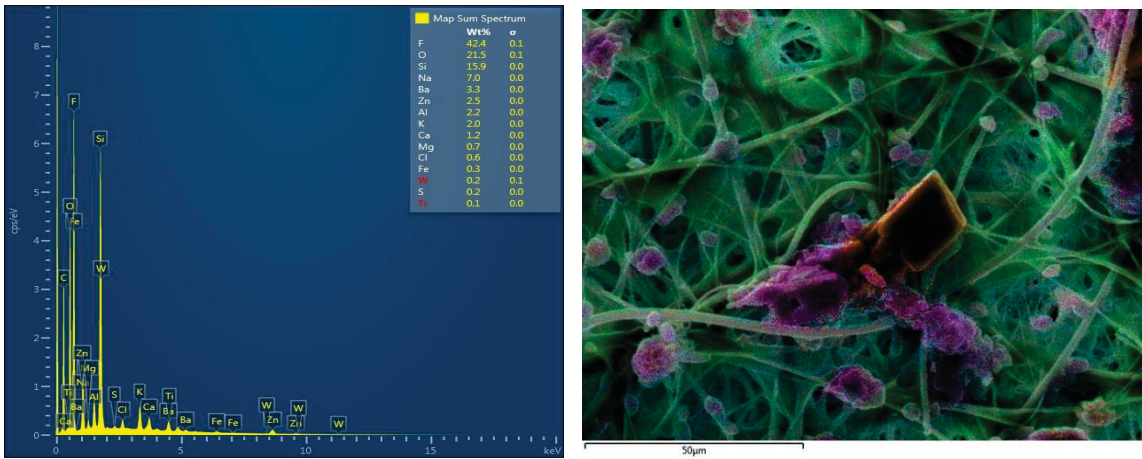


FIGURE 46: Elemental composition spectrum (left) from the central particle (left) and colour image highlighting K-(orange), Na-(yellow), Mg-(purple) containing particle (right).

Particles with Na, Si and Al represent 50 % of the total number of particles analyzed. Cl, K and Fe also appeared, but at a lesser frequency. In a previous study, during the 2014 dry season (FRAUND et al, 2017), organic compounds were found to

be the major constituent. Ammonium, Chloride, Nitrate, Sulfate and Black carbon were also quantified only in the range of 3.2 to 5.6 μm , where fragments of fungal spores were found above and below the canopy (CHINA et al., 2016).

For the sample in the range of 2 to 4 μm , mainly amorphous carbonaceous, mineral and salt particles were found (FIGURE 47). Minor elements quantified were Fe, Mg, Al, Ba, Cl, K, Mg, Ca, Zn and S. From the 25 particles analysed, 2 had more than 10 % Iron. Potassium is less than 2 % by composition of all particles. Nitrogen appeared just once, also as a minor compound.

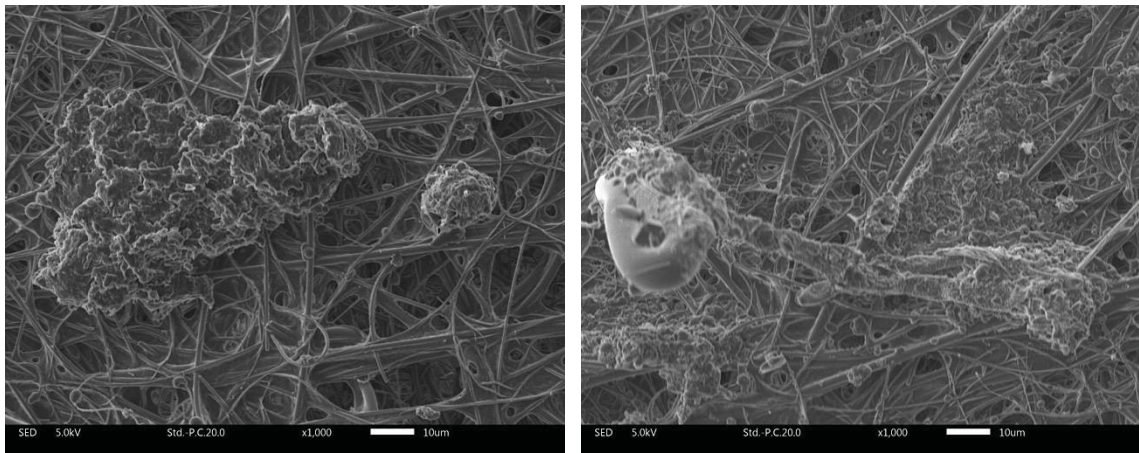


FIGURE 47: Images with 1000x magnification of particles from 2 to 4 μm sampled with fiberfilm filter, scale bar: 10 μm . Example of C-, O-containing amorphous particles (left), and Si-, O-, Na- and Mg-containing particles (right).

From the 140 single particles analysed for elemental composition it was determined that the sampled particles can be qualitatively classified as organic and biological, followed by mineral and finally salt particles. This main relative composition is similar for all the stages from 2 to 16 μm , as shown in TABLE 6.

TABLE 6: Relative cluster classification of single particles in the range of 2 to 16 μm sampled at 80 m height during 2016 dry season. Results in percentage (%).

	Organic/Biological	Mineral	Salt
2 to 4 μm	56	28	16
4 to 8 μm	47	31	22
8 to 16 μm	47	41	12

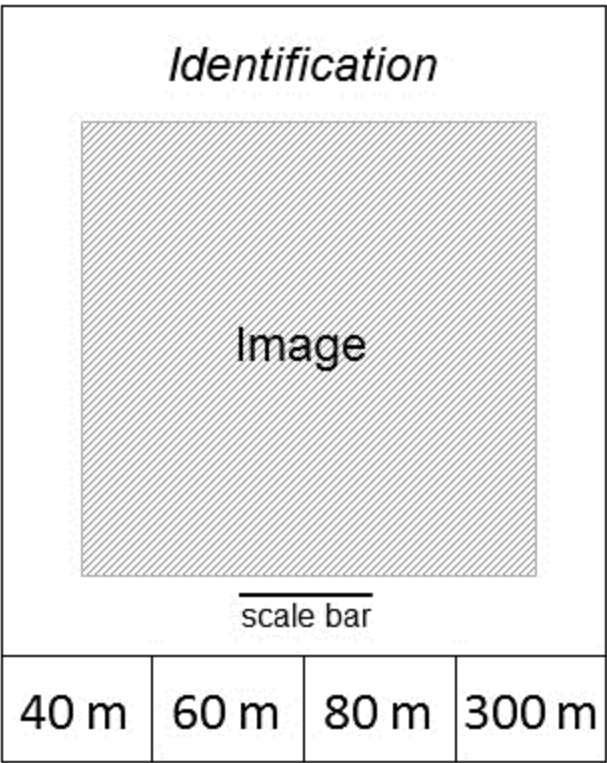
Canopy debris are the dominant type of particles in suspension (TABLE 4), in agreement with the prevalence of organic and biological microparticles, as shown by the SEM/X-ray data about the particles composition (TABLE 6). Those results spread

the scope for future investigations, aiming to identify and quantify the canopy compounds. A different technique is needed to fully characterize these coarse particles, e.g. to detect a potential dominance of micronic-sized wax and lipid leaf surface debris.









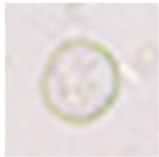

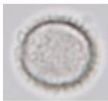

The results corroborate what was shown with the pollen sampler results. Almost 75 % of the samples content, classified as canopy debris can be formed by organic/biological material, mineral and salt particles, but mainly biological particles or fragments. Organic and biological particles accounted for half of the material sampled across the different size cuts from 2 to 16 μm . Combined analytical techniques can be used in a future work to assess the composition of the canopy debris, since this is the major component detected throughout the samples.

APPENDIX C: BIOAEROSOL ATLAS

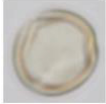

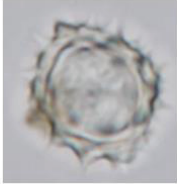
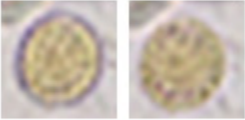
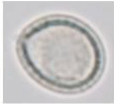

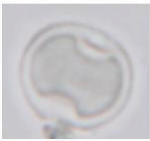
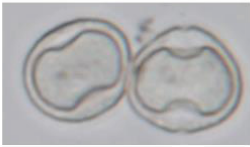




All the biological particles sampled were imaged at 400 x magnification with a 40 x objective lens, unstained. After categorization into broad types, an attempt was made to identify each pollen and fungal spore. The following pages show images of each particle without image color post-processing and with the respective scale bar (20 μm for pollen grains and 10 μm for spores), and at the bottom is the height(s) of occurrence marked in black. Each category is arranged in order from smallest to largest particle diameter. The images follow the format below:








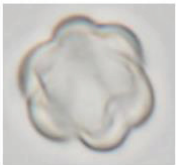


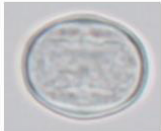



APPENDIX C.1: POLLEN GRAINS (1/10)

<div><p><i>Moraceae</i></p><p>20 μm</p></div> <div><div>40 m</div><div>60 m</div><div>80 m</div><div>300 m</div></div>	<div><p><i>Fabaceae</i></p><p>20 μm</p></div> <div><div>40 m</div><div>60 m</div><div>80 m</div><div>300 m</div></div>	<div><p><i>Fabaceae</i></p><p>20 μm</p></div> <div><div>40 m</div><div>60 m</div><div>80 m</div><div>300 m</div></div>
<div><p><i>Fabaceae</i></p><p>20 μm</p></div> <div><div>40 m</div><div>60 m</div><div>80 m</div><div>300 m</div></div>	<div><p><i>Moraceae</i></p><p>20 μm</p></div> <div><div>40 m</div><div>60 m</div><div>80 m</div><div>300 m</div></div>	<div><p><i>Moraceae</i></p><p>20 μm</p></div> <div><div>40 m</div><div>60 m</div><div>80 m</div><div>300 m</div></div>
<div><p><i>Identification</i></p><p>20 μm</p></div> <div><div>40 m</div><div>60 m</div><div>80 m</div><div>300 m</div></div>	<div><p><i>Asteraceae</i></p><p>20 μm</p></div> <div><div>40 m</div><div>60 m</div><div>80 m</div><div>300 m</div></div>	<div><p><i>Identification</i></p><p>20 μm</p></div> <div><div>40 m</div><div>60 m</div><div>80 m</div><div>300 m</div></div>
<div><p><i>Identification</i></p><p>20 μm</p></div> <div><div>40 m</div><div>60 m</div><div>80 m</div><div>300 m</div></div>	<div><p><i>Asteraceae</i></p><p>20 μm</p></div> <div><div>40 m</div><div>60 m</div><div>80 m</div><div>300 m</div></div>	<div><p><i>Fabaceae</i></p><p>20 μm</p></div> <div><div>40 m</div><div>60 m</div><div>80 m</div><div>300 m</div></div>

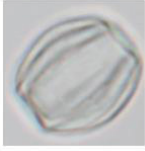







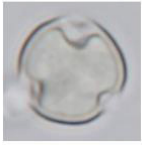
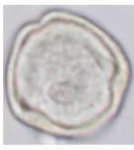
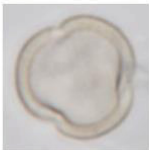
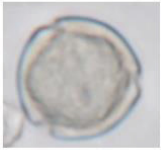
POLLEN GRAINS (2/10)

<p><i>Euphorbiaceae</i></p>  <p>20 μm</p> <p>40 m 60 m 80 m 300 m</p>	<p><i>Malpighiaceae</i></p>  <p>20 μm</p> <p>40 m 60 m 80 m 300 m</p>	<p><i>Identification</i></p>  <p>20 μm</p> <p>40 m 60 m 80 m 300 m</p>
<p><i>Asteraceae</i></p>  <p>20 μm</p> <p>40 m 60 m 80 m 300 m</p>	<p><i>Identification</i></p>  <p>20 μm</p> <p>40 m 60 m 80 m 300 m</p>	<p><i>Moraceae</i></p>  <p>20 μm</p> <p>40 m 60 m 80 m 300 m</p>
<p><i>Identification</i></p>  <p>20 μm</p> <p>40 m 60 m 80 m 300 m</p>	<p><i>Identification</i></p>  <p>20 μm</p> <p>40 m 60 m 80 m 300 m</p>	<p><i>Identification</i></p>  <p>20 μm</p> <p>40 m 60 m 80 m 300 m</p>
<p><i>Caesalpinaceae</i></p>  <p>20 μm</p> <p>40 m 60 m 80 m 300 m</p>	<p><i>Identification</i></p>  <p>20 μm</p> <p>40 m 60 m 80 m 300 m</p>	<p><i>Caesalpinaceae</i></p>  <p>20 μm</p> <p>40 m 60 m 80 m 300 m</p>



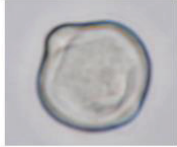

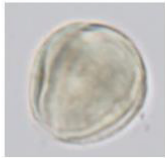



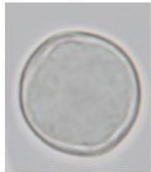

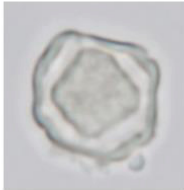

POLLEN GRAINS (3/10)

<p><i>Arecaceae</i></p>  <p>20 μm</p> <p>40 m 60 m 80 m 300 m</p>	<p><i>Identification</i></p>  <p>20 μm</p> <p>40 m 60 m 80 m 300 m</p>	<p><i>Malpighiaceae</i></p>  <p>20 μm</p> <p>40 m 60 m 80 m 300 m</p>
<p><i>Identification</i></p>  <p>20 μm</p> <p>40 m 60 m 80 m 300 m</p>	<p><i>Euphorbiaceae</i></p>  <p>20 μm</p> <p>40 m 60 m 80 m 300 m</p>	<p><i>Meliaceae</i></p>  <p>20 μm</p> <p>40 m 60 m 80 m 300 m</p>
<p><i>Sapindaceae</i></p>  <p>20 μm</p> <p>40 m 60 m 80 m 300 m</p>	<p><i>Myrtaceae</i></p>  <p>20 μm</p> <p>40 m 60 m 80 m 300 m</p>	<p><i>Identification</i></p>  <p>20 μm</p> <p>40 m 60 m 80 m 300 m</p>
<p><i>Meliaceae</i></p>  <p>20 μm</p> <p>40 m 60 m 80 m 300 m</p>	<p><i>Identification</i></p>  <p>20 μm</p> <p>40 m 60 m 80 m 300 m</p>	<p><i>Meliaceae</i></p>  <p>20 μm</p> <p>40 m 60 m 80 m 300 m</p>


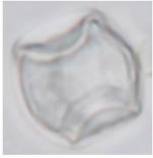
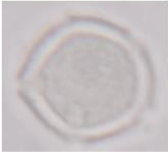


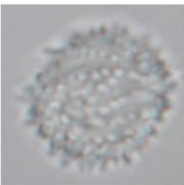
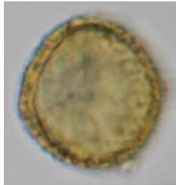
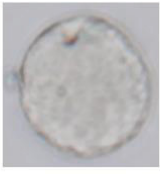


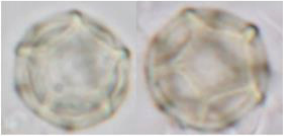

POLLEN GRAINS (4/10)

<p><i>Identification</i></p>  <p>20 μm</p> <p>40 m 60 m 80 m 300 m</p>	<p><i>Identification</i></p>  <p>20 μm</p> <p>40 m 60 m 80 m 300 m</p>	<p><i>Anacardiaceae</i></p>  <p>20 μm</p> <p>40 m 60 m 80 m 300 m</p>
<p><i>Identification</i></p>  <p>20 μm</p> <p>40 m 60 m 80 m 300 m</p>	<p><i>Identification</i></p>  <p>20 μm</p> <p>40 m 60 m 80 m 300 m</p>	<p><i>Caesalpiniaceae</i></p>  <p>20 μm</p> <p>40 m 60 m 80 m 300 m</p>
<p><i>Meliaceae</i></p>  <p>20 μm</p> <p>40 m 60 m 80 m 300 m</p>	<p><i>Myrtaceae</i></p>  <p>20 μm</p> <p>40 m 60 m 80 m 300 m</p>	<p><i>Fagaceae</i></p>  <p>20 μm</p> <p>40 m 60 m 80 m 300 m</p>
<p><i>Simarubaceae</i></p>  <p>20 μm</p> <p>40 m 60 m 80 m 300 m</p>	<p><i>Euphorbiaceae</i></p>  <p>20 μm</p> <p>40 m 60 m 80 m 300 m</p>	<p><i>Meliaceae</i></p>  <p>20 μm</p> <p>40 m 60 m 80 m 300 m</p>

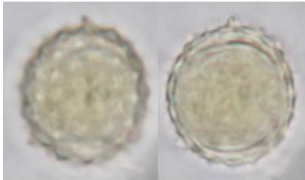
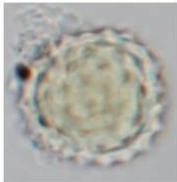
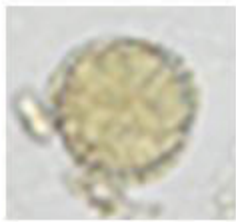

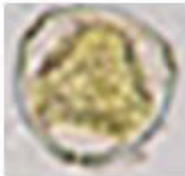



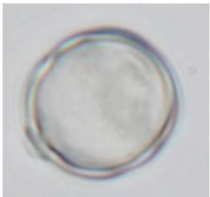
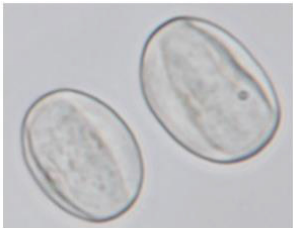


POLLEN GRAINS (5/10)

<i>Identification</i>  20 μ m 40 m 60 m 80 m 300 m	<i>Identification</i>  20 μ m 40 m 60 m 80 m 300 m	Solanaceae  20 μ m 40 m 60 m 80 m 300 m
Fabaceae  20 μ m 40 m 60 m 80 m 300 m	<i>Identification</i>  20 μ m 40 m 60 m 80 m 300 m	Fabaceae  20 μ m 40 m 60 m 80 m 300 m
<i>Identification</i>  20 μ m 40 m 60 m 80 m 300 m	<i>Identification</i>  20 μ m 40 m 60 m 80 m 300 m	<i>Identification</i>  20 μ m 40 m 60 m 80 m 300 m
<i>Identification</i>  20 μ m 40 m 60 m 80 m 300 m	Meliaceae  20 μ m 40 m 60 m 80 m 300 m	Saxifragaceae  20 μ m 40 m 60 m 80 m 300 m






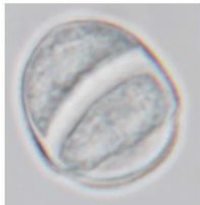
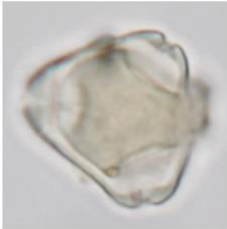

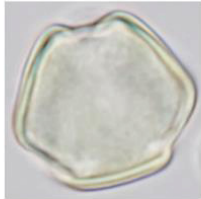
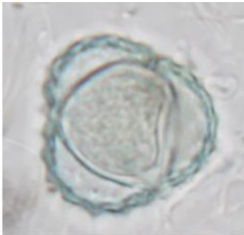


POLLEN GRAINS (6/10)

<i>Identification</i>  20 μ m 40 m 60 m 80 m 300 m	<i>Identification</i>  20 μ m 40 m 60 m 80 m 300 m	<i>Oleaceae</i>  20 μ m 40 m 60 m 80 m 300 m
<i>Identification</i>  20 μ m 40 m 60 m 80 m 300 m	<i>Amaranthaceae</i>  20 μ m 40 m 60 m 80 m 300 m	<i>Amaranthaceae</i>  20 μ m 40 m 60 m 80 m 300 m
<i>Identification</i>  20 μ m 40 m 60 m 80 m 300 m	<i>Identification</i>  20 μ m 40 m 60 m 80 m 300 m	<i>Flacourtiaceae</i>  20 μ m 40 m 60 m 80 m 300 m
<i>Identification</i>  20 μ m 40 m 60 m 80 m 300 m	<i>Amaranthaceae</i>  20 μ m 40 m 60 m 80 m 300 m	<i>Identification</i>  20 μ m 40 m 60 m 80 m 300 m













POLLEN GRAINS (7/10)

<p><i>Amaranthaceae</i></p>  <p>20 µm</p>	<p><i>Identification</i></p>  <p>20 µm</p>	<p><i>Amaranthaceae</i></p>  <p>20 µm</p>
40 m 60 m 80 m 300 m	40 m 60 m 80 m 300 m	40 m 60 m 80 m 300 m
<p><i>Identification</i></p>  <p>20 µm</p>	<p><i>Myricaceae</i></p>  <p>20 µm</p>	<p><i>Identification</i></p>  <p>20 µm</p>
40 m 60 m 80 m 300 m	40 m 60 m 80 m 300 m	40 m 60 m 80 m 300 m
<p><i>Amaranthaceae</i></p>  <p>20 µm</p>	<p><i>Fabaceae</i></p>  <p>20 µm</p>	<p><i>Identification</i></p>  <p>20 µm</p>
40 m 60 m 80 m 300 m	40 m 60 m 80 m 300 m	40 m 60 m 80 m 300 m
<p><i>Fabaceae</i></p>  <p>20 µm</p>	<p><i>Meliaceae</i></p>  <p>20 µm</p>	<p><i>Simarubaceae</i></p>  <p>20 µm</p>
40 m 60 m 80 m 300 m	40 m 60 m 80 m 300 m	40 m 60 m 80 m 300 m

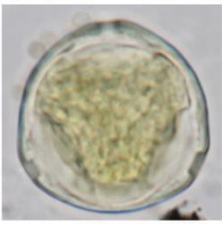


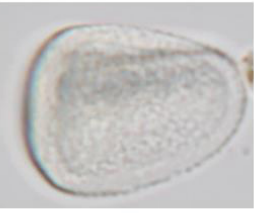








POLLEN GRAINS (8/10)

<p><i>Identification</i></p>  <p>20 μm</p> <p>40 m 60 m 80 m 300 m</p>	<p><i>Identification</i></p>  <p>20 μm</p> <p>40 m 60 m 80 m 300 m</p>	<p><i>Identification</i></p>  <p>20 μm</p> <p>40 m 60 m 80 m 300 m</p>
<p><i>Betulaceae</i></p>  <p>20 μm</p> <p>40 m 60 m 80 m 300 m</p>	<p><i>Identification</i></p>  <p>20 μm</p> <p>40 m 60 m 80 m 300 m</p>	<p><i>Podocarpaceae</i></p>  <p>20 μm</p> <p>40 m 60 m 80 m 300 m</p>
<p><i>Myrtaceae</i></p>  <p>20 μm</p> <p>40 m 60 m 80 m 300 m</p>	<p><i>Identification</i></p>  <p>20 μm</p> <p>40 m 60 m 80 m 300 m</p>	<p><i>Fabaceae</i></p>  <p>20 μm</p> <p>40 m 60 m 80 m 300 m</p>
<p><i>Identification</i></p>  <p>20 μm</p> <p>40 m 60 m 80 m 300 m</p>	<p><i>Combretaceae</i></p>  <p>20 μm</p> <p>40 m 60 m 80 m 300 m</p>	<p><i>Identification</i></p>  <p>20 μm</p> <p>40 m 60 m 80 m 300 m</p>




POLLEN GRAINS (9/10)



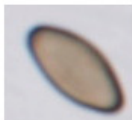
<p><i>Cyperaceae</i></p>  <p>20 μm</p>	<p><i>Identification</i></p>  <p>20 μm</p>	<p><i>Areaceae</i></p>  <p>20 μm</p>
40 m 60 m 80 m 300 m	40 m 60 m 80 m 300 m	40 m 60 m 80 m 300 m
<p><i>Identification</i></p>  <p>20 μm</p>	<p><i>Bambusoideae</i></p>  <p>20 μm</p>	<p><i>Parianaceae</i></p>  <p>20 μm</p>
40 m 60 m 80 m 300 m	40 m 60 m 80 m 300 m	40 m 60 m 80 m 300 m
<p><i>Identification</i></p>  <p>20 μm</p>	<p><i>Identification</i></p>  <p>20 μm</p>	<p><i>Identification</i></p>  <p>20 μm</p>
40 m 60 m 80 m 300 m	40 m 60 m 80 m 300 m	40 m 60 m 80 m 300 m
<p><i>Poaceae</i></p>  <p>20 μm</p>	<p><i>Identification</i></p>  <p>20 μm</p>	<p><i>Identification</i></p>  <p>20 μm</p>
40 m 60 m 80 m 300 m	40 m 60 m 80 m 300 m	40 m 60 m 80 m 300 m




POLLEN GRAINS (10/10)



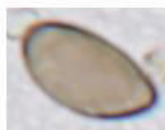
<p><i>Identification</i></p>  <p>20 μm</p>	<p><i>Identification</i></p>  <p>20 μm</p>	<p><i>Identification</i></p>  <p>20 μm</p>
40 m 60 m 80 m 300 m	40 m 60 m 80 m 300 m	40 m 60 m 80 m 300 m
<p><i>Cyperaceae</i></p>  <p>20 μm</p>	<p><i>Cyperaceae</i></p>  <p>20 μm</p>	<p><i>Cyperaceae</i></p>  <p>20 μm</p>
40 m 60 m 80 m 300 m	40 m 60 m 80 m 300 m	40 m 60 m 80 m 300 m
<p><i>Identification</i></p>  <p>20 μm</p>	<p><i>Poaceae</i></p>  <p>20 μm</p>	<p><i>Identification</i></p>  <p>20 μm</p>
40 m 60 m 80 m 300 m	40 m 60 m 80 m 300 m	40 m 60 m 80 m 300 m
<p><i>Identification</i></p>  <p>20 μm</p>	<p><i>Podocarpaceae</i></p>  <p>20 μm</p>	<p><i>Podocarpaceae</i></p>  <p>20 μm</p>
40 m 60 m 80 m 300 m	40 m 60 m 80 m 300 m	40 m 60 m 80 m 300 m

APPENDIX C.2: FUNGAL SPORES (1/17) – PHYLUM: ASCOMYCOTA

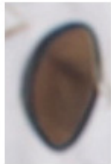

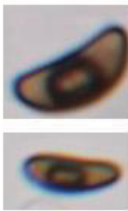









<i>Identification</i>				<i>Identification</i>				<i>Identification</i>			
											
10 µm				10 µm				10 µm			
40 m	60 m	80 m	300 m	40 m	60 m	80 m	300 m	40 m	60 m	80 m	300 m

<i>Ascospore</i>				<i>Ascospore</i>				<i>Ascospore</i>			
											
10 µm				10 µm				10 µm			
40 m	60 m	80 m	300 m	40 m	60 m	80 m	300 m	40 m	60 m	80 m	300 m













<i>Ascospore</i>				<i>Ascospore</i>				<i>Ascospore</i>			
											
10 µm				10 µm				10 µm			
40 m	60 m	80 m	300 m	40 m	60 m	80 m	300 m	40 m	60 m	80 m	300 m

<i>Identification</i>				<i>Identification</i>				<i>Identification</i>			
											
10 µm				10 µm				10 µm			
40 m	60 m	80 m	300 m	40 m	60 m	80 m	300 m	40 m	60 m	80 m	300 m









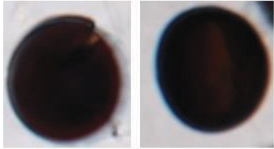



FUNGAL SPORES (2/17) - PHYLUM: ASCOMYCOTA

<i>Identification</i>  10 µm 40 m 60 m 80 m 300 m	<i>Identification</i>  10 µm 40 m 60 m 80 m 300 m	<i>Xylaria</i>  10 µm 40 m 60 m 80 m 300 m
<i>Identification</i>  10 µm 40 m 60 m 80 m 300 m	<i>Identification</i>  10 µm 40 m 60 m 80 m 300 m	<i>Ascospore</i>  10 µm 40 m 60 m 80 m 300 m
<i>Ascospore</i>  10 µm 40 m 60 m 80 m 300 m	<i>Ascospore</i>  10 µm 40 m 60 m 80 m 300 m	<i>Ascospore</i>  10 µm 40 m 60 m 80 m 300 m
<i>Identification</i>  10 µm 40 m 60 m 80 m 300 m	<i>Ascospore</i>  10 µm 40 m 60 m 80 m 300 m	<i>Venturia</i>  10 µm 40 m 60 m 80 m 300 m













FUNGAL SPORES (3/17) - PHYLUM: ASCOMYCOTA

<p><i>Identification</i></p>  <p>10 μm</p>	<p><i>Identification</i></p>  <p>10 μm</p>	<p><i>Identification</i></p>  <p>10 μm</p>
40 m 60 m 80 m 300 m	40 m 60 m 80 m 300 m	40 m 60 m 80 m 300 m
<p><i>Venturia</i></p>  <p>10 μm</p>	<p><i>Venturia</i></p>  <p>10 μm</p>	<p><i>Venturia</i></p>  <p>10 μm</p>
40 m 60 m 80 m 300 m	40 m 60 m 80 m 300 m	40 m 60 m 80 m 300 m
<p><i>Identification</i></p>  <p>10 μm</p>	<p><i>Identification</i></p>  <p>10 μm</p>	<p><i>Venturia</i></p>  <p>10 μm</p>
40 m 60 m 80 m 300 m	40 m 60 m 80 m 300 m	40 m 60 m 80 m 300 m
<p><i>Identification</i></p>  <p>10 μm</p>	<p><i>Bispora</i></p>  <p>10 μm</p>	<p><i>Identification</i></p>  <p>10 μm</p>
40 m 60 m 80 m 300 m	40 m 60 m 80 m 300 m	40 m 60 m 80 m 300 m







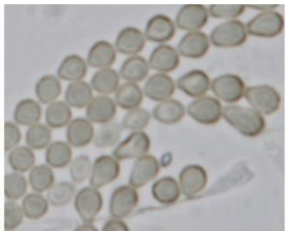
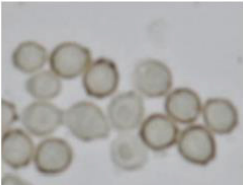



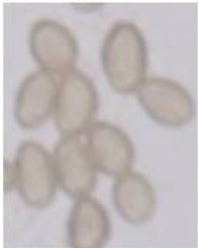
FUNGAL SPORES (4/17) - PHYLUM: ASCOMYCOTA

<p><i>Identification</i></p>  <p>10 μm</p> <p>40 m 60 m 80 m 300 m</p>	<p><i>Identification</i></p>  <p>10 μm</p> <p>40 m 60 m 80 m 300 m</p>	<p><i>Identification</i></p>  <p>10 μm</p> <p>40 m 60 m 80 m 300 m</p>
<p><i>Venturia</i></p>  <p>10 μm</p> <p>40 m 60 m 80 m 300 m</p>	<p><i>Bispora</i></p>  <p>10 μm</p> <p>40 m 60 m 80 m 300 m</p>	<p><i>Xylaria</i></p>  <p>10 μm</p> <p>40 m 60 m 80 m 300 m</p>
<p><i>Periconia</i></p>  <p>10 μm</p> <p>40 m 60 m 80 m 300 m</p>	<p><i>Nigrospora</i></p>  <p>10 μm</p> <p>40 m 60 m 80 m 300 m</p>	<p><i>Nigrospora</i></p>  <p>10 μm</p> <p>40 m 60 m 80 m 300 m</p>
<p><i>Spegazzinia</i></p>  <p>10 μm</p> <p>40 m 60 m 80 m 300 m</p>	<p><i>Spegazzinia</i></p>  <p>10 μm</p> <p>40 m 60 m 80 m 300 m</p>	<p><i>Spegazzinia</i></p>  <p>10 μm</p> <p>40 m 60 m 80 m 300 m</p>













FUNGAL SPORES (5/17) - PHYLUM: ASCOMYCOTA

<p><i>Torula</i></p>  <p>10 μm</p>	<p><i>Identification</i></p>  <p>10 μm</p>	<p><i>Identification</i></p>  <p>10 μm</p>
40 m 60 m 80 m 300 m	40 m 60 m 80 m 300 m	40 m 60 m 80 m 300 m
<p><i>Identification</i></p>  <p>10 μm</p>	<p><i>Identification</i></p>  <p>10 μm</p>	<p><i>Identification</i></p>  <p>10 μm</p>
40 m 60 m 80 m 300 m	40 m 60 m 80 m 300 m	40 m 60 m 80 m 300 m
<p><i>Identification</i></p>  <p>10 μm</p>	<p><i>Identification</i></p>  <p>10 μm</p>	<p><i>Identification</i></p>  <p>10 μm</p>
40 m 60 m 80 m 300 m	40 m 60 m 80 m 300 m	40 m 60 m 80 m 300 m
<p><i>Identification</i></p>  <p>10 μm</p>	<p><i>Identification</i></p>  <p>10 μm</p>	<p><i>Identification</i></p>  <p>10 μm</p>
40 m 60 m 80 m 300 m	40 m 60 m 80 m 300 m	40 m 60 m 80 m 300 m








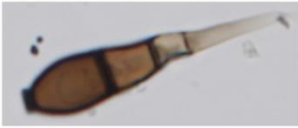




FUNGAL SPORES (6/17) - PHYLUM: ASCOMYCOTA

<p><i>Identification</i></p>  <p>10 μm</p>	<p><i>Identification</i></p>  <p>10 μm</p>	<p><i>Identification</i></p>  <p>10 μm</p>
40 m 60 m 80 m 300 m	40 m 60 m 80 m 300 m	40 m 60 m 80 m 300 m
<p><i>Identification</i></p>  <p>10 μm</p>	<p><i>Identification</i></p>  <p>10 μm</p>	<p><i>Identification</i></p>  <p>10 μm</p>
40 m 60 m 80 m 300 m	40 m 60 m 80 m 300 m	40 m 60 m 80 m 300 m
<p><i>Penicillium</i></p>  <p>10 μm</p>	<p><i>Penicillium</i></p>  <p>10 μm</p>	<p><i>Penicillium</i></p>  <p>10 μm</p>
40 m 60 m 80 m 300 m	40 m 60 m 80 m 300 m	40 m 60 m 80 m 300 m
<p><i>Identification</i></p>  <p>10 μm</p>	<p><i>Identification</i></p>  <p>10 μm</p>	<p><i>Identification</i></p>  <p>10 μm</p>
40 m 60 m 80 m 300 m	40 m 60 m 80 m 300 m	40 m 60 m 80 m 300 m





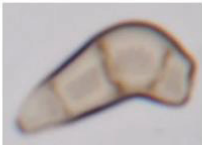



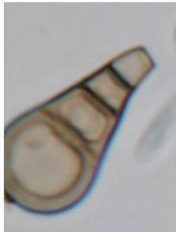



FUNGAL SPORES (7/17) - PHYLUM: ASCOMYCOTA

<p><i>Identification</i></p>  <p>10 μm</p>	<p><i>Identification</i></p>  <p>10 μm</p>	<p><i>Cladosporium</i></p>  <p>10 μm</p>
40 m 60 m 80 m 300 m	40 m 60 m 80 m 300 m	40 m 60 m 80 m 300 m
<p><i>Cladosporium</i></p>  <p>10 μm</p>	<p><i>Cladosporium</i></p>  <p>10 μm</p>	<p><i>Cladosporium</i></p>  <p>10 μm</p>
40 m 60 m 80 m 300 m	40 m 60 m 80 m 300 m	40 m 60 m 80 m 300 m
<p><i>Identification</i></p>  <p>10 μm</p>	<p><i>Identification</i></p>  <p>10 μm</p>	<p><i>Identification</i></p>  <p>10 μm</p>
40 m 60 m 80 m 300 m	40 m 60 m 80 m 300 m	40 m 60 m 80 m 300 m
<p><i>Identification</i></p>  <p>10 μm</p>	<p><i>Identification</i></p>  <p>10 μm</p>	<p><i>Identification</i></p>  <p>10 μm</p>
40 m 60 m 80 m 300 m	40 m 60 m 80 m 300 m	40 m 60 m 80 m 300 m




FUNGAL SPORES (8/17) - PHYLUM: ASCOMYCOTA



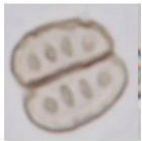
<p><i>Identification</i></p>  <p>10 μm</p>	<p><i>Identification</i></p>  <p>10 μm</p>	<p><i>Identification</i></p>  <p>10 μm</p>
40 m 60 m 80 m 300 m	40 m 60 m 80 m 300 m	40 m 60 m 80 m 300 m
<p><i>Identification</i></p>  <p>10 μm</p>	<p><i>Identification</i></p>  <p>10 μm</p>	<p><i>Identification</i></p>  <p>10 μm</p>
40 m 60 m 80 m 300 m	40 m 60 m 80 m 300 m	40 m 60 m 80 m 300 m
<p><i>Identification</i></p>  <p>10 μm</p>	<p><i>Alternaria</i></p>  <p>10 μm</p>	<p><i>Identification</i></p>  <p>10 μm</p>
40 m 60 m 80 m 300 m	40 m 60 m 80 m 300 m	40 m 60 m 80 m 300 m
<p><i>Identification</i></p>  <p>10 μm</p>	<p><i>Identification</i></p>  <p>10 μm</p>	<p><i>Identification</i></p>  <p>10 μm</p>
40 m 60 m 80 m 300 m	40 m 60 m 80 m 300 m	40 m 60 m 80 m 300 m

FUNGAL SPORES (9/17) - PHYLUM: ASCOMYCOTA



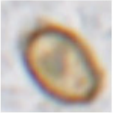



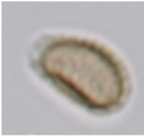




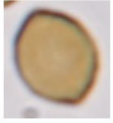
<p><i>Identification</i></p>  <p>10 μm</p>	<p><i>Identification</i></p>  <p>10 μm</p>	<p><i>Identification</i></p>  <p>10 μm</p>
40 m 60 m 80 m 300 m	40 m 60 m 80 m 300 m	40 m 60 m 80 m 300 m
<p><i>Curvularia</i></p>  <p>10 μm</p>	<p><i>Curvularia</i></p>  <p>10 μm</p>	<p><i>Curvularia</i></p>  <p>10 μm</p>
40 m 60 m 80 m 300 m	40 m 60 m 80 m 300 m	40 m 60 m 80 m 300 m
<p><i>Alternaria</i></p>  <p>10 μm</p>	<p><i>Identification</i></p>  <p>10 μm</p>	<p><i>Alternaria</i></p>  <p>10 μm</p>
40 m 60 m 80 m 300 m	40 m 60 m 80 m 300 m	40 m 60 m 80 m 300 m
<p><i>Identification</i></p>  <p>10 μm</p>	<p><i>Identification</i></p>  <p>10 μm</p>	<p><i>Identification</i></p>  <p>10 μm</p>
40 m 60 m 80 m 300 m	40 m 60 m 80 m 300 m	40 m 60 m 80 m 300 m

FUNGAL SPORES (10/17) - PHYLUM: ASCOMYCOTA

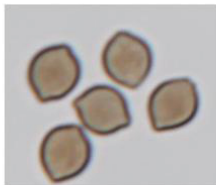
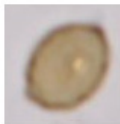

<i>Identification</i>  10 µm				<i>Leptosphaerulina</i>  10 µm				<i>Leptosphaerulina</i>  10 µm			
40 m	60 m	80 m	300 m	40 m	60 m	80 m	300 m	40 m	60 m	80 m	300 m




<i>Identification</i>  10 µm				<i>Identification</i>  10 µm				<i>Identification</i>  10 µm			
40 m	60 m	80 m	300 m	40 m	60 m	80 m	300 m	40 m	60 m	80 m	300 m

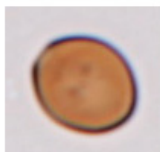
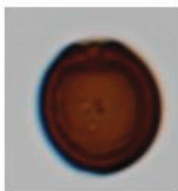

FUNGAL SPORES (11/17) - PHYLUM: BASIDIOMYCOTA

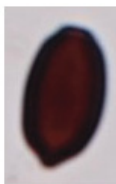

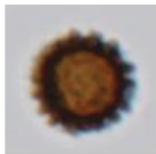
<p><i>Ganoderma</i></p>  <p>10 μm</p>	<p><i>Ganoderma</i></p>  <p>10 μm</p>	<p><i>Ganoderma</i></p>  <p>10 μm</p>
40 m 60 m 80 m 300 m	40 m 60 m 80 m 300 m	40 m 60 m 80 m 300 m
<p><i>Ganoderma</i></p>  <p>10 μm</p>	<p><i>Ganoderma</i></p>  <p>10 μm</p>	<p><i>Ganoderma</i></p>  <p>10 μm</p>
40 m 60 m 80 m 300 m	40 m 60 m 80 m 300 m	40 m 60 m 80 m 300 m
<p><i>Ganoderma</i></p>  <p>10 μm</p>	<p><i>Ganoderma</i></p>  <p>10 μm</p>	<p><i>Ganoderma</i></p>  <p>10 μm</p>
40 m 60 m 80 m 300 m	40 m 60 m 80 m 300 m	40 m 60 m 80 m 300 m
<p><i>Ganoderma</i></p>  <p>10 μm</p>	<p><i>Ganoderma</i></p>  <p>10 μm</p>	<p><i>Conocybe</i></p>  <p>10 μm</p>
40 m 60 m 80 m 300 m	40 m 60 m 80 m 300 m	40 m 60 m 80 m 300 m

FUNGAL SPORES (12/17) - PHYLUM: BASIDIOMYCOTA





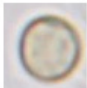



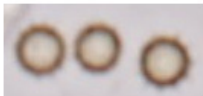



<i>Conocybe</i>				<i>Conocybe</i>				<i>Conocybe</i>			
											
<div>10 μm</div>				<div>10 μm</div>				<div>10 μm</div>			
40 m	60 m	80 m	300 m	40 m	60 m	80 m	300 m	40 m	60 m	80 m	300 m

<i>Coprinoid</i>				<i>Coprinoid</i>				<i>Coprinoid</i>			
											
<div>10 μm</div>				<div>10 μm</div>				<div>10 μm</div>			
40 m	60 m	80 m	300 m	40 m	60 m	80 m	300 m	40 m	60 m	80 m	300 m

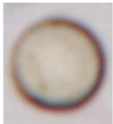


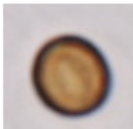
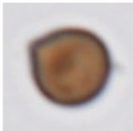


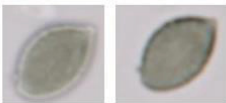

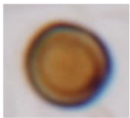


<i>Coprinoid</i>				<i>Coprinoid</i>				<i>Coprinoid</i>			
											
<div>10 μm</div>				<div>10 μm</div>				<div>10 μm</div>			
40 m	60 m	80 m	300 m	40 m	60 m	80 m	300 m	40 m	60 m	80 m	300 m

<i>Coprinoid</i>				<i>Scleroderma</i>				<i>Scleroderma</i>			
											
<div>10 μm</div>				<div>10 μm</div>				<div>10 μm</div>			
40 m	60 m	80 m	300 m	40 m	60 m	80 m	300 m	40 m	60 m	80 m	300 m



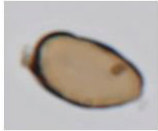

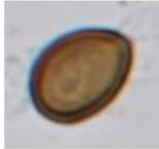

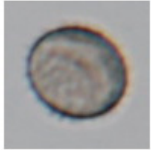
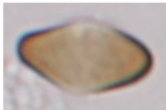


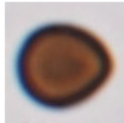

FUNGAL SPORES (13/17) – OTHER PHYLA

<p><i>Identification</i></p>  <p>10 μm</p>	<p><i>Identification</i></p>  <p>10 μm</p>	<p><i>Identification</i></p>  <p>10 μm</p>
40 m 60 m 80 m 300 m	40 m 60 m 80 m 300 m	40 m 60 m 80 m 300 m
<p><i>Identification</i></p>  <p>10 μm</p>	<p><i>Identification</i></p>  <p>10 μm</p>	<p><i>Identification</i></p>  <p>10 μm</p>
40 m 60 m 80 m 300 m	40 m 60 m 80 m 300 m	40 m 60 m 80 m 300 m
<p><i>Identification</i></p>  <p>10 μm</p>	<p><i>Identification</i></p>  <p>10 μm</p>	<p><i>Identification</i></p>  <p>10 μm</p>
40 m 60 m 80 m 300 m	40 m 60 m 80 m 300 m	40 m 60 m 80 m 300 m
<p><i>Identification</i></p>  <p>10 μm</p>	<p><i>Identification</i></p>  <p>10 μm</p>	<p><i>Identification</i></p>  <p>10 μm</p>
40 m 60 m 80 m 300 m	40 m 60 m 80 m 300 m	40 m 60 m 80 m 300 m









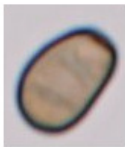
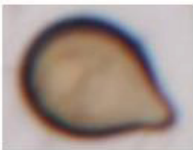


FUNGAL SPORES (14/17) - OTHER PHYLA

<p><i>Identification</i></p>  <p>10 μm</p>	<p><i>Identification</i></p>  <p>10 μm</p>	<p><i>Identification</i></p>  <p>10 μm</p>
40 m 60 m 80 m 300 m	40 m 60 m 80 m 300 m	40 m 60 m 80 m 300 m
<p><i>Identification</i></p>  <p>10 μm</p>	<p><i>Identification</i></p>  <p>10 μm</p>	<p><i>Identification</i></p>  <p>10 μm</p>
40 m 60 m 80 m 300 m	40 m 60 m 80 m 300 m	40 m 60 m 80 m 300 m
<p><i>Identification</i></p>  <p>10 μm</p>	<p><i>Identification</i></p>  <p>10 μm</p>	<p><i>Identification</i></p>  <p>10 μm</p>
40 m 60 m 80 m 300 m	40 m 60 m 80 m 300 m	40 m 60 m 80 m 300 m
<p><i>Identification</i></p>  <p>10 μm</p>	<p><i>Identification</i></p>  <p>10 μm</p>	<p><i>Identification</i></p>  <p>10 μm</p>
40 m 60 m 80 m 300 m	40 m 60 m 80 m 300 m	40 m 60 m 80 m 300 m


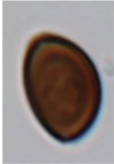

FUNGAL SPORES (15/17) - OTHER PHYLA

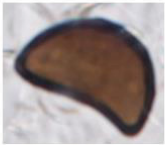


<p><i>Identification</i></p>  <p>10 μm</p>	<p><i>Identification</i></p>  <p>10 μm</p>	<p><i>Identification</i></p>  <p>10 μm</p>
40 m 60 m 80 m 300 m	40 m 60 m 80 m 300 m	40 m 60 m 80 m 300 m
<p><i>Identification</i></p>  <p>10 μm</p>	<p><i>Identification</i></p>  <p>10 μm</p>	<p><i>Identification</i></p>  <p>10 μm</p>
40 m 60 m 80 m 300 m	40 m 60 m 80 m 300 m	40 m 60 m 80 m 300 m
<p><i>Identification</i></p>  <p>10 μm</p>	<p><i>Identification</i></p>  <p>10 μm</p>	<p><i>Identification</i></p>  <p>10 μm</p>
40 m 60 m 80 m 300 m	40 m 60 m 80 m 300 m	40 m 60 m 80 m 300 m
<p><i>Identification</i></p>  <p>10 μm</p>	<p><i>Identification</i></p>  <p>10 μm</p>	<p><i>Identification</i></p>  <p>10 μm</p>
40 m 60 m 80 m 300 m	40 m 60 m 80 m 300 m	40 m 60 m 80 m 300 m

FUNGAL SPORES (16/17) - OTHER PHYLA







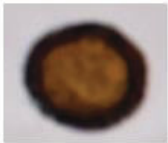





<p><i>Identification</i></p>  <p>10 μm</p>	<p><i>Identification</i></p>  <p>10 μm</p>	<p><i>Identification</i></p>  <p>10 μm</p>
40 m 60 m 80 m 300 m	40 m 60 m 80 m 300 m	40 m 60 m 80 m 300 m
<p><i>Identification</i></p>  <p>10 μm</p>	<p><i>Identification</i></p>  <p>10 μm</p>	<p><i>Identification</i></p>  <p>10 μm</p>
40 m 60 m 80 m 300 m	40 m 60 m 80 m 300 m	40 m 60 m 80 m 300 m
<p><i>Identification</i></p>  <p>10 μm</p>	<p><i>Identification</i></p>  <p>10 μm</p>	<p><i>Identification</i></p>  <p>10 μm</p>
40 m 60 m 80 m 300 m	40 m 60 m 80 m 300 m	40 m 60 m 80 m 300 m
<p><i>Identification</i></p>  <p>10 μm</p>	<p><i>Identification</i></p>  <p>10 μm</p>	<p><i>Identification</i></p>  <p>10 μm</p>
40 m 60 m 80 m 300 m	40 m 60 m 80 m 300 m	40 m 60 m 80 m 300 m

FUNGAL SPORES (17/17) - OTHER PHYLA






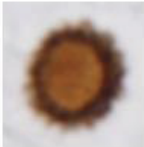
<p><i>Identification</i></p>  <p>10 µm</p>				<p><i>Identification</i></p>  <p>10 µm</p>				<p><i>Identification</i></p>  <p>10 µm</p>			
40 m	60 m	80 m	300 m	40 m	60 m	80 m	300 m	40 m	60 m	80 m	300 m

<p><i>Identification</i></p>  <p>10 µm</p>				<p><i>Identification</i></p>  <p>10 µm</p>				<p><i>Identification</i></p>  <p>10 µm</p>			
40 m	60 m	80 m	300 m	40 m	60 m	80 m	300 m	40 m	60 m	80 m	300 m







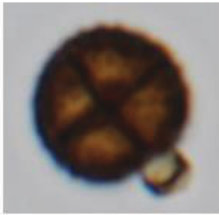





APPENDIX C.3: FERN SPORES (1/2)

<p><i>Identification</i></p>  <p>10 μm</p>	<p><i>Identification</i></p>  <p>10 μm</p>	<p><i>Identification</i></p>  <p>10 μm</p>
40 m 60 m 80 m 300 m	40 m 60 m 80 m 300 m	40 m 60 m 80 m 300 m
<p><i>Identification</i></p>  <p>10 μm</p>	<p><i>Identification</i></p>  <p>10 μm</p>	<p><i>Identification</i></p>  <p>10 μm</p>
40 m 60 m 80 m 300 m	40 m 60 m 80 m 300 m	40 m 60 m 80 m 300 m
<p><i>Identification</i></p>  <p>10 μm</p>	<p><i>Identification</i></p>  <p>10 μm</p>	<p><i>Identification</i></p>  <p>10 μm</p>
40 m 60 m 80 m 300 m	40 m 60 m 80 m 300 m	40 m 60 m 80 m 300 m
<p><i>Identification</i></p>  <p>10 μm</p>	<p><i>Identification</i></p>  <p>10 μm</p>	<p><i>Identification</i></p>  <p>10 μm</p>
40 m 60 m 80 m 300 m	40 m 60 m 80 m 300 m	40 m 60 m 80 m 300 m





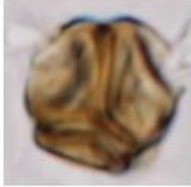







FERN SPORES (2/2)

<p><i>Identification</i></p>  <p>10 μm</p>	<p><i>Identification</i></p>  <p>10 μm</p>	<p><i>Identification</i></p>  <p>10 μm</p>
<p>40 m 60 m 80 m 300 m</p>	<p>40 m 60 m 80 m 300 m</p>	<p>40 m 60 m 80 m 300 m</p>
<p><i>Identification</i></p>  <p>10 μm</p>	<p><i>Identification</i></p>  <p>10 μm</p>	<p><i>Identification</i></p>  <p>10 μm</p>
<p>40 m 60 m 80 m 300 m</p>	<p>40 m 60 m 80 m 300 m</p>	<p>40 m 60 m 80 m 300 m</p>



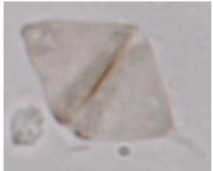






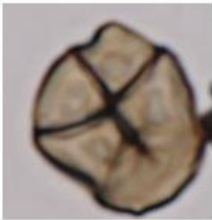


APPENDIX C.4: UNKNOWN PARTICLES (1/4)

<p><i>Identification</i></p>  <p>10 μm</p> <table border="1"> <tr> <td>40 m</td> <td>60 m</td> <td>80 m</td> <td>300 m</td> </tr> </table>	40 m	60 m	80 m	300 m	<p><i>Identification</i></p>  <p>10 μm</p> <table border="1"> <tr> <td>40 m</td> <td>60 m</td> <td>80 m</td> <td>300 m</td> </tr> </table>	40 m	60 m	80 m	300 m	<p><i>Identification</i></p>  <p>10 μm</p> <table border="1"> <tr> <td>40 m</td> <td>60 m</td> <td>80 m</td> <td>300 m</td> </tr> </table>	40 m	60 m	80 m	300 m
40 m	60 m	80 m	300 m											
40 m	60 m	80 m	300 m											
40 m	60 m	80 m	300 m											
<p><i>Identification</i></p>  <p>10 μm</p> <table border="1"> <tr> <td>40 m</td> <td>60 m</td> <td>80 m</td> <td>300 m</td> </tr> </table>	40 m	60 m	80 m	300 m	<p><i>Identification</i></p>  <p>10 μm</p> <table border="1"> <tr> <td>40 m</td> <td>60 m</td> <td>80 m</td> <td>300 m</td> </tr> </table>	40 m	60 m	80 m	300 m	<p><i>Identification</i></p>  <p>10 μm</p> <table border="1"> <tr> <td>40 m</td> <td>60 m</td> <td>80 m</td> <td>300 m</td> </tr> </table>	40 m	60 m	80 m	300 m
40 m	60 m	80 m	300 m											
40 m	60 m	80 m	300 m											
40 m	60 m	80 m	300 m											
<p><i>Identification</i></p>  <p>10 μm</p> <table border="1"> <tr> <td>40 m</td> <td>60 m</td> <td>80 m</td> <td>300 m</td> </tr> </table>	40 m	60 m	80 m	300 m	<p><i>Identification</i></p>  <p>10 μm</p> <table border="1"> <tr> <td>40 m</td> <td>60 m</td> <td>80 m</td> <td>300 m</td> </tr> </table>	40 m	60 m	80 m	300 m	<p><i>Identification</i></p>  <p>10 μm</p> <table border="1"> <tr> <td>40 m</td> <td>60 m</td> <td>80 m</td> <td>300 m</td> </tr> </table>	40 m	60 m	80 m	300 m
40 m	60 m	80 m	300 m											
40 m	60 m	80 m	300 m											
40 m	60 m	80 m	300 m											
<p><i>Identification</i></p>  <p>10 μm</p> <table border="1"> <tr> <td>40 m</td> <td>60 m</td> <td>80 m</td> <td>300 m</td> </tr> </table>	40 m	60 m	80 m	300 m	<p><i>Identification</i></p>  <p>10 μm</p> <table border="1"> <tr> <td>40 m</td> <td>60 m</td> <td>80 m</td> <td>300 m</td> </tr> </table>	40 m	60 m	80 m	300 m	<p><i>Identification</i></p>  <p>10 μm</p> <table border="1"> <tr> <td>40 m</td> <td>60 m</td> <td>80 m</td> <td>300 m</td> </tr> </table>	40 m	60 m	80 m	300 m
40 m	60 m	80 m	300 m											
40 m	60 m	80 m	300 m											
40 m	60 m	80 m	300 m											


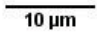
UNKNOWN PARTICLES (2/4)


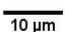
<p><i>Identification</i></p>  <p>10 μm</p>	<p><i>Identification</i></p>  <p>10 μm</p>	<p><i>Identification</i></p>  <p>10 μm</p>
40 m 60 m 80 m 300 m	40 m 60 m 80 m 300 m	40 m 60 m 80 m 300 m
<p><i>Identification</i></p>  <p>10 μm</p>	<p><i>Identification</i></p>  <p>10 μm</p>	<p><i>Identification</i></p>  <p>10 μm</p>
40 m 60 m 80 m 300 m	40 m 60 m 80 m 300 m	40 m 60 m 80 m 300 m
<p><i>Identification</i></p>  <p>10 μm</p>	<p><i>Identification</i></p>  <p>10 μm</p>	<p><i>Identification</i></p>  <p>10 μm</p>
40 m 60 m 80 m 300 m	40 m 60 m 80 m 300 m	40 m 60 m 80 m 300 m
<p><i>Identification</i></p>  <p>10 μm</p>	<p><i>Identification</i></p>  <p>10 μm</p>	<p><i>Identification</i></p>  <p>10 μm</p>
40 m 60 m 80 m 300 m	40 m 60 m 80 m 300 m	40 m 60 m 80 m 300 m


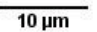
UNKNOWN PARTICLES (3/4)


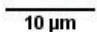
<p><i>Identification</i></p>  <p>10 μm</p>	<p><i>Identification</i></p>  <p>10 μm</p>	<p><i>Identification</i></p>  <p>10 μm</p>
40 m 60 m 80 m 300 m	40 m 60 m 80 m 300 m	40 m 60 m 80 m 300 m
<p><i>Identification</i></p>  <p>10 μm</p>	<p><i>Identification</i></p>  <p>10 μm</p>	<p><i>Identification</i></p>  <p>10 μm</p>
40 m 60 m 80 m 300 m	40 m 60 m 80 m 300 m	40 m 60 m 80 m 300 m
<p><i>Identification</i></p>  <p>10 μm</p>	<p><i>Identification</i></p>  <p>10 μm</p>	<p><i>Identification</i></p>  <p>10 μm</p>
40 m 60 m 80 m 300 m	40 m 60 m 80 m 300 m	40 m 60 m 80 m 300 m
<p><i>Identification</i></p>  <p>10 μm</p>	<p><i>Identification</i></p>  <p>10 μm</p>	<p><i>Identification</i></p>  <p>10 μm</p>
40 m 60 m 80 m 300 m	40 m 60 m 80 m 300 m	40 m 60 m 80 m 300 m


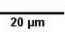
UNKNOWN PARTICLES (4/4)

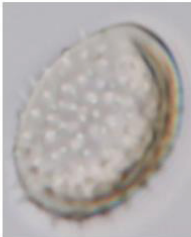
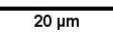
<i>Identification</i>				
				
				
40 m	60 m	80 m	300 m	


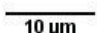
<i>Identification</i>				
				
				
40 m	60 m	80 m	300 m	

<i>Identification</i>				
				
				
40 m	60 m	80 m	300 m	

<i>Identification</i>				
				
				
40 m	60 m	80 m	300 m	

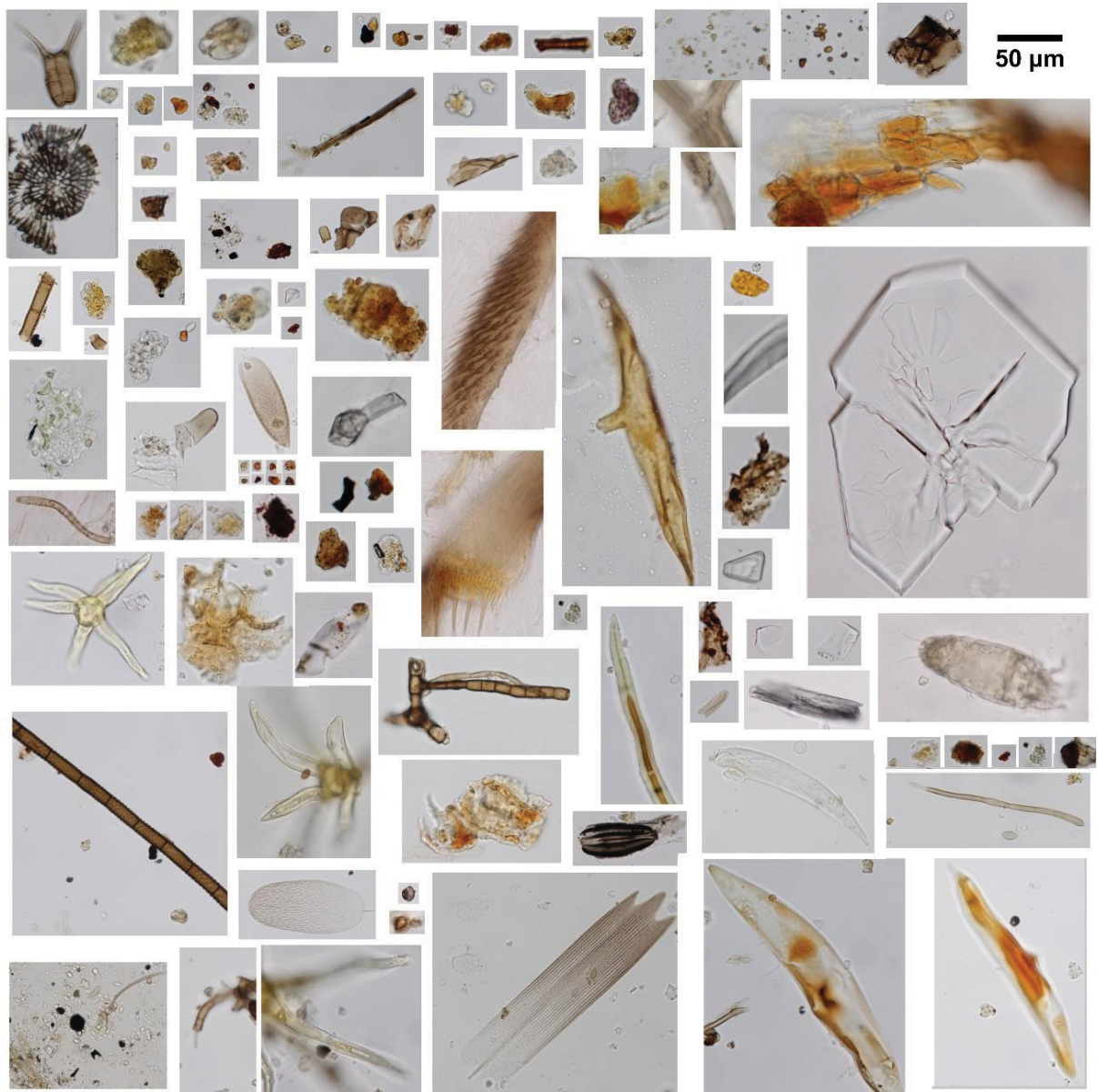
<i>Identification</i>				
				
				
40 m	60 m	80 m	300 m	

<i>Identification</i>				
				
				
40 m	60 m	80 m	300 m	

<i>Identification</i>				
				
				
40 m	60 m	80 m	300 m	

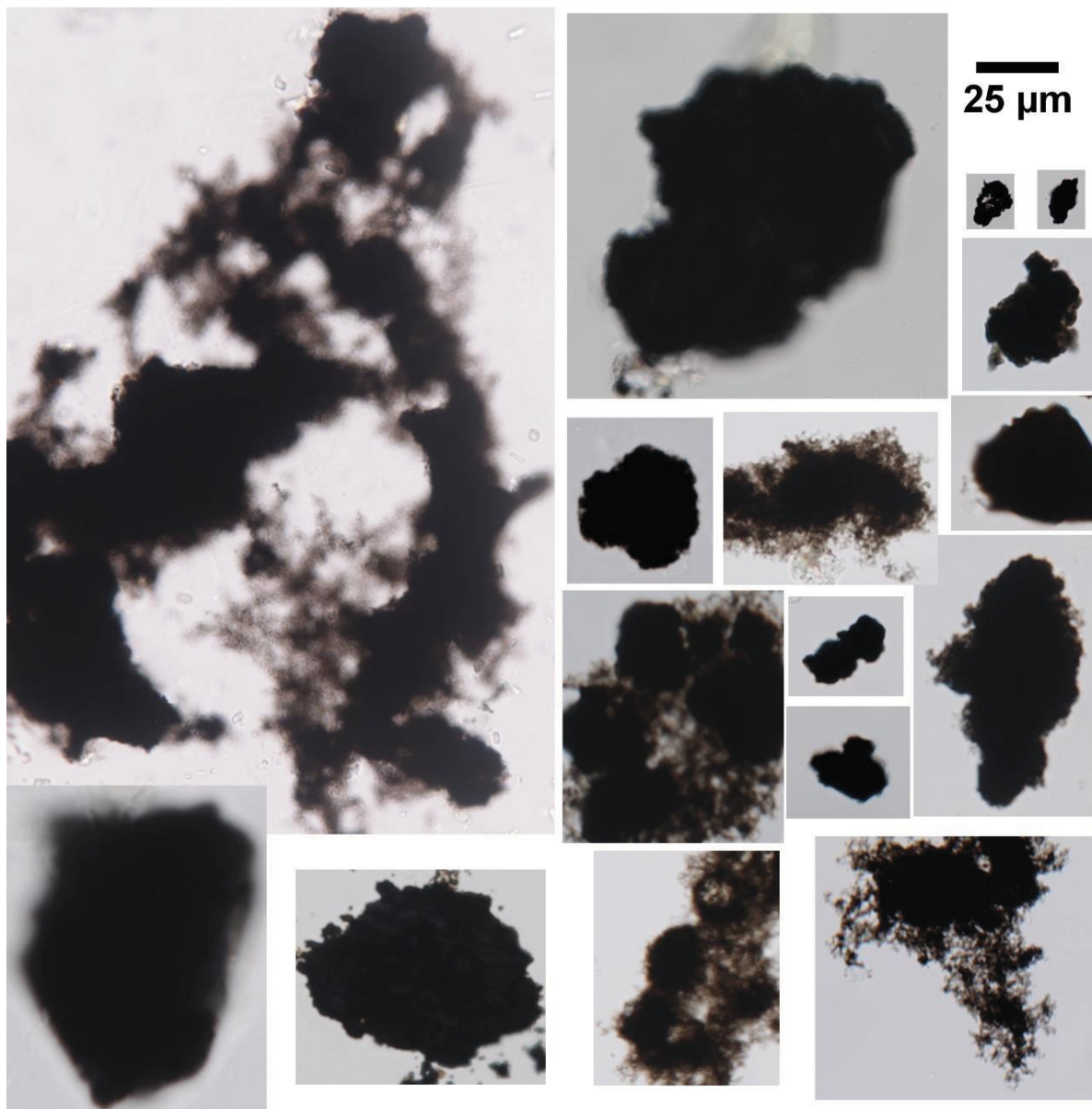
CANOPY DEBRIS (1/1)

Example of structures classified as canopy debris. The general scale is 50 μm .



SOOT (1/1)

Examples of black amorphous structures classified as soot. General scale: 25 μm .



REFERENCES

- BARTH, O.M.; JUSTO, R.L.; BARROS, M.A. Sistematic catalogue of arboreal plant pollen grains of southern Brazil. XXX: Meliaceae. Rev. Brasil. Biol., 58 (3), 497-509, 1998.
- BRAGA, J.A.; SALES, E.O.; SOARES NETO, J.; CONDE, M.M.; BARTH, O.M.; LORENZON, M.C. Floral sources to *Tetragonisca angustula* (Hymenoptera: Apidae) and their pollen morphology in a Southeastern Brazilian Atlantic Forest. Int. J. Trop. Biol., 60 (4), 1491-1501, 2012.
- CARRIJO, T.T.; FOURNY, A.C.S.; FREITAS, M.F.; GONCALVES-ESTEVEES, V.; PEIXOTO, A.L. Insights on *Ardisia* and *Stylogyne* (Myrsinoideae–Primulaceae) based on pollen morphology. Plant Syst. Evol., 297, 261–269, 2011.
- CARVALHO, C. A. L.; MORETI, A. C. C. C.; MARCHINI, L. C.; ALVES, R. M. O.; OLIVEIRA, P. C. F. Pollen spectrum of honey of “URUÇU” bee (*Melipona scutellaris* LATREILLE, 1811), Rev. Brasil. Biol., 61(1), 63-67, 2001.
- COLINVAUX, P.; OLIVEIRA, P. E. De; PATINO, J. E. M. Amazon pollen manual and atlas. 413 p. Taylor & Francis, Amsterdam, The Netherlands, 2005.
- FERREIRA, M.G.; ABSY, M.L. Pollen analysis of honeys of *Melipona* (*Michmelia*) *seminigra merrillae* and *Melipona* (*Melikerria*) *interrupta* (Hymenoptera: Apidae) bred in Central Amazon, Brazil. Grana, 1-14, 2017.
- FERREIRA, M.G.; ABSY, M.L. Pollen niche and trophic interactions between colonies of *Melipona* (*Michmelia*) *seminigra merrillae* and *Melipona* (*Melikerria*) *interrupta* (Apidae: Meliponini) reared in floodplains in the Central Amazon. Arthropod-Plant Interactions, 9, 263-279, 2015.
- GURGEL, E.S.C.; CARREIRA, L.M.M.; KALUME, M.A.A. Leguminosas da Amazônia Brasileira - XV. O pólen do gênero *Bocoa* Aubl. (Leguminosae - Papilionoideae), Acta bot. bras., 18(3), 431-435, 2004.
- LEWIS, W. H.; VINAY, P.; ZENGER, V. E. Airborne and allergic pollen of North America. The Johns Hopkins University Press, Baltimore, 254 p., 1983.
- MORGADO, L. N.; RESENDES, R.; MOURA, M.; VENTURA, M. A. M. Pollen resources used by *Chrysoperla agilis* (Neuroptera: Chrysopidae) in the Azores, Portugal, Eur. J. Entomol., 111(1), 143–146, 2014.
- MOURA, C. O.; ABSY, M.L.; SANTOS, F.A.R.; MARQUES-SOUZA, A.C. Pollen morphology of Central Amazonia floodplain and flooded forest species. Acta Amazonica, 34 (1), 15-19, 2004.
- NOVAIS, J.S.; ABSY, M.L. Palynological examination of the pollen pots of native stingless bees from the Lower Amazon region in Pará, Brazil. Palynology, 37 (2), 218-230, 2013.
- RODRIGUES, I.D.; ABSY, M.L.; SILVA-CAMINHA, S.A.F.; GONCALVES-ESTEVEES, V.; MENDONCA, C.B.F.; FERREIRA, M.G.; MOURA, C.O. Pollen morphology of 25 species in the family Apocynaceae from the Adolpho Ducke Forest Reserve, Amazonas, Brazil. Palynology, 41 (2), 278-296, 2017.
- SEKINE, E. S.; TOLEDO, V. A. A.; CAXAMBU, M. G.; SHMURA, S.; TAKASHIBA, E. H.; SEREIA, M. J.; MARCHINI, L. C.; MORETI, A. C. C. C. Melliferous flora and pollen characterization of honey samples of *Apis mellifera* L., 1758 in apiaries in the counties of Ubiratã and Nova Aurora, PR. Annals of the Brazilian Academy of Sciences, 85 (1), 307-326, 2013.
- SOUZA, H. R.; CORREA, A. M.S.; CRUZ-BARROS, M.A.V.; ALBUQUERQUE, P.M.C. Espectro polínico da própolis de *Scaptotrigona* aff. *postica* (Hymenoptera, Apidae, Meliponini) em Barra do Corda, MA, Brasil. Acta Amazonica, 45 (3), 307-316, 2015.
- TRESSO, M. R.; CORREA, A.M.S. Flora Polínica da Reserva do Parque Estadual das Fontes do Ipiranga (São Paulo, Brasil). Hoehnea, 42 (1), 33-39, 2015.
- TRYON, R. M.; TRYON, A. F. Ferns and Allied Plants. Springer-Verlag, New York, 857 p., 1982.
- ZIDKO, A.; RODRIGUES, L.A.; MENDONCA, C.B.F.; ABSY, M.L.; FERREIRA, M.G.; SAMPAIO, P.T.B.; ESTEVES, V. Pollen morphology of *Carapa* species (Meliaceae) from the Brazilian Amazon. Acta Amazonica, 46 (3), 333-336, 2016.